Monograph

PROSPECTIVE GLOBAL SCIENTIFIC TRENDS

MODERN TECHNOLOGIES AND CONCEPTS OF RESEARCHING FOR SHIP POWER PLANTS OF COMBINED PROPULSION COMPLEXES

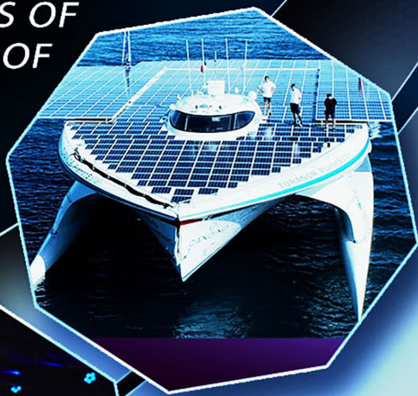

Book 7. Part 7

'2021

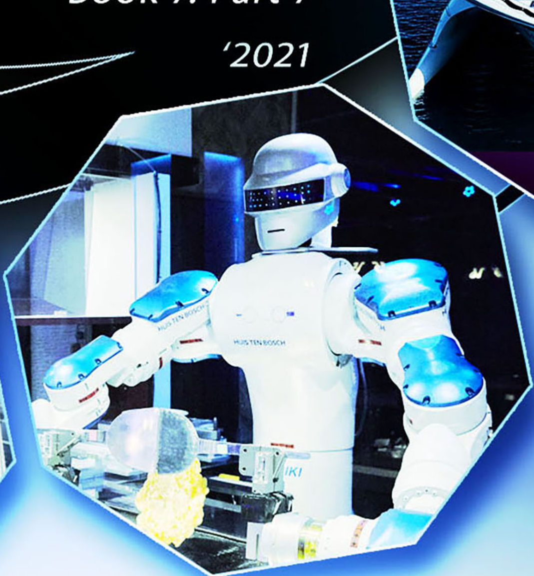

SWorld
Germany

Budashko V.V.

PROSPEKTIVE GLOBALE WISSENSCHAFTLICHE TRENDS

MODERNE TECHNOLOGIEN UND FORSCHUNGSKONZEPTE FÜR SCHIFFSKRAFTWERKE KOMBINIERTER ANTRIEBSANLAGEN

PROSPECTIVE GLOBAL SCIENTIFIC TRENDS

MODERN TECHNOLOGIES AND CONCEPTS OF RESEARCHING FOR SHIP POWER PLANTS OF COMBINED PROPULSION COMPLEXES

Monographic series «European Science»
Book 7. Part 7.

In internationalen wissenschaftlich-geometrischen Datenbanken enthalten
Included in International scientometric databases

MONOGRAPHIE

MONOGRAPH

ScientificWorld-NetAkhatAV
Karlsruhe 2021

*Monographic series «**European Science**»*

UDC 629.56.064.5+620.9

Author:
Budashko V.V.

Recommended for printing by
Decision of the Scientific Council of National University «Odessa Maritime Academy» Ministry of Education and Science of Ukraine
(protocol № 9 from 25.06.2020).

Reviewers:
Sagin S.V., D.Sc., professor, Lokarev V.I., D.Sc., professor,
Gerega O.M., D.Sc., professor, Nikulina O.L., Ph.D., profes-sor,
Bukaros A.U., Ph.D., associate professor

Prospektive globale wissenschaftliche Trends: Moderne technologien und forschungskonzepte für schiffskraftwerke kombinierter antriebsanlagen. Monografische Reihe «Europäische Wissenschaft». Buch 7. Teil 7. 2021.

Prospective global scientific trends: Modern technologies and concepts of researching for ship power plants of combined propulsion complexes. Monographic series «European Science». Book 7. Part 7. 2021.

The monograph presents a set of new ideas, methods and results of research related to improving the efficiency of ship power plants of combined propulsion complexes. The main motivation for writing the monograph is the current requests for practice and the presence of unresolved problems on the lines of propellers, power systems of engines, thrusters motors and power distribution systems.
The monograph is intended for scientific-pedagogical, engineering-technical workers, ship engineering and technical staff and higher education graduates who work and study in the specialty "River and maritime transport" of specializa-tions: "Operation and maintanance of ship electrical equipment and automation equipment" and "Management of ship technical systems and complexes»

ISBN 978-3-949059-43-8
DOI: 10.30890/2709-2313.2021-07-07

Published by:
ScientificWorld-NetAkhatAV
Lußstr. 13
76227 Karlsruhe, Germany
in conjunction with Institute «SE&E»
e-mail: orgcom@sworld.education
site: www.sworld.education

ÜBER DIE AUTOREN / ABOUT THE AUTHORS

Budashko Vitalii Vitaliiovych

Doctor of Technical Sciences, Professor

National University «Odessa Maritime Academy»

 ISBN 978-3-949059-43-8

Inhalt / *Content*

 ISBN 978-3-949059-43-8

 ISBN 978-3-949059-43-8

List of Conditional Abbreviations

Abbreviations	Explanation
AD	Actuator Disk
AGE	Alternative generating elements
AHTS	Anchor-handling Tug/Supply
AHV	Anchor Handling Vessel
AES	Alternative energy source
AM	Asynchronous motor
APSC	Azimuth propeller-steering column
ASK	Automatic Station Keeping
AVR	Automatic Voltage Regulator
Azipod®	Electric podded azimuth thruster produced by ABB Group
Azippul	Rolls-Royce plc azimuthing pulling propeller
BMS	Battery management system
BEM	Board electric motor
BMA	Battery module assemblies
BSPS	Battery storage power station
CAHV	Construction anchor handling vessel
CFD	Computational Fluid Dynamics
CFE	Complete factorial experiment
CLV	Cable laying vessel
Contaz®	Rolls-Royce plc azimuth thruster with contra-rotating propellers
CPICS	Classical PI control strategy with SOC's regulation
CPP	A controllable–pitch propeller or variable–pitch propeller is a type of propeller
CPP	Controllable Pitch Propeller
CRP	Contra-rotating propeller
CRP Azipod®	Propulsion Concept
CS	Control system
CSD	Cutter Suction Dredger
CSI	Current source inverter
CSg	Control signals
DC–link	Direct current link
DCM	Discrete-continuous models
DEPC	Diesel-electric propulsion complex
DEPV	Diesel-electric Passenger Vessel
DFA	Dynamic functional analogue
DMS	Data Management System
DP	Dynamic Positioning
DM	Decision maker
DSLCM	Digital Synchronizer and Load Control Module

ISBN 978-3-949059-43-8

Abbreviations	Explanation
DSS	Decision Support System
DTC	Direct Torque Control
EBR	Engine-boiler room
EC	Electronic computer
ECMS	Equivalent consumption minimization strategy
EDG	Emergency diesel generator
EDLC	Electric double-layer capacitor
EDCS	Electricity distribution control system
EEDI	Energy Efficience Design Index
EEMS	External energy maximization strategy with SOC's regulation
EEOI	Energy Efficiency Operational Index
ELTON	Elton is a global information technology, consulting and outsourcing company
EMDEC	Electro-Motive Diesel Engine Control system
EMS	Energy Management System
ESS	Energy Storage System
FACTS	Flexible Alternative Current Transmission Systems
Fanbeam®	DP reference system
FDSMCS	Frequency decoupling and state machine control strategy with SOC's regulation
FFE	Fractional factor experiment
FMEA	Failure modes and effects analysis
FPP	A fixed–pitch propeller is a type of propeller
FRV	Fisheries research vessel
Fr	Froude numbers
GNSS	Global Navigation Satellite System
HART	Highway Addressable Remote Transducer Protocol
HELMI	Helsinki Multi-category sea-ice model
HVSB	High voltage switchboard
ICE-HICE	Mermaid podded propulsors ICE and HICE produced by Rolls-Royce plc
IM	Inductional Motor
IMO	International Maritime Organization
ITTC	International Towing Tank Conference
K-POS	Single Dynamic Positioning system
LCI	Load Commutated Inverter
L-Drive	An L-drive is a type of azimuth thruster in which the pod–mounted propellers
LFC	Live Fish Carrier
LIB	Lithium-ion batteries
LNG	Liquefied natural gas
LNGCF	LNG Car Ferry

Abbreviations	Explanation
LSB	Large Scale Battery
LVSB	Low voltage switchboard
MLS	Method of the least squares
MSB	Main switchboard
MARPOL	International Convention for the Prevention of Pollution from Ships
MatLab/Simulink	Simulation and Model Based Design
Mermaid™	Electric podded azimuth thruster produced by Rolls-Royce plc
MGTV	Multipurpose Geotechnical & Soil Investigation Vessel
MOV	Multipurpose Offshore Vessel
MPM	Main propulsion motor
MRSV	Multipurpose field & ROV Support Vessel
MSDG	Medium speed diesel-generator
MSE	Medium speed engines
OCV	Offshore Construction Vessel
ORV	Oceanographic Research Vessel
OSCV	Offshore Subsea Construction Vessel
PCT	Product/Chemical Tankers
PEM	Propulsion electric motor
PLC	Programmable Logic Controller
PID	Proportional-integral-derivative
PMD	Person who makes a decision
PMR	Power Management Relay
PMS	Power Management System
PST	Purse Seiner/Pelagic Trawler
PT	Power Transducers
PUSH	Mermaid Push podded propulsors produced by Rolls-Royce plc
PVGS	Photovoltaic (PV) generation system
PWM	Pulse Width Modulation
RANS	Reynolds-averaged Navier-Stokes
Re	Reynolds numbers
RBU	Resistor back unit
ReFRESCO	Reliable&Fast Rans Equations (solver for) Ships, Cavitation (and) Offshore
Rolls-Royce	Rolls-Royce Marine Power Operations Limited, a subsidiary of Rolls-Royce plc
RO-RO	Roll-on/Roll-off ships
ROV	Remotely operated underwater vehicle
RPU	Redundant Power Management Processors Unit
SAPP	Ship automated power plants
SB	Storage batteries

Abbreviations	Explanation
SBV	Stand-by and Guard Vessels
SEEMP	Ship Energy Efficiency Management Plan
SEES	Ships electrical energy system
SFC	Specific fuel consumption
Ships CPC	Ships Combined Propulsion Complexes
SLDR	Stationary self-lifting tower
SSDR	Semi-submersible self-propelled drilling rigs
SLS	Seabed Logging Ship
SMCS	State machine control strategy
SOC	State-of-Charge
SP	Steering propeller
SPAR	Single Point mooring And Reservoir
SPS	Ship power systems
SPU	Signal Processing Unit
SRV	Seismic Research Vessel
SWATH	Small Waterplane Area Twin Hull
Swing-UP	Rolls-Royce plc swing-up/combi thrusters type
TD	Thruster drives
THD	Total harmonic distortion
THR	Thruster
TLP	Tension-leg platform
TML	Twin Marine Lifter
TT-PM	The Permanent magnet tunnel thruster produced by Rolls-Royce plc
UL	Rolls-Royce plc retractable azimuth thruster type
UPS	Uninterruptible Power Supply
VFD	Variable Frequency Drive
VSD	Variable Speed Drives
VSI	Voltage source inverter
VSP	Variable Speed Pumping
WSCC	Western System Coordinating Council
Z-Drive	Is a type of marine propulsion unit. Specifically, it is an azimuth thruster

 ISBN 978-3-949059-43-8

EINFÜHRUNG / *INTRODUCTION*

In recent decades the growth of capacity, energy-efficiency, increasing prices for fuel and materials, enhanced operational modes, which is associated, first of all, with the development of the offshore fleet, have substantially aggravated the problems of design, construction and operation of the optimal combined propulsion complexes (CPC) and ship power plants (SPP) that provide their power. Today, in the design of ships, along with traditional desire for optimization of dynamic characteristics, more attention is paid to the increase in reliability of the system “propulsion – shaft – hull – engine”, taking into account specificity of their work under conditions that are constantly changing. A great complexity of these tasks predetermines the main way to solve them – a physical model experiment and operational and technical economic calculations based on it. The results of such research, as a rule, are published in professional publications, technical materials of the sessions of the International Towing Tank Conference (ITTC) and scientific and technical societies, usually inaccessible when conducting research calculations. The publications that exist in this country mostly do not meet modern requirements as far as applied methods, designations and terminology are concerned [129] .

For example, the definition of the tow and established power and towing resistance of the designed ship with the accuracy enough for practice is possible only according to the results of the tests of geometrically similar models under conditions of partial dynamic similarity, which called into existence various methods of processing of obtained results and recalculation for the real conditions.

Mentioned methods have been used for decades and are improved in towing tanks of different countries, which greatly complicated comparison of the obtained intermediate results. A similar pattern is observed in the research of the interaction in the system housing – propulsion, SPP – CPC, etc. Since the beginning of the 20th century systematic tests of series models were conducted to judge the effect of certain parameters that characterize the shape of the underwater part of the hull, the resistance change or parameters, which would increase the SPP efficiency to change the dynamic CPC characteristics. In these cases, a group of models are designed and tested based on the basic models that differ by a regular change of separate elements (adopted in the shipbuilding practice) while other papramaters were unvariable. Before the 70-ies of the last century, the results of serial testing were processed by the accepted in a certain organization methods and were used to construct their own empirical methods of calculation of towing resistance of ships with bypasses of installed capacity of SPP, dynamic characteristics of CPC, etc., built according to the rules in this series or slightly different from them [19]. The accepted method of research by way of "changing the settings one by one” is inaccurate in principle because both the shape of the ship's surface, the dynamic CPC characteristics and SPP effectiveness are the functions of a large number of parameters dependent on each other in various degree, so changing one of them changes others automatically.

As for SPP for a particular type of CPC, then their choice is generally not optimized, neither from the point of view of the efficiency of CPC itself, nor from the point of view of improvement of the operational SPP modes that can be made only by integral methods [137].

With the advent of computer technology, it became possible to process primary results of serial and single model tests using methods of multifactor analysis and to present the results in the form of multi-dimensional surface described in the form of polynomials of the second-third degree of the shape of the hull, hydrodynamic criteria of similarity and SPP efficiency criteria. The work of determining coefficients of polynomials performed over the last decade allowed creating dozens of methods of forecasting of towing and installed capacity of vessels of various types, while the accuracy of these forecasts are substantially higher than traditional methods described, for example, in [66, 116].

With regard to a great complexity of the calculations by these methods, they are implemented mainly in the form of a thoroughly tested computer software that allows users not to challenge the accuracy of the calculations carried out with proper choice of appropriate methodological series considering all the restrictions, provided the initial information was entered correctly.

In recent years, the data of the coefficients of the interaction between propulsions and vessel’s hull, fuel and lubricants consumption efficiency, etc., have been processed similarly, which created the basis for creating methods of estimation of influence of structural factors on the propulsive characteristics of ships and efficiency of operational CPC modes.

Software products that were developed in recent years make it possible for an engineer to carry out not only determining the towing and installed capacity, optimal propulsion, but also selecting necessary SPP components. The usage of modern methods increases the culture of designing and gives a researcher an opportunity to learn how to work with professional software products in performing research, which elevates the level of scientific-research work to international standards.

CPC provides continuous abutments on the propulsions (rowing pods) in the movement of the ship to overcome resistance of water and inertia of the hull due to SPP energy providing for maximal efficiency. In the mode, for example, of a dynamic positioning (DP), SPP efficiency takes up not very important, but not the last place. As different types of main engines are used in the CPC for energy generation, however, SPP with diesel as a source of mechanical energy (over 80%) gained the widest popularity. Modern CPC can be distinguished by the following main SPP types by way of control of progressive movement:

– with heat or electric engines, as well as their combination operating with fixed propeller pitch (FPP) – with these settings the control of the ship’s progressive movement is reduced to changing the engine modes;

– with heat or electric engines, as well as their combination operating with controllable propeller pitch (CPP) – with these settings the control of the ship’s progressive movement is carried out by the change in operation modes of the main engines and the propeller screw step;

– with heat or electric engines, as well as their combination running on FPP of reverse rotation;

– with heat or electric engines operating on FPP or CPP and electric engines that run on FPP with azimuth degree of freedom;

– with electric engines operating on FPP with azimuth degree of freedom.

The attached SPP CPC graduation is not final, and has a lot of cross–combinations, so to define clearly the type of SPP on the stage of design, to complete the chosen CPC is quite difficult. Therefore the built ships after a certain period of time, sometimes very brief, need recompleting because of the impossibility of working in some operating modes, or due to the decrease in their efficiency.

Control of the ship’s progressive movement or keeping the vessel at the desired location is carried out by a combined method using power management systems (PMS) and various regulators and stabilization systems depending on the type of installed components that ensure the start, stop, reverse and frequency change in a propeller screw rotation.

The most suitable for solving various problems of designing SPP CPC are the decision support systems (DSS) that are interactive computer-aided systems (software packages), which are designed to aid and support various kinds of research or project activity when making decisions regarding the solution of design or research problems (structured or unstructured). The application of DSS should provide a comprehensive and unbiased analysis of the subject field, making decisions under conditions of continuous development and SPP CPC complexity [46, 127, 151]. The support of DSS computer tools in various approaches should provide the opportunity to design, select and directly compare alternative solutions.

There are many technologies, criteria and, as a result, the methods used in DSS for the design of SPP CPC. And the choice of one or another way with the final goal of obtaining the rankings of alternative solutions should rely on the initial data, knowledge and the results obtained in the process of decision-making.

On the other hand, the lack of qualified personnel in connection with their departing research institutions, increasing requirements to the intensity and quality of production, competition in the sector of design and construction of SPP CPC are additional factors that determine the relevance of the DSS. Methods and simulation tppls used in this area do not fully correspond to modern problems. At the same time, research in the field of artificial intelligence and expert systems, in particular, have shown the efficiency of application of intelligent DSS in such cases, based on expert knowledge. However, in the area of providing energy efficiency of designed SPP CPC, especially in the modes of dynamic positioning, development and industrial application of DSS remains unsolved.

Thus we can state that the development of DSS in the design and research of SPP CPC, with the introduction of its components in energy processes in order to increase the effectiveness of the decisions is a relevant issue, especially when choosing one or another CPC structure, setting up various regulators, contributing to the improvement of operational modes of a ship.

Tighter requirements on environmental protection, the future transition to the more expensive grade of fuel with low sulfur content, reducing harmful emissions, noise characteristics of vessels in certain areas of navigation are reduced, highlight certain areas of shipping and ports, which the work of marine diesel engines are excludes, causing the need alternative energy sources to find that meet the requirements of maritime and environmental legislation increased [1, 90, 144].

Exploring of alternative diesel and gas engines for SPP CPC, which focuses on heat recovery systems, exhaust, leading to significant savings in annual operating costs, but did not solve environmental problems. The use of heat recovery, which cover part of the electricity consumption, and devices to reduce harmful emissions into the atmosphere promising direction of building SPP CPC, but today is one that is losing relevance.

This fact forced to rethink critically the experience of using the ship electricity storage, solar and hydrogen energy sources, ensure the safety of their operation and improve their production technology and obtain approval of the leading classification societies [4, 43, 46, 154]. An important feature, such as advanced battery systems, is the possibility of charged from the selection of heat recovery of marine cranes modes braking of shaft generator and from renewable energy sources, such as solar and hydrogen elements. So today, the design and construction of modern SPP CPC, we have to reckon with this fact.

Operation the majority of ship power systems (SPS) as components of Energy

Management System (EMS), carried out the simultaneous operation of two or more diesel generators (DG), one disconnected and one emergency diesel generator (EDG). In normal mode, usually two workers DG loaded to 20÷45 % of its rated capacity, while load any of these generators to the level of 80 % of the rated power is switched to parallel work power network the third generator, the emergency diesel generator switched on for 30 seconds after the power failure. There are some SPS, where the normal mode of operation only one main DG and the other is on standby and ready for connection in parallel with the main generator. For most vehicles specified feature SPS operation due to security requirements, since the operation of the vessel necessarily required dynamic provision of electricity, which require Maritime Register of Ukraine, Russia, Japan and others [26, 78, 151].

The presence of such the significant (not less than 100 %) of the dynamic reserve of energy is the need of effective damping unpredictable peak loads in the SPS that can cause disabling and even major customers around the CPC. This requirement arises also because to run disconnected DG followed its synchronization with the ship's network is needed though short time (see Table 1), but this is the time during which the vessel blackouts can occur fatal accident [48, 63, 82]. Proposed that the technical component of the traditional approach to building SPS suitable for use in many types of vessels.

Table 1

The time from submission of the signal to automatically start receiving the time to load nominal value for the DG, prepared for rapid load acceptance.

Power, kW	Time, s
To 100	10
From 100 to 500 including	20
From 500 to 1000 including	30
More than 1000	40

The peak load on SPS may arise due to the nature of ship operation, the specific type of process performed by ships (dynamic positioning oil rigs, hooks and trawls al.). The inclusion of powerful contingent of consumers, especially the narrow ship passage and weather conditions.

It should be noted that the generator sets, automatic launch system hardware, between expectations are in “hot standby”. This means that at least made permanent shirts heated engine (for power liquid-cooled). Power station with automatic start–up can take the load after few seconds (see Table 1), after power failure in the external network, it does not need extra time to warm up the engine. Also, no need to make manual switch in the fuse board – all necessary switching performed automatically and during DG carried automatic maintenance frequency output voltage and power engine speed. For particularly difficult conditions, special SPS DG can work in this mode when the engine is running continuously, but the generator load is not connected or minimum. In this mode, fuel consumption, though not very big, but is also available. Remember that when switching to emergency mode, guaranteed job batteries. Therefore, during normal operation SPS necessary to provide and charging batteries, in which also consumes fuel [71].

It is also clear that the total fuel consumption for the two partially loaded DG significantly higher than in other DG working under similar stress. But for security fee shipping. However, in order to save fuel and at the expense of safety, often in the vessel's practice are cases of gross neglect safety rules when the ship is at one and the second included DG that, at best, is in the “hot standby”. So urgent task, which is aimed at solving the existing problems simultaneously improve navigation safety and efficiency of operation of ship electric power systems.

KAPITEL 1 / *CHAPTER 1*
DECISION SUPPORT SYSTEM'S CONCEPT FOR DESIGN OF COMBINED PROPULSION COMPLEXES

While solving the problems of a system approach in making decisions in research work at SPP CPC designing, a number of uncertainties [142] occurs, such as:

– the problem of the choice of adequate targets and goals in the study of energy processes in the power transfer in SPP CPC with many interdependent criteria;

– the uncertainty of the impact of unidentified state of the environment that are uncontrollable while affecting operational modes;

– the absence or lack of sufficient knowledge about the nature of the origin of the disturbing factors and their influence on energy processes;

– the ambiguity of expectations of the SPP CPC development with a prospect of upgrade;

– the vagueness of directions and strategies of the development of the SPP CPC components, or the so-called diversity of approaches from different manufacturers at the evaluation of parameters and SPP CPC characteristics;

– fuzzy and diverse information space in coverage and interpretation of research results of processes and objects, as well as the absence or unavailability of authoritative evidence on the reliability of existing information.

In addition to the mentioned above, worth noting are:

– uncertainty of structures and parameters of the models of studied SPP CPC;

– difficulties of system analysis and quality of evaluation of the models parameters;

– the absence or unavailability of statistics of the observed systems, which are a part of amount of the data with available omissions, pulse emissions, disturbing influences and errors (noise) in measurement;

– ambiguity of methodology research from various, sometimes unrecognized data processing techniques or solving problems;

– the impossibility of organizing all the possible options of SPP CPC set, which derives from all the types of uncertainties and is essentially caused by them.

In [78] the design and implementation of SPP CPC in the DP mode with the help of simulation of a hardware loop in the controller of regulation speed of a rowing engine was implemented, but the problem of dynamic load of mathematical models and practical realization of the work remained.

The problem of topology and design of power transformers is considered by the authors in [20], but evaluating the effectiveness, design and potential operation characteristics in SPP CPC use remained unsolved. Also unanswered is the question of comparison with other types of power transformers to establish whether a specific type of transformer has potential by its topology to improve the operational SPP and CPC characteristics.

Today there is not a unified strategy for DSS construction in the design and study of SPP CPC but the main principles have already been formed. Thus, DSS that is developed should be: at the level of the user – cooperative, which allows a designer or a researcher (a person who makes a decision – PMD) to modify, improve and complete the solutions offered by the system, sending these changes in the opposite direction for testing; at the technical level – a local system, which may be installed on one computer, due to the necessity of PMD mobility; at the conceptual level – model-driven (DSS) and provide access to the study of mathematical models (statistical, DMI–models, optimizing, imitation); depending on the types of data that DSS will work with is strategic, based on the analysis of large volumes of various information from alternative sources [106].

In [149] the issue of modern DSS SPP CPC were developed in the direction of definition of requirements for the general structure of the system of design and PMD training but simultaneous modelling of SPP and CPC structures and their implementation led the authors to difficulties with DSS practical usage.

In particular, in [67] this issue was partially solved in terms of the application of new generation of DSS to provide a wider range of possible solutions and reduce costs, but the choice of performance criteria and their approach to the dynamics of physical models did not produce desired results.

And finally in [144] the authors tackled the issue of optimization of dynamic characteristics and initiated the design of control strategy of SPP CPC, but the study of models of nonlinear controllers and simulation models SPP CPC in Matlab/Simulink was performed without adapting the software to other DSS. The problem of matching and dispersal of parameters that are explored in the case of deviation of SPP capacity was also not considered.

The most important aim of the created DSS is to improve the most rational options of SPP CPC set, taking into account the influence of various factors with the possibility of deep consideration of the data, knowingly converted for convenient use in the decision-making process and to work out the rules for making decisions, which on the basis of the data, accordingly consolidated, will enable a PMD to justify making a decision, using improving factors when upgrading SPP CPC and increase their efficiency. DSS should be based on multi–dimensional principles of representation and analysis of the data [117].

Goals and purpose of DSS can be defined as follows:

– creating the conditions for understanding the problem to be solved that is problem structuring, generating the main and auxiliary tasks, identifying existing advantages and disadvantages, formation of criteria;

– asisstance in solving problems, that is a possibility of generating and selecting different types of models and methods, collection, processing, and preparation of data, calculation, design, delivery and adjustment of the results;

– assistance in conducting regressive analyses, etc., an explanation of the selected ways of decision;

– ability to analyze similar and alternative solutions and availability of results [156]. A cognitive process is mainly used for the functional structuring of DSS at the design of the SPP CPC (Table 1.1) [102].

Table 1.2.
Process of cognitive design of DSS

Scientific tools	Scientific problems (stages)	Scientific results, methods of implementation
Processing of the results of the analysis of periodicals	Substantiation of the relevance of DSS design at SPP CPC projection	Recommendations for further DSS improvement
Protocol of initial data collection and the problem decomposition	Statement and decomposition of problems for DSS	Table of necessary requirements to DSS
The list of existing and possible limitations during making decisions in the design process	Definition and the list of limitations that can arise in the decision-making process	The list of specific problems for a certain task
Necessary DSS functions at SPP CPC design	Definition of functional capacities of DSS	The list of available DSS functions
The list of methods and existing rules for the decision selection	The design of methodology and ways of making decisions	Functional structuring
Systems of automatical projection, algorithmic languages, visualization programs	Typification of dialogue windows, DSS control principles and usage of necessary software medium	Block-schemes of algorithm, verbal algorithms of work, engineering methods
Simulation software products	Developing software medium and its approbation, protocol of approbation	Algorithms, block-schemes, graph-schemes, programs, identification *m*-files

Logical steps in creating the DSS will be detailing of the stages in the design of SPP CPC, functional structuring of its architecture and the substantiation of the process of implementation. Using the deepest data analysis, complex of engineering knowledge, etc., linked to the relevant tasks of the DSS designed computing procedures, then connect functions and procedures, and, eventually, to realize all the stages of the programming of all the functional system modules, including the design and programming of interface between PMD and DSS.

Therefore, making the conclusion, we can state that from the point of view of modern requirements, the present situation requires creation of DSS at the design and

ISBN 978-3-949059-43-8

study of SPP CPC, which will give an opportunity: to manage data; to have sufficinet information about the decision-making that hides original assumptions, quantitative and qualitative evaluation; to control calculation and modelling, including flexibility and the capacity to generate DMI-models of SPP and CPC; to have an opportunity to improve the made decision, as well as SPP CPC efficiency, typification and design of the software elements, testing simulation models, comparing the results of running tests and laboratory studies with theoretical works.

1.1. The setting and decomposition of the problems considering boundary conditions and criteria

The aim of the studies is the synthesis of a decision-making support system in the design of ship power plants (SPP) combined propulsive complexes (CPC), required for the improvement of occurring energy processes in SPP CPC.

To achieve this aim the following tasks were set:

– statement and decomposition of the problems regarding DSS in the design and study of energy processes in SPP CPC with determining operational and combinatorial constraints and substantiation of the functionality of DSS in the design and study of SPP CPC;

– ensuring functional compliance of modeling steps of the processes of power transfer, composition of operating modes and criteria for the evaluation of SPP CPC effectiveness, information correction, automation of analysis with the ability of logical conclusions, support of presentation of the results and improvement of the quality of the made decision;

– development of methods and ways of improvement of the made decision from the point of view of SPP CPC efficiency, development of the elements of the software medium and their testing in the simulation modeling in real conditions during running tests and laboratory studies.

When performing decomposition of the main goal, situational purpose was set, that is the study and identification of mathematical models of operational modes of

SPP CPC in existing software complexes, other DSS in order to detect drawbacks and existing assumptions and criteria, on the basis of which the present dynamics of problem solving were formed by way of consistent interactive analysis of situational data, when the formed problem or its absence is considered as a result of solving or complicating (refinement) of the previous one.

Achieving situational purposes, the criteria of selection decisions were formed and combined based on a set of both SPP CPC and operating modes in which they operate. In some cases herewith the problems of knowledge occurred, in which the clarity of strategy and selection rules of alternative criterion were lost. Based on the fact that most of the criteria had numeric character, the necessity arose to perform complex calculations in the process of merging various, sometimes, at first glance, incompatible criteria that led to dividing them into determining and defining.

For example, integral criteria of effectiveness allow making a decision at variation of any significant parameters of SPP CPC that would provide the increase of energy efficiency, and therefore if the adequacy of mathematical models is provided, the criteria can be considered objective and applicable for assessing the efficiency of the power transmission in this SPP CPC with any types of engines on the shafts lines. In the stationary movement of the ship with CPC, the resistance to the body that moves, is proportional to the traction, but in general case the resistance to movement R and the traction T should not necessarily be equal and opposite, and the ship in this case may accelerate and react to other external forces. In this case, the coefficients, that take into account the reduction of the traction, can be identified using the replacement of the resistance by the relevant efforts for all three planes of the movement (surge, sway, yaw) [12, 26]:

$$C_{F_{Lh}} = \frac{F_L(V,n) - T_{ux}(V,n) - F_L(V,0)}{T_u(V,n)}, \qquad (1.1)$$

$$C_{F_{Th}} = \frac{F_T(V,n) - T_{uy}(V,n) - F_T(V,0)}{T_u(V,n)}, \qquad (1.2)$$

$$C_{N_h} = \frac{N(V,n) - T_{uy}(V,n)X_p - T_{ux}(V,n)Y_p - N(V,0)}{T_{uy}(V,n)X_p - T_{ux}(V,n)Y_p}, \quad (1.3)$$

where: $F_L(V,n)$, $F_T(V,n)$ i $N(V,n)$ are the general forces (H), acting on the vessel in the absence of other external disturbances at the flow velocity v (m/s) and the relevant number of FPP turns n (r/min); $F_L(V,0)$, $F_T(V,0)$ and $N(V,0)$ are the relevant forces (H) in the case of fixed propeller screw (for example, flow); $T_{uy}(V,n)$ and $T_{ux}(V,n)$ are the tractions (H) by the relevant axis relative to the plane of the movement.

Based on the formulas for calculating the capacity for any engine, directly transmitted to the propeller screw, we find the expression for the calculation of the coefficients of efficiency on the shaft line under the influence of forces that act in a certain plane, where these forces have the advantage. For example, for the induction motor [18]:

$$P_{AD} = \eta_{TRM} \times 2\pi \times Q_{AD} \times n, \quad (1.4)$$

where η_{TRM} is the transmission efficiency, Q_{AD} is the torque on the shaft IM, [Nm], and considering the expressions (1.1), (1.2), (1.3), (1.4), for the plane surge, we receive:

$$H_{pr\_surge} = \eta_{TRM} \frac{\int_0^L (\left|(Q_{AD\_F_L}(l) - Q_{AD\_ux}(l))n\right| - Q_{AD\_F_L})dl}{\int_0^L (\left|(Q_{AD\_F_L}(l) - Q_{AD\_ux}(l))n\right| - Q_{AD\_F_L})dl + \sum_{j=1}^{n}\int_0^L \Delta Q_j(l)\,dl}, \quad (1.5)$$

Similarly we receive expressions for calculating IM efficiency for the other two planes:

$$H_{pr\_sway} = \eta_{TRM} \frac{\int_0^T (\left|(Q_{\mathrm{AD}\_F_T}(t) - Q_{\mathrm{AD}\_uy}(t))n\right| - Q_{\mathrm{AD}\_F_T})dt}{\int_0^T (\left|(Q_{\mathrm{AD}\_F_T}(t) - Q_{\mathrm{AD}\_uy}(t))n\right| - Q_{\mathrm{AD}\_F_T})dt + \sum_{j=1}^{n}\int_0^T \Delta Q_j(t)\,dt}, \quad (1.6)$$

$$H_{pr\_yaw} = \eta_{TRM}\left(\frac{\oiint\limits_{XY}\left|(Q_{AD\_N}(t) - Q_{AD\_uy}(t)) - Q_{AD\_ux}(t)n\right|}{\oiint\limits_{XY}\left|(Q_{AD\_N}(t) - Q_{AD\_uy}(t)) - Q_{AD\_ux}(t)n\right| + \sum\limits_{X=Y}^{X}\oiint\limits_{XY}\Delta Q_{XY}(t)dt} - \right.$$

$$-\frac{Q_{AD\_T}dt}{\oiint\limits_{XY}\left|(Q_{AD\_N}(t) - Q_{AD\_uy}(t)) - Q_{AD\_ux}(t)n\right| + \sum\limits_{X=Y}^{X}\oiint\limits_{XY}\Delta Q_{XY}(t)dt} -$$

$$\left.-\frac{Q_{AD\_N}dt}{\oiint\limits_{XY}\left|(Q_{AD\_N}(t) - Q_{AD\_uy}(t)) - Q_{AD\_ux}(t)n\right| + \sum\limits_{X=Y}^{X}\oiint\limits_{XY}\Delta Q_{XY}(t)dt}\right). \tag{1.7}$$

On the other hand, for promising concepts of SPP CPC with hybrid ship installations with contra-rotating pods (CRP), working in the mode DP where gravitational forces dominate and Froude law of similarity applies, to receive which the equality of numbers for the model and nature is needed, i.e. $F_{rM} = F_{rN}$, criteria of similarity are necessary to express through the values characteristic for a given mode.

When water flows around the ship hull in a characteristic linear size, they choose the length of the ship between perpendiculars on the waterline and forward in the direction of the flow, and as the characteristic speed – the speed of the flow attack. The Froude similarity criteria for our case is obtained from the general criterion of hydrodynamic similarities of Newton, substituting the force of gravity to this equation, $G = mg$:

$$\frac{v_S^2}{g_S \cdot l_S} = \frac{v_M^2}{g_M \cdot l_M}, \tag{1.8}$$

where v is the running flow speed, m/sec; g is the force of gravity, [m/sec^2]; l is the length, m, accordingly ($_S$) of the ship and ($_M$) of the model.

It is necessary to receive main parameters of all emerging flows from the equation (1.8) taking into account the extent of the similarities. We calculate in which dependencies speed, thrusts and torques for the model and the ship are in the case of modeling by the Froude’s law. Records of cavitation occurrence is carried out by maintaining the criteria of similarity F_r, R_e and equality of numbers E_u for the model and the ship.

In fact, the resistance of a ship consists of both the resistance to friction and wave resistance, caused by waves, that forms on the free surface of the water under the force of gravity. However, later PMD will meet the next complication: if the size of the model is 100 times less than the size of the actual ship, then by the equation, to keep the Froude's number F_r unchanged, one needs to take the speed of v by 10 times less than the speed of the actual vessel, and in order to keep the Reynolds number R_e also unchanged, the coefficient of density ρ must be taken by 1000 times lower than the density water coefficient. But it is impossible to do in practice, that is why the test should be conducted in the same medium, to use the same water and the friction resistance should be determined by the special research formulas, and residual resistance, i.e. wave resistance, has to be recalculated according to the law of similarity for ideal incompressible liquid that is under the influence of gravity force.

Resistance to the movement of the vessel depends on the shape of the hull. Studying the influence of the hull's shape, it is necessary to expand the class of motions and examine the movement of the family of hulls, formed by some law depending on geometrical parameters, the change of which characterizes the studied geometric features of the contours. It is very important in practice to highlight the following options from infinite variety of parameters that characterize geometric properties of the shape of hulls, such options that are very important for the residual resistance.

Experimental research in the field of hydrodynamic simulations show [50] that the main parameters for all sorts of geometrically dissimilar contours of the hulls of usual types of ships that determine the coefficient of resistance is a Froude's number and a coefficient of sharpness. Instead of a Froude's number by length, it is possible to take Froude's number by the volume water tonnage Δ:

$$F_{r\Delta} = \frac{v}{\sqrt{g\sqrt[3]{\Delta}}} = F_r\sqrt{\lambda}, \qquad (1.9)$$

where λ is the coefficient of longitudinal hull sharpness (Fig. 1.1) [5].

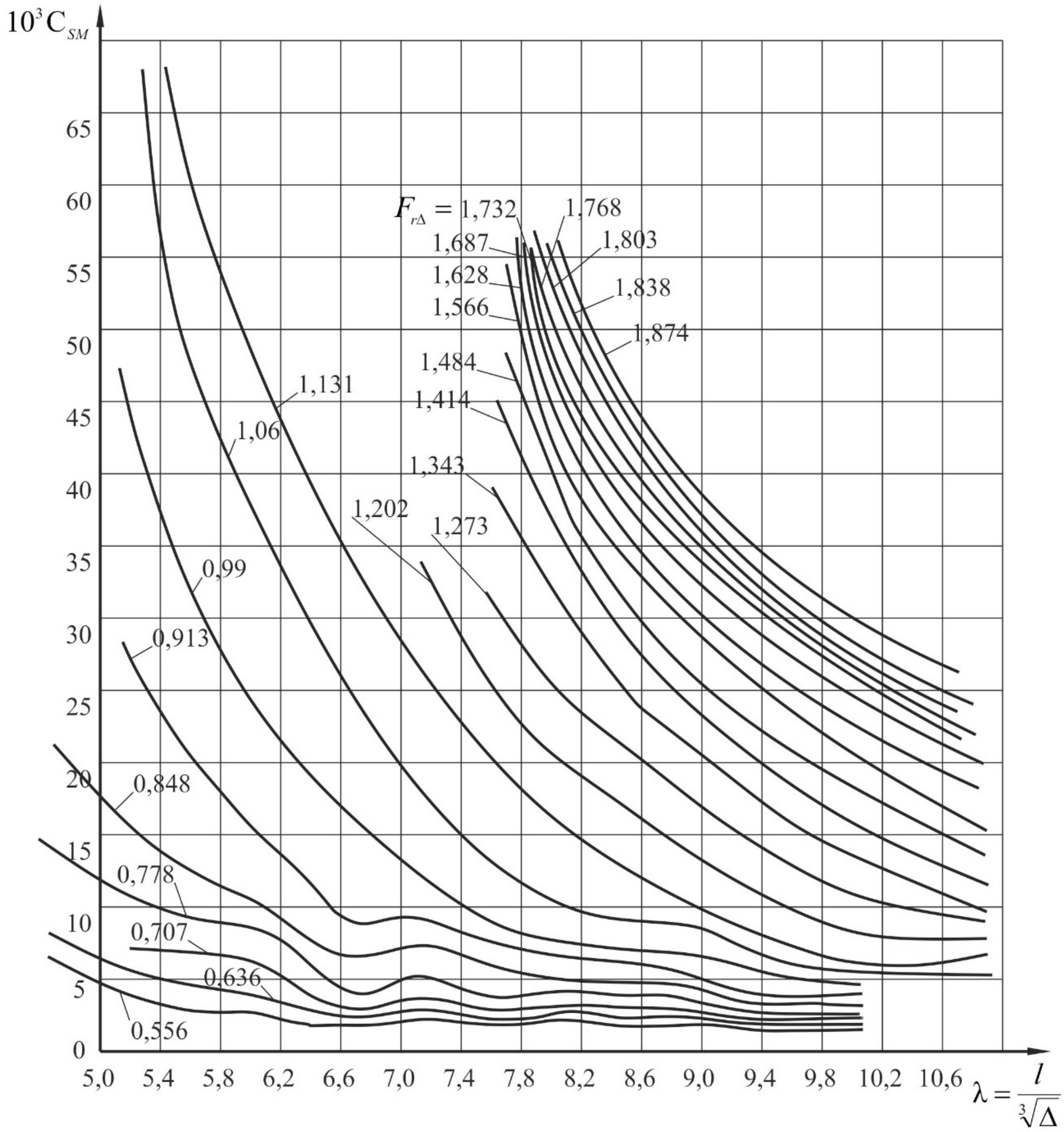

Fig. 1.1. Experimental dependencies of the ratio of resistance on a ton of water tonnage in the function of coefficient of longitudinal hull sharpness and Froude's number.

If for the real conditions and the conditions of the test of a model the acceleration of gravity $g_S \neq g_M$, then from (1.8) we receive:

$$\frac{v_S}{v_M} = \sqrt{\frac{l_S \cdot \rho_1}{l_M \cdot \rho_2}} = \sqrt{\lambda_{SM}}, \qquad (1.10)$$

where ρ_1, ρ_2 are the densities of the media, [kg/m^3], that is the speed of a model water flow should be decreased by $\sqrt{\lambda_{SM}}$ under condition of compliance with Archimedes criterion for a real and a simulation medium.

So, the abutments of the model and the ship pods should be in dependence:

$$\frac{T_S}{T_M} = \frac{n_S \cdot v_S}{n_M \cdot v_M} = \lambda_{SM}^2 \sqrt{\lambda_{SM}} = \lambda_{SM}^{2,5}, \qquad (1.11)$$

where n_S, n_M are the frequencies of pod rotation, r/min; that is, if an abutment of the ship pod T_S, then at the smaller by l_{SM} times model, the abutment of the pod should be lower by $\lambda_{SM}^{2,5}$ times under condition of compliance with geometrical criteria of similarity.

The ratio of torques on the pods’ shafts, and therefore the capacity consumed by the drive engines, considering the correlation (1.8), (1.9), (1.10), (1.11), i.e.

$$\frac{Q_S}{Q_M} = \frac{D_S \cdot v_S}{D_M \cdot v_M} = \lambda_{SM}^{2,5} \sqrt{\lambda_{SM}} = \lambda_{SM}^3, \qquad (1.12)$$

where D_S, D_M are the diameters of pods, [m].

Similarly, through the linear scale one can deduce the values of the scale factors for other parameters.

Based on (1.8), (1.9), (1.10), (1.11) and (1.12), a system of equations that describes the electromagnetic and electromechanical processes in the thruster’s propulsion’s motor and takes the nonlinear nature of the processes in the motors is of the form (1.13), where m – is the number of phases; p – is the number of pairs of poles; U_{1s}, U_{2s} – are components of the stator voltage; Ψ_{1s}, Ψ_{2s}, Ψ_{1r}, Ψ_{2r} – are components of the stator and rotor coupling; I_{1s}, I_{2s}, I_{1r}, I_{2r} – are the constituent currents of the stator and rotor; R_s, R_r, – are the active stator and rotor supports, M_d – is the induction motor torque:

 ISBN 978-3-949059-43-8

$$\begin{cases} U_{1s} = \lambda_{SM}^{2,5}\left(\dfrac{d\Psi_{1s}}{dt} - \Psi_{2s}\omega_k\right) + \dfrac{R_s I_{1s}}{\lambda_{SM}^{2,5}} \\ U_{2s} = \lambda_{SM}^{2,5}\left(\dfrac{d\Psi_{2s}}{dt} - \Psi_{1s}\omega_k\right) + \dfrac{R_s I_{2s}}{\lambda_{SM}^{2,5}} \\ 0 = \lambda_{SM}^{2,5}\left(\dfrac{d\Psi_{1r}}{dt} - (\omega_k - p\omega)\Psi_{2r}\right) + \dfrac{R_r I_{1r}}{\lambda_{SM}^{2,5}} \\ 0 = \lambda_{SM}^{2,5}\left(\dfrac{d\Psi_{2r}}{dt} + (\omega_k - p\omega)\Psi_{1r}\right) + \dfrac{R_r I_{2r}}{\lambda_{SM}^{2,5}} \\ M_d = \lambda_{SM}^{2,5}\left(\dfrac{mpK_r}{2}\left|\Psi_r \times I_s\right|\right)\left|\left(1 - \lambda_{SM}^{2,5}\right)\right| \end{cases}; \tag{1.13}$$

1.2. Support of functional compliance of the processes with the design problems

Technologies of the design of SPP CPC require the following functions to support decision-making by PMD:

1. Modeling of the processes of power tranfer. With the help of existing models of real processes, or in the process of creating the new ones, it is necessary to have a

possibility to apply, based on the regressive approach of the subsystem of forecasting their further process and subsystem of synthesis of optimal and adaptive solutions that are based on current data, or observations [25, 69].

2. Composition of operating modes and criteria for evaluation of effectiveness of SPP CPC. With the help of mathematical methods of finding tools or rules to combine automatically those properties that characterize different operating modes of SPP CPC for removal of cognitive limitations of PMD.

3. Information correction. Reading, saving and processing of information, data, results using integrated computer technologies, due to which the capacities of PMD in decision–making and data processing expand significantly.

4. Analysis automation with the ability of logical conclusions using artificial intelligence methods and numerical methods that will allow improving the quality of

the results and reduce the time for solving similar problems in future.

5. Support for the presentation of the results with the implementation of the functions of access to databases and knowledge bases of other DSS, using the tools of computer graphics and language processing as well.

6. Improvement of the quality of decision making in order to eliminate errors in systematics, stemming from the quantitative analysis and heuristic calculation, by the introduction of statistical and other methods of correction results with functional design and selection of specific procedures of calculation and analysis for the implementation of each function of the DSS within the existing group of experts who design it, to eliminate external and cognitive restrictions that affect making a decision.

For example, it is possible to display the reservation index of the ship technical means and equipment by a function of coefficients of reservation, i.e. the ratio of the number of installed objects onboard to the required number of these objects, according to the rules of the Register. Each element of the SPP CPC requires the analysis of evaluation from PMD considering requirements depending on the type of the ship, operating modes and the area of navigation.

The rules of registers concerning the number of main engines are not set. The number of main engines is defined according to the technical specifications for a ship design and, consequently, by a ship owner, so it is advisable to exclude the main engines from a number of factors of the reservation indicator.

The number of main sources of electric power is chosen based on the results of the calculation of the power of the ship's electric plant. In addition, each self–propelled vessel must be provided with not less than two main sources of energy (two generators driven by own source of energy; a generator driven by own source of energy and a shaft generator; a generator driven by own source of energy and a storage battery). But the power from the main sources of electricity must ensure that in the case of failure of a single source, the remaining ones provide the electricity supply to critical devices in the running, maneuvering and emergency modes. That is, the operation of a ship in the mode, for example, of staying put, based on these terms, is not specified. In reality, there are four or more major sources of electrical energy on the ships of the class DP. Besides, the rules of the registers imply the need for the installation of emergency sources of electric energy beyond the Engine-boiler room (EBR).

The performed analyses [82] considering various types of vessels justify PMD decision and the requirements of the registers and European requirements for the number of sources of electrical energy are different, that is why the sources of electrical energy is expedient to include into a number of factors that affect the indicator of the reservation.

According to the registers rules, the vessels of DP class must be provided with one main fire–extinguishing pump and the pump as a part of the ballast system, except for the vessels longer than 100 m, where there must be two main fire pumps and two pumps that are able to work with the ballast system. Besides, oil and drilling vessels longer than 100 m must be provided with at least one emergency fire pump.

And in this case the performed tests [103] considering vessels of different types allow PMD to make a decision that the requirements of the registers and European requirements for the number of fire and ballast pumps are not identical, so the fire and ballast pumps are also included in the number of factors that affect the indicator of the reservation.

Finally, regarding the drainage pumps, each vessel must be provided with not less than two drainage pumps, one of the pumps must be ballast, included into the drainage and ballast systems and working in a DP mode. The second pump may be ballast, sanitary, of general usage, with water or steam ejector and not included in the process of calculating SPP power. In other words, it may be stated that according to the analysis [14], the requirements of the registers and European prescriptions concerning the number of drainage pumps for certain types of ships, operatingg in a DP mode, do not exist at present at all, so the drainage pumps are also included in the number of factors that affect the indicator of the reservation. From the point of view of supporting the compliance functionality, there is no sense to apply quality criteria, which might be imposed on PMD, because in our conditions they are not relevant, in particular as a result of poor competitiveness of domestic scientific decisions in the domestic market. The next step is likely to be highlighting primary (initial) processes in the design and study of SPP CPC, that is the description of physical processes with which the PMD will be required to interact.

1.3. Technology of DSS SPP CPC implementation including intellectual, behavioral anf cognitive restrictions of PMD

SPP CPC design from the point of view of considering all functional restrictions within a single operating mode presents a cognitive (in synergy with the engineering) research process of making a decision that includes gradual improvement of the data that come from the study of a particular operational mode of a vessel and SPP operation as well, together with modern technological operational DSS base. One of the steps was considered in previous subchapters. Modern requirements in the support of decision making were found in advance at the stage of substantiation of requirements to functional compliance with the processes of the design problems.

Requirements to support decision making in the design of SPP CPC determine functional restrictions which PMD who uses DSS should bypass. The next stage specifies specific needs in support of the decision that integrate with developed and implemented methods within the DSS based on the characteristics of the operational mode without the use of supporting scientific research tools, i.e. only on the basis of available data and the results of other works within existing DSS. In this way a conversion of a specific request in support of making a decision into a functional project of SPP CPC is achieved. The main technological tool that is needed at this stage is more or less precise substantiation and application of technological DSS base, which in its turn, is based on functional qualities and defined criteria explored above. A mathematical apparatus used in the design and implementation of SPP CPC within DSS is shown in Fig. 1.2 [28, 32]. According to the given classification (Fig. 1.2), simulation of real processes, control systems or SPP CPC control within DSS that is created should be carried out with an ability of choice of alternative decisions, a diverse toolkit for information retrieval, methods of automated analysis and applications for the presentation of results, implementation and improvement of the quality of made decisions. Each model should be built taking into account modern techniques with the ability to implement the support functions. The use of one or another method within each subsystem of DSS should be based on defined and proven criteria and dimensions that determine the level of their adequacy in a particular configuration of SPP CPC.

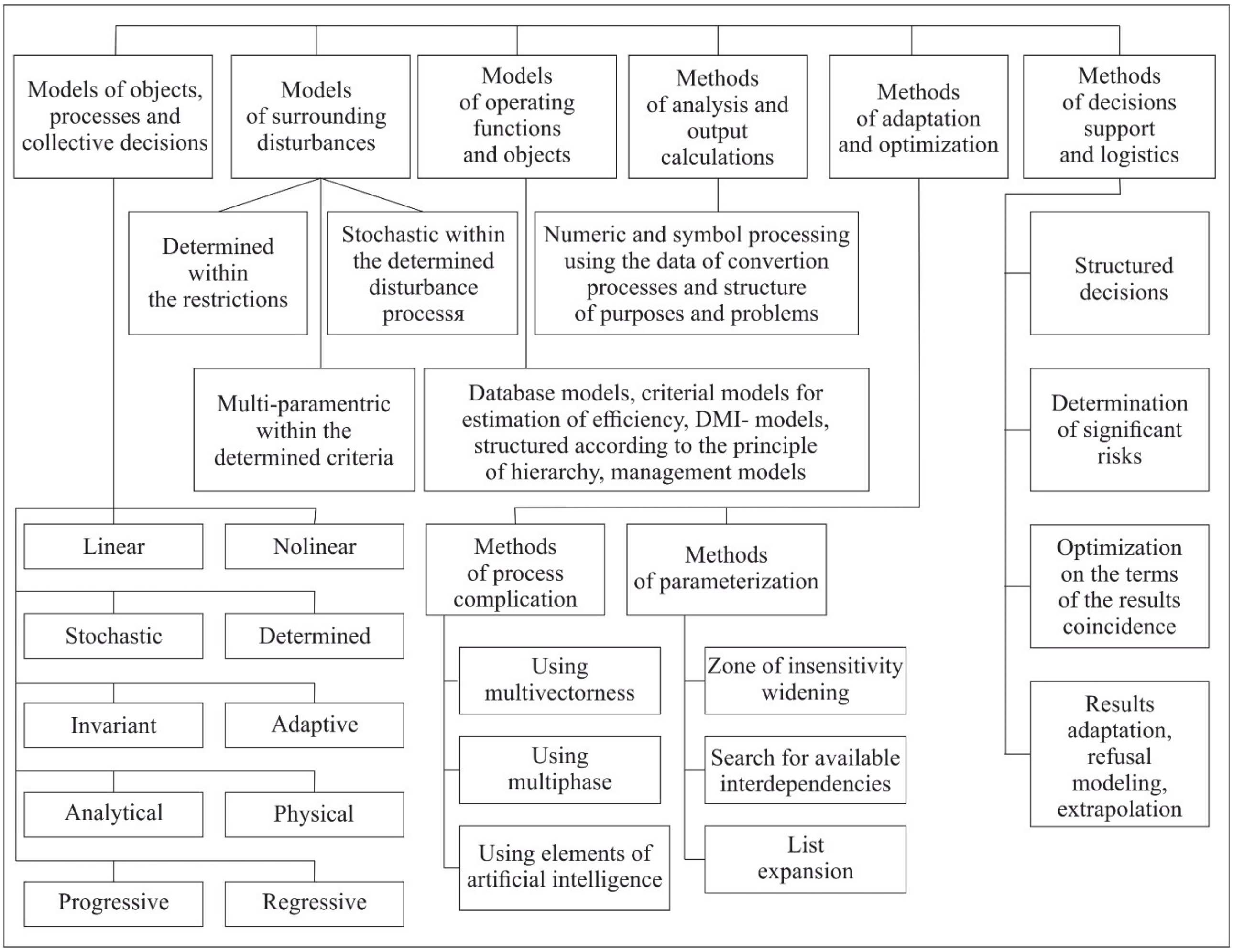

Fig. 1.2. Classification of mathematical apparatus of DSS in the design and research of SPP CPC.

It follows that the classification presented in Fig. 1.2 not only directs the PMD in the appropriate direction, but also specifies the issues of making a decision that is considered when choosing a method of SPP CPC study for its further implementation within DSS. Certainly, the classification presented in Fig. 1.2 does not provide comprehensive support for the design of SPP CPC but determines the list of available modern technologies for its implementation and methodology of research within the defined methods and specifies tools for comparative analysis. For the implementation of deep comprehensive analysis of the made decision regarding the projected SPP CPC it should have a set of recognized rules, based on reliable data from decision making in this area, which were collected by decomposition of specific operational problems which would have enabled to implement the developed SPP CPC at the lowest risks for operational inefficiency.

1.4. Computer simulation of the processes in SPP CPC as a DSS component

Fig. 1.3 presents a computer model for setting thrusters configuration on the example of CPC of the ship of the type Supply Vessel

According to the method described in [58, 139], a computer model was created of identification of the parameters (Fig. 1.3) of the ship, the type Supply Vessel, the *m-file* text of which is given in the item 5 of the research results.

For the step ratio $p_{Di}=H_P/D_i$ the values of thrusts and torques are determined by the force vector τ_T, that is described by the equation

$$\tau_T = T_{matrix} K_{Tmatrix} u_T, \tag{1.14}$$

where T_{matrix} is the matrix of thrusters configuration (1.17), (1.18), (1.19), (1.20); $K_{Tmatrix}$ is the matrix of coefficients of pods thrusts (1.16); u_T is the vector of removable thrusters thrusts applied to the ship (1.15).

The thrusts applied to the ship in a dynamic positioning mode, due to thrusters work, are determined by the force (thrusts) vector (1.14):

$$u_T = \Big[|p_{D1} - p_{D10}|(p_{D1} - p_{D10}), |p_{D2} - p_{D20}|(p_{D2} - p_{D20}), \ldots,$$
$$|p_{Dk_{TR}} - p_{Dk_{TR}0}|(p_{Dk_{TR}} - p_{Dk_{TR}0}) \Big]^{T_{matrix}}, \tag{1.15}$$

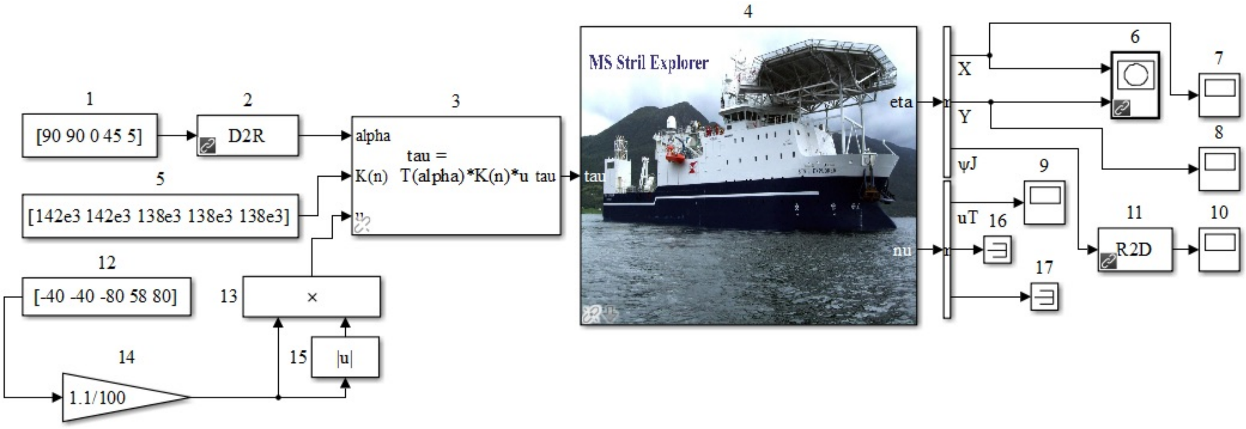

Fig. 1.3. Computer simulation in MatLab/Simulink of the configuration of thrusters for the ship of the type Supply Vessel: 1 is setting the angle of the location of azimuth devices relative to diametral plane of the vessel, α_A, degree; 2 is the block of conversion degrees to radians; 3 is the CPC model; 4 is the model of identification of the ship parameters; 5 is setting the coefficient of the pod’s abutment, K_T; 6 is the plotter of XY-coordinates; 7 – 10 are the oscilloscope fixing: XY are the coordinates of the ship, m; value of weighted force that applied to the ship u_T, $H\times10^6$; an angle of the ship yaw ψ_J, grade, accordingly; 11 is the block of conversion of radians to degrees; 12 is setting the step ratio of pods H_P, –100 % ÷ +100 %; 13 is the function of multiplying; 14 is the block of calculation of step ratio $p_D=H_P/D$, where D is the pod diameter, m; 15 is the block of calculation of absolute value; 16, 17 are the devices of absorbtion of outgoing signals of the ship which are not tracked.

where p_{Di0} ($i0 = 1\ldots k_{TR}$) is the step ratio of separate thrusters pod, maximal quanity of which is determined by the number $k_{TR.}$

Coefficients of pods thrusts are determined by the diagonal matrix:

$$K_{Tmatrix} = \begin{pmatrix} K_{T1}(n_1) & 0 & \ldots & 0 \\ 0 & K_{T2}(n_2) & \ldots & 0 \\ \ldots & \ldots & \ldots & \ldots \\ 0 & 0 & \ldots & K_{Tr}(n_r) \end{pmatrix}, \qquad (1.16)$$

where n_i ($i = 1\ldots r$) is the frequency of i thrusters pod rotation, r/min.

 ISBN 978-3-949059-43-8

Forces of thrusters thrusts determined by the vector , are divided into the lengthwise, crosscut and angle (yaw) components by the matrix of thrusters configuration.

For example, on the ship of the type Supply Vessel four azimuth thrusters are installed (two main and two auxiliary, located between the diametral plane and the fore part to stand out from the hull), which can be rotated at any angle α_A relative to a diametral plane of the vessel and one fore tunnel thrusters. Based on this, we have the following configuration of the thrusts applied to the ship: $u_{T1,2}$ are the thrusts of main azimuth thrusters; $u_{T3,4}$ are the thrusts of auxiliary thrusters; u_{T5} is the thrust of the bow thrusters. Then the matrix of thrusters configuration will have the following look:

$$T_{matrix(0)} = \begin{pmatrix} cos\alpha_{A1} & cos\alpha_{A2} & cos\alpha_{A3} & cos\alpha_{A4} & 0 \\ sin\alpha_{A1} & sin\alpha_{A2} & sin\alpha_{A3} & sin\alpha_{A4} & 1 \\ l_{T1}sin\alpha_{A1} & l_{T2}sin\alpha_{A2} & l_{T3}sin\alpha_{A3} & l_{T4}sin\alpha_{A4} & l_{T5} \end{pmatrix}. \qquad (1.17)$$

where l_{Ti} (i = 1…5) is the strength or distance from the place of thrust application of this thrusters to the projection of the force vector τ_T to the plane of the ship's movement.

Moreover, it should be taken into account that positive movement of the ship in the x-direction is a forward movement, in the y-direction is the movement to the right, in z-direction (yaw) – movement back, i.e. contrary to a minute arrow.

For this vessel, as a test of the effectiveness of the existing installation of SPP CPC within the developed DSS, in addition, besides the main, three possible thrusters configurations were tested which are determined by the respective matrices $T_{matrix(1)}$ (1.18); $T_{matrix(2)}$ (1.19); $T_{matrix(3)}$ (1.20).

Configuration (1): two main classical FPP of the left and right sides in the stern of the ship; one azimuth thrusters that stands out of the hull in the fore of the vessel, which can be rotated at any angle α_A relative to diametral plane of the vessel, and one fore tunnel thrusters ($u_{T1,2}$ – thrusts of the main classical FPP; u_{T3} – thrust of auxiliary azimuth thrusters, u_{T4} – thrust of the bow thrusters:

 ISBN 978-3-949059-43-8

$$T_{matrix(1)} = \begin{pmatrix} 1 & 1 & cos\alpha_{A3} & 0 \\ 0 & 0 & sin\alpha_{A3} & 1 \\ l_{T1} & -l_{T2} & l_{T3}sin\alpha_{A3} & l_{T4} \end{pmatrix}. \quad (1.18)$$

Configuration (2): two main classical FPP of the left and right sides in the stern of the ship; two stern tunnel thrusters; one azimuth thrusters that stands out of the hull in the fore part of the vessel, which can be rotated at any angle α_A relative to diametral plane of the vessel; one fore tunnel thrusters ($u_{T1,2}$ – thrusts of the main classical FPP; $u_{T3,4}$ – thrusts of the stern tunnel thrusters; u_{T5} – thrust of the auxiliary azimuth thrusters, u_{T6} – thrust of the bow thrusters):

$$T_{matrix(2)} = \begin{pmatrix} 1 & 1 & 0 & 0 & 0 & cos\alpha_{A6} \\ 0 & 0 & 1 & 1 & 1 & sin\alpha_{A6} \\ l_{T1} & -l_{T2} & -l_{T3} & -l_{T4} & l_{T5} & l_{T6}sin\alpha_{A6} \end{pmatrix}. \quad (1.19)$$

Configuration (3): three azimuth thrusters (two main left and right sides and one auxiliary, located between the diametral plane and the fore part that stands out of the hull) which can be rotated at any angle α_A relative to to diametral plane; one stern tunnel thrusters; one bow tunnel thruster ($u_{T1,2}$ – thrusts of the main azimuth thrusters; u_{T3} – thruster of the stern thrusters; u_{T4} – thrust of auxiliary azimuth thruster, u_{T5} – thruster of the bow tunnel thruster):

$$T_{matrix(3)} = \begin{pmatrix} cos\alpha_{A1} & cos\alpha_{A2} & 0 & cos\alpha_{A4} & 0 \\ sin\alpha_{A1} & sin\alpha_{A2} & 1 & sin\alpha_{A4} & 1 \\ l_{T1}sin\alpha_{A1} & l_{T2}sin\alpha_{A2} & -l_{T3} & l_{T4}sin\alpha_{A4} & l_{T5} \end{pmatrix}. \quad (1.20)$$

Simulation was performed in the computer laboratory MatLab/Simulink.

Changing the parameters of matrices of thrusters configurations, mutual location of azimuth devices and their position relative to the diametral plane of the vessel, as well as the step ratio of the pods, we obtained the diagrams of XY-coordinates and the angle of the ship yaw.

1.5. Results of the study of a ship behavior at different parameters of propulsion complex

We developed *m*-files of indefication parameters for different types of vessels for their further implementation into a spatial model of SPP with the aim of obtaining optimal *XY*-movement from the point of view of minimization.

m-file of indefication parameters of the ship, type Supply Vessel, which is in a dynamic positioning mode, is given below:

function xdot = *supply_vessel*(*x*,*Ttau*)

% function *xdot* = *supply_vessel*(*x*,*Ttau*) returns speed derivative by time *xdot* = *E***Ttau* + *F***x* state vector: *x* = [*u v r x y psi*]' for Supply Vessel of the length *L* = 76 m.

% Model of Zero speed (DP)

% *u* = speed of longitudinal movement, [m/sec]

% *v* = speed of lateral movement, [m/sec]

% *r* = yaw speed, [rad/sec]

% *x* = position in *x*-direction, [m]

% *y* = position in *y*-direction, [m]

% *psi* = yaw angle, [rad]

% *Ttau* = [*X*, *Y*, *N*]' thrust/point vector

% Parameters of the ship

Ls = 76,4; % length of the ship, [m]

gs = 9,8; % acceleration of the force of gravity, [m/c^2]

tonn = 3657*e*3; % weight, [kg]

Tm = *diag*([1 1 1 1 *Ls*]);

Tminv = *diag*([1 1 1 1 1/*Ls*]);

% Matrices of models

Kmod = [1,1323 0 0 0 0

0 0 0 1,9101 –0,0751

0 0 0 –0,0567 0,1312];

ISBN 978-3-949059-43-8

```
Cmod = [0,0401 0 0 0 0
 0 0 0 0,1211 –0,0131
 0 0 0 –0,0038 0,0312];
 % Checking the initial and original sizes
 if (length(x) ~= 6),error('x-vector must have a dimension 6 !');end
 if (length(Ttau) ~= 3),error('u-vector must have a dimension 3 !');end
 K = (tonn*Tminv^2)*(Tm*Kmod*Tminv);
 C = (tonn*Tminv^2)*(sqrt(gs/Ls)*Tm*Cmod*Tminv);
 F = [ zeros(3,3) eye(3)
 zeros(3,3) –inv(K)*C ];
 E = [zeros(3,3); inv(K) ];
 % Definition of derivative status
 xdot = E*Ttau + F*x;
```

Fig. 1.4, Fig. 1.5, accordingly, present the diagrams of the changes of *XY*-coordinates and an angle of yaw ψJ in the function of time during 200 sec from the vessel of the type *Supply Vessel* at different configurations of thrusters, mutual position of the axes of the main and auxiliary pods relative to diametral plane; values and coefficients of step ratios and thrusts coefficients.

By analysing the diagrams in Fig. 1.4, Fig. 1.5, it is possible to make a conclusion that the optimal from the point of view of the ship moving in the *XY*-plane is the configuration (2) thrusters, which is determined by the matrix (1.19).

 ISBN 978-3-949059-43-8

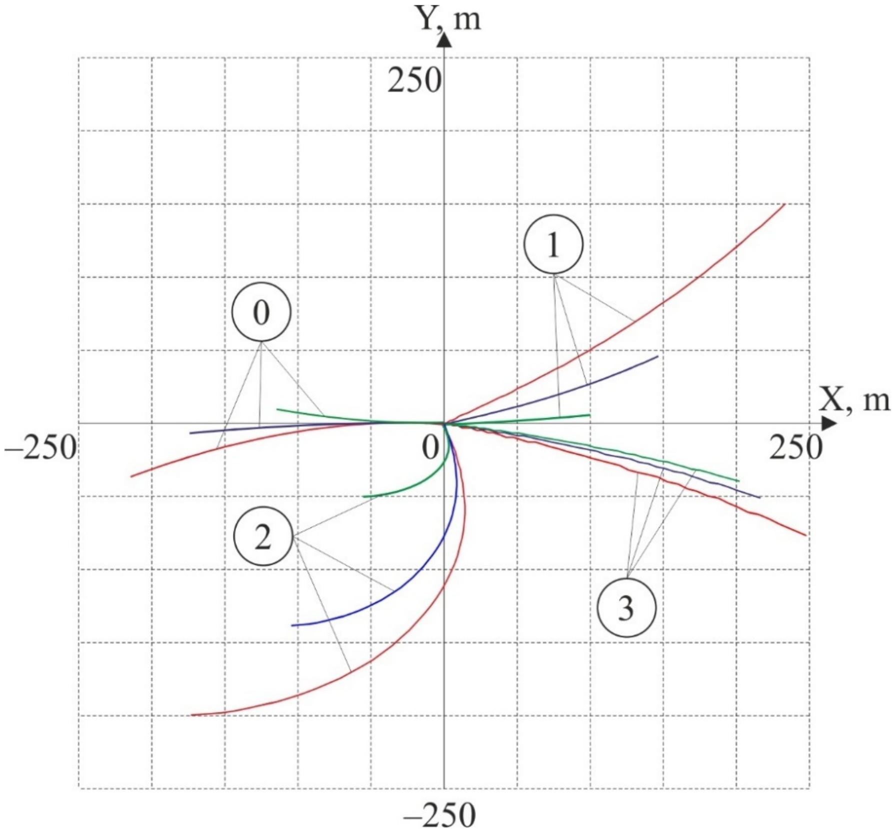

Fig. 1.4. Changing coordinates of the vessel, type Supply Vessel, length 76 m, at different thrusters configuration: 0÷3 – numbers of appropriate configurations (1.17), (1.18), (1.19), (1.20): ——— – mutial perpendicular axis location of the main and auxiliary pods with unchanged values of step ratios and thrusts coefficients; ——— – mutial perpendicular axis location of the main and auxiliary pods with regulated values of step ratios and thrusts coefficients; ——— – optimal location of the axes of the main and auxiliary pods with values of step ratios and thrusts coefficients that meet the criterion of minimum change in the *XY*–coordinates of the ship.

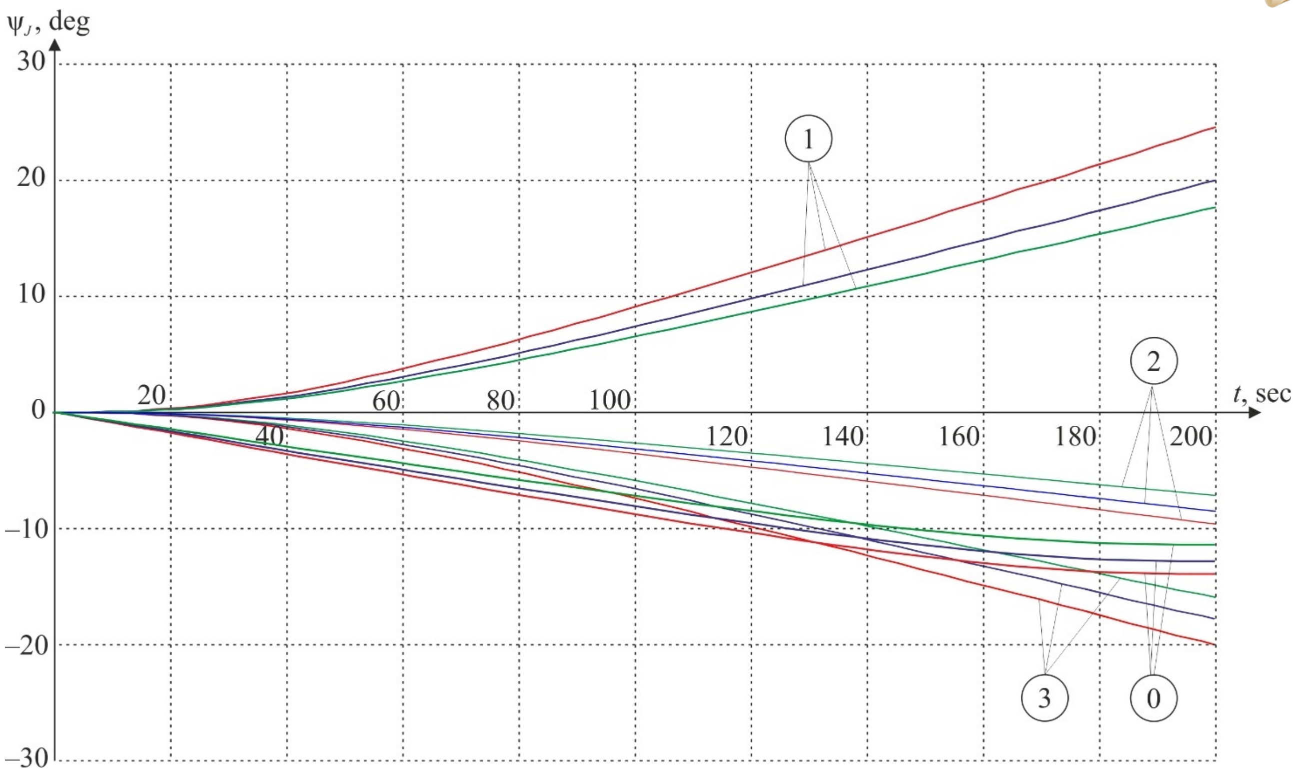

Fig. 1.5. Diagrams of dependency of yaw angle of the ship, type Supply Vessel, length 76 m, in the time function: 0÷3 – numbers of appropriate configurations (1.17), (1.18), (1.19), (1.20): —— – mutial perpendicular axis location of the main and auxiliary pods with unchanged values of step ratios and thrusts coefficients; —— – mutial perpendicular axis location of the main and auxiliary pods with regulated values of step ratios and thrusts coefficients; —— – the optimal location of the axes of the main and auxiliary pods with values of step ratios and thrusts coefficients that meet the criterion of minimum change in the *XY*-coordinates of the ship.

1.6. Design proposals with the possibility of multiple design changes

The proposed approach to the design of DSS SPP CPC allows predicting total quantity and the type of thrusters and pods, power system of electric motors with possibility of multiple design changes even in the presence of minimal data of the existing project and can be used practically for any type of the ship. DSS also allows upgrading various types of vessels for their adaptation to dynamic positioning mode and gives the possibility to synthesize recommendations for thrusters developers, controllers and power systems for ships, working in a mode of dynamic positioning. This is achieved due to the fact that the proposed approach is based on the cognitive (in sinergy with engineering) research process of decision-making that includes gradual improvement of the data that comes from the study of a particular operational mode of the vessel operation. Its characteristic difference is the application of the method of reciprocal implementation of the characteristic spatial vectors of energy processes in SPP and hydrodynamic processes in CPC. Due exactly to this difference, the developed DSS does not require the application of the criteria of similarity and allows multiple analysis of the SPP and CPC structure at minimal original data.

The ability to change thrusters settings, in particular: the values of the step ratios, thrusts coefficients and the location of the axes of the main and auxiliary pods, for a specific ship greatly expanded the use of the approach from the point of view of acceleration of convergence of synthesized DMI-models of ships, and for a given speed of pod rotation, traction, torque and stepper attitude allowed establishing that the coefficient of traction (thrust) increases with the change of mutual thrusters location relative to one another and the diametral plane of the ship. It was also found that the correlation of thrusts coefficient is better correlated to the coefficients of power than to the step coefficients of pod, which gives the reason to think about the opportunity to improve the energy efficiency of SPP CPC in operational modes and include obtained results to the database for other similar DSS to provide developers and researchers with the necessary information for creating new concepts of SPP CPC or to modify existing ones.

Experimental research for applied configurations of thrusters is planned to be performed on a physical model of CPC [34, 35, 36, 108].

KAPITEL 2 / *CHAPTER 2*
MODERNIZATION OF HYBRID ELECTRIC-POWER SYSTEM FOR COMBINED PROPULSION COMPLEXES

2.1. The basic principle of the proposed modifications

The basic principle of the proposed modifications SPS concluded that in many cases the practical operation of vessels, the work of the main DG may be at loadings up to 80 % of the nominal value and the dynamic reserve of energy will be an additional source of static electricity [32].

This approach is known, but its technical implementation to date has been virtually impossible because of the lack of highly static energy, which is significantly higher than for its technical and operational characteristics classic batteries and variety of peak load and supply of electricity are provides. It to use SPS extra battery, which is made up of Electric double–layer capacitor (EDLC) is proposed [80, 162]. There EDLC decision on the use of road transport and electric networks in some special purpose.

The device EDLC – static electrochemical, organic or inorganic electrolyte "covers" which is the electric double layer at the interface between the electrodes and the electrolyte. Functionally EDLC is the hybrid capacitor and chemical current sources and refers to the storage of electricity molecular types. Capacitors symmetrical double electric layer capacitors are different from the classical fact that the spatial separation of opposite charges, which create working electric field using polarized microscopic layer at the boundary surface between two media distribution.

Modern bipolar EDLC is sealed and the technological design based on activated carbon in bound water and an alkaline electrolyte and has a very high energy and powerful performance. Properties EDLC allow its effective use as charging pulse current source of operating voltage charge to several hundred volts and the number of charge-discharge cycles at least the million. Modern EDLC with high stored energy density and little leakage of charge. There EDLC batteries with specific energy stored more than 50 J/cm^3 (two orders of magnitude more specific energy of any classical capacitors) and specific average power of 10 [kW/kg]. The latter figure is much higher than traditional power density of acidic or alkaline batteries and allows EDLC as damper sources in SPS.

For example, the company ELTON advanced technology of electrochemical capacitors "asymmetric" type developed and patented. This design negative electrode made of activated carbon materials (polarized electrode), and the positive electrode is unpolarized (faradic). The positive electrode made of nickel hydroxide as the electrolyte used an aqueous solution of alkali used in alkaline batteries and therefore has low price. This asymmetrical design has created and mass produces electrochemical capacitors with high specific capacity and energy, low internal resistance, weakly dependent on the temperature during operation and storage. Moreover, such EDLC does not require maintenance, have a wide operating temperature range, store performance at extremely low (–50°C) temperatures, able to withstand without fracture and failure of heightened tension.

Super capacitors based elements 400÷500 series has weight of 200 [kg], 5 [MJ] energy and peak power of 200 [kW]. For comparison – 4 acid battery weight in 4×50 = 200 [kg], with power consumption of 20 [MJ], but peak power less than 40 [kW]. It is clear that acid batteries require special care, ventilation, etc., and is notable given greater peak power, which is necessary in the short-term loads in SPS.

One of the important issues – is the official definition of the place of use of ship power systems using EDLC. But it is not technical but organizational type and entirely dependent on experience (which is not) operation, the recognition of SPS Maritime Register, classification authorities, engineering companies.

One of the issues – is the cost of such complex Ships electrical energy system (SEES). It should be noted that the prices of electrochemical capacitor EDLC is constantly declining. Thus, in 1996, 1 F EDLC capacity cost \$0,75 at the total cost of almost \$284 for the 1,0 [kJ] of energy. Already in 2006, 1 F containers had to spend \$0,01 and the 1 kJ of energy – \$2,85. In 2014, 1 [F] EDLC capacity needed to spend only \$0,0045 and 1 [kJ] of energy around \$1,0. Obviously, in 18 years the share price fell by nearly 1 [kJ] 300 times, and 1 [F] capacity – 150 times, and this decline continue.

At first glance, these amounts are small, but you must remember that:

a) only few EDLC battery with sufficient and necessary additional electronic devices;

b) the voltage of one element EDLC small – about 2 [V];

c) the sequential IM same identical elements in the EDLC battery, the total battery capacity C_Σ, F, is given by:

$$C_\Sigma = 1/C_1 + 1/C_2 + 1/C_3 + ... + 1/C_n, \quad (2.21)$$

where $C_1 = C_2 = C_3 = ... = C_n$ – the capacity of individual elements of the same type EDLC, i.e. the total battery capacity of successive elements is significantly reduced;

d) work with EDLC as storage (buffer) capacitor power energy systems, they quickly lose up to half of the output voltage of the initial voltage, giving up to 75 % of stored energy.

That is, the necessary energy E, J, calculated from the known formula:

$$E = C_\Sigma \cdot U^2/2, \quad (2.22)$$

where U – working battery voltage must agree to four times higher.

Estimated value of energy:

$E = 2 \cdot C_\Sigma \cdot U^2$, (2.23)leading to the substantial increase in capacity have required batteries.

Depending on the time of $\Delta\tau$ in buffered mode and the required power (easier – and of current consumption I) is easy to calculate the required number of individual elements EDLC as follows:

$$C_\Sigma = (I \cdot \Delta\tau)/U. \quad (2.24)$$

As result of previous calculations can be seen that only cost EDLC battery can be tens of thousands of dollars.Therefore, from the practical point of view, as an emergency (buffer) source used by SEES EDLC is quite possible, but needs to address for number of research tasks. First, the task EDLC battery, which could have the capacity of several thousand farad.

 ISBN 978-3-949059-43-8

Secondly, this task is the connection of individual elements in the EDLC battery with ensuring uniform distribution of voltage between the battery cells. Thirdly, it is to stabilize the output DC voltage under load EDLC. There is an extremely important task of converting direct current into three-phase alternating current with the ability to instantly sync with SPS.

In addition, the need to solve the problem of theoretical and economic assessment of the possibility of using EDLC in SPS, selecting parameters and calculating its basic characteristics, identifying variables EDLC, simulation of static energy and SPS with EDLC in static and dynamic modes, the theoretical justification and constructive solutions of electronic charge and voltage stabilization formation algorithms included in EDLC SPS, technological and structural study of the entire system and for number of others.

Thus, SEES offered must include the following elements:

– an electronic device providing charge (charging) battery EDLC of the ship's electrical network or from the shore network;

– EDLC battery, comprising individual elements (banks) EDLC [80] voltage distribution system, its own monitoring system, control and protection;

– an electronic device stabilize the output voltage based on the pulse converters, such chopper-booster types (power factor correction, booster converter) ;

– controlled static generator (converter “voltage direct current – voltage three-phase”), for example – based on industrial frequency converters with ensuring its constant readiness to sync with SPS;

– microcontroller systems management connecting the parallel operation of EDLC SPS using speed sensors voltage, frequency, current, if necessary – the temperature of the executive contactors;

– alarm system monitoring, diagnosis, protection of the system.

This material was fairly new solutions for the SPS and requires further research.

 ISBN 978-3-949059-43-8

2.2. Conceptualization of design for hybrid electric propulsion complexes

Stringent requirements of environmental protection, the future transition to a more expensive fuel grades with low sulfur content, reduction of harmful emissions, reduction of the noise characteristics of vessels in certain areas of navigation, allocation of certain areas of shipping and ports, which excludes the work of ship diesel engines cause the need to find alternative energy sources that meet the increased requirements of maritime and environmental legislation [90].

Research of alternative diesel and gas engines for SPP of CPC, which focuses on the system of exhaust heat recovery, led to significant savings in annual operating costs, but did not solve environmental problems.

The use of heat recovery systems, which compensate a part of the electricity consumption, and devices to reduce harmful emissions into the atmosphere is promising direction of SPP CPC building, but today is one that is losing relevance.

This fact forced to critically rethink an experience of use of accumulator, solar and hydrogen energy sources for the purposes of ship electricity, ensure the safety of their operation and improve their production technology and obtain an approval of the leading Classification societies [1]. An important feature of advanced battery systems is their ability to be charged from the heat extraction systems, recovery from the ship cranes during the braking modes, for shaft generators and renewable energy sources such as solar and hydrogen elements. So today, it is necessary takes into account this fact for design and building of modern SPP CPC.

The object of research is a hybrid Diesel-electric propulsion complex (DEPC). The variant of its block diagram is shown in Fig. 2.1. Other decisions related to the integration improvement of providing hybrid DEPCs and SPPs are given in [13, 44, 76, 77, 96, 98, 145].

 ISBN 978-3-949059-43-8

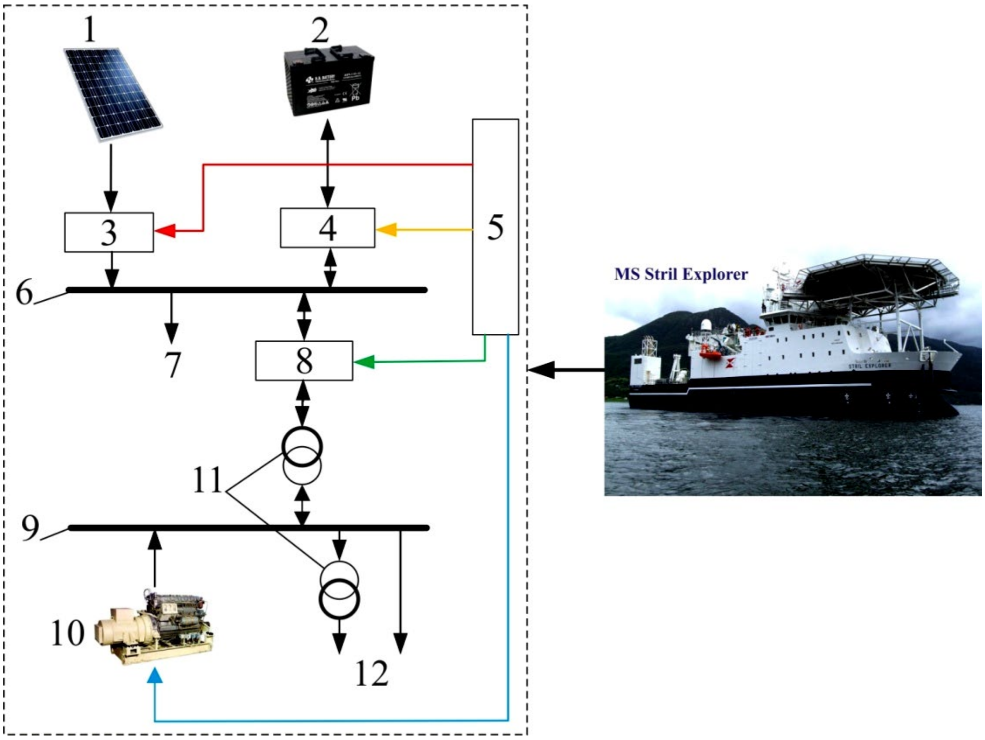

Fig. 2.6. Block functional diagram of combined (hybrid) propulsion complex: 1 – Photovoltaic (PV) generation system (PVGS); 2 – Energy Storage System (ESS); 3, 4 – DC/DC converter; 5 – control system (CS) of hybrid diesel-electric propulsion complex (DEPC); 6 – DC-link; 7 – to DC consumers – such as Resistor back unit (RBU); 8 – Voltage source inverter (VSI) or Current source inverter (CSI), 9 – High voltage switchboard (HVSB); 10 – ships power plant (SPP) with Medium speed engines (MSE); 11 – voltage transformers, 12 – to AC consumers, in particular, Board electric motor (BEM), Thruster (THR) and Low voltage switchboard (LVSB)

Hybrid DEPC is shown in Fig. 2.1. It is based on the electric power complex of offshore ship, operating in dynamic positioning mode and consists of the following elements:

KC200GT-based PVGS modules with nominal power of 10 kW (maximum 11,5 kW) and output voltage of 30-60 V.

Lithium-ion batteries (LIB)-based ESS with system voltage of 48 V and a capacity of 4,000 A×h.

Power DC/DC converters of PSC18 type with nominal power of 40 kW, nominal current and voltage on the DC-link of 200 A and 450 B, respectively, are designed to enhance and regulate the voltage in the PVGS output and limits the input current and to discharge and recharge of ESS batteries. These converters are bidirectional and allow to regulate the output voltage of the current limit and are used to redistribute of the power between the components of hybrid DEPC.

VSI power modules of PWS-F (PWS-W) type with the maximum total capacity of 300 kW, a voltage of 450 VDC, 440 VAC and 50 Hz, which allow to adjust the power factor depending on MSE load.

RBU with capacity of 5 kW intended to avoid overload of PVGS and ESS.

Power three-phase transformers with respective power are used for coordination between HVSB and LVSB of hybrid DEPC.

CS of hybrid DEPC distributes the power between PVGS, ESS and SPP according to the chosen strategy of power consumption:

− State machine control strategy (SMCS).

− Classical PI Control Strategy with State-of-Charge (SOC's) Regulation.

− Frequency decoupling and state machine control strategy with SOC's regulation).

− Equivalent consumption minimization strategy.

− External energy maximization strategy with SOC's regulation.

The main purpose of PVGS as Alternative energy source (AES) in the given hybrid DEPC is SPP activation after power failure and power support of the ship operation in the maneuvering modes, one of which is the mode of dynamic positioning (DP). Depending on the chosen strategy of power consumption, CS regulates the power of each energy source according to the specified output voltage and maximum current of PVGS, ESS and converters (DC/DC converters, VSI).

The disadvantages of given block diagram of hybrid DEPC are:

− Inconsistency of MSE parameters with other components, leading to uneven magnetic flux regulation and voltage amplitudes, which causes further increase additional ripple voltage in the outputs of converters and an emergence of equalization currents during synchronous operation.

− High level of harmonics in the current of energy consumers.

− Reduced reliability, efficiency, increased size and weight that occur through the use of high power elements and sets of equipment for them.

− Inability to balancing of three-phase power supply system with uneven loading phases.

The aim of design – to improve the control system of power processes in ships hybrid DEPCs performed with the use of AESs.

To achieve this aim it is necessary to perform the following tasks:

1. Prove the possible ways of improving the structural and block diagrams of hybrid DEPCs developed using AESs taking into account modern results in their development.

2. Identify the most important factors of operating modes for hybrid DEPCs with AESs affecting the quality of consumed electricity in terms of non-determined load.

3. Make comparative mathematical modeling of energy processes in hybrid DEPCs with AESs in different operating modes for their parameterization and determination of boundary conditions for trouble-free operation.

Renewable energy sources, especially solar, wind power are more penetrating in the shipbuilding sector. However, long-term storage of energy is a universal problem in securing support for renewable sources on the basis of electricity with the high availability depending on the season. One way of overcoming this problem is to use hydrogen as an energy vector by which solar and wind energy is transformed, stored and restored at the right time. Hydrogen that derived from water using electrolysis is stored as a compressed gas or metal hydride, and then used from the repository to generate electricity in a fuel cell.

In [52] the authors identified the benefits and problems of various types of fuel cells. Possible opportunities for emission limitation of different types of fuel cells, real devices for merchant ships and warships and projects of the potential innovation and research needs for area of fuel cells are considered.

Detailed analysis of the effectiveness of the ship DC hybrid power system was made in [154]. Also, the authors have developed algorithms for optimizing control systems by the criterion of minimum fuel consumption under different load conditions and achieved 15 % fuel savings of optimally adjusted energy storage in the investigated DC system.

Serious environmental pollution and low efficiency of traditional SPPs, which power is predetermined only by the number of diesel generators, can be reduced by proper integration of renewable energy sources. In recent years, photovoltaic elements have been used in SPP in order to reduce greenhouse gas emissions, increase energy efficiency and strengthen SPP stability. However, the use of too many solar panels can increase the cost of capital investment and make the power system is unstable due to the uncertainty associated with solar energy [147]. In addition, a wide range of studies [4, 8, 43, 155, 160, 162] found that the use of energy storage systems (ESS) is one of the most effective solutions for quality, reliability and power of SPP and contributes to greater development of efficient energy distribution. Some studies [17, 42] showed that the optimal control of ESS in SPP with multiple bus structures that are built using Flexible Alternative Current Transmission Systems (FACTS) and are the Western System Coordinating Council (WSCC) with the uneven impedance distribution will reduce the peak load, the cost of power supply renovation and compensate the negative impact on the environment.

Hybrid SPP concepts were investigated in the works [48, 85]. Lithium-ion batteries in the integration of diesel SPP for CPC modes with loading and unloading operations was investigated in [48]. To maximize a fuel economy, ESSs were used in the rebuilding of bulker for electric propulsion in [85]. In other works, various strategies that solve problems to maximize battery life and reduce fuel consumption were developed [95, 107].

Many studies of hybrid power systems were published in [32, 95, 119, 122, 159]. In particular, the economic and environmental benefits of hybrid DEPC using SPP and storage of energy in ESS were analyzed in [32]. The optimal distribution scheme for independent DEPC with integrated wind turbine (WT) and SPP in conditions of their uncertainty in terms of minimizing energy costs and maximum reliability was proposed in [95, 119]. Best practices for improving DEPC and SPP

CPC were also proposed in [122, 159].

It should be noted that hybrid CPCs in the modern periodic sources not take a first place [73, 128]. In [73], SPPs is used in SPPs for reducing fuel costs. Evaluation of stability and economic analysis of hybrid DEPCs was considered in [91]. The authors of [120] proposed a preliminary analysis of measures to reduce harmful emissions into the environment in the port area. In addition, an integration of significant PVGS and ESS power in SPP in reducing CO_2 emissions is a challenge. Electricity production by PVGS in SPP depends on its position in the ocean. Previous studies [54, 91, 120, 128, 150] of PVGS use take into account the calendar conditions, local time, time zone, operating coordinates in terms of power providing for moving ship. In [128] proposed the optimal choice of hybrid DEPC sizes taking into account different slope angles of PVGS panels. Corrections to the output settings of PVGS panels depending on their location on the ship were obtained because of the strong dependence of parameters and quality of PVGS from climatic conditions such as time of year, local time, operating coordinates. The authors [120] proposed an optimal fundamental structure of hybrid DEPC with wind turbines and various environmental conditions with the methods of gradual PVGS adaptation to the operating conditions. Detailed models of hybrid DEPC with PVGS were created and optimized in [54, 91] that taking into account the actual environmental conditions and uncertain operating situation. An evaluation method of global illumination depending on the PVGS slope was developed in [150], which took into account the temperature and distribution of the solar spectrum.

Analysis of Fig. 2.1 allow to conclude that the control of hybrid DEPC is a very complex process that requires taking into account a large number of factors of energy and operating components. For example, such component of hybrid DEPC as PVGS is based on the use of lithium-ion batteries (LIB) [111].

Fig. 2.2 shows a functional block diagram of hybrid DEPC with PVGS fragmentation.

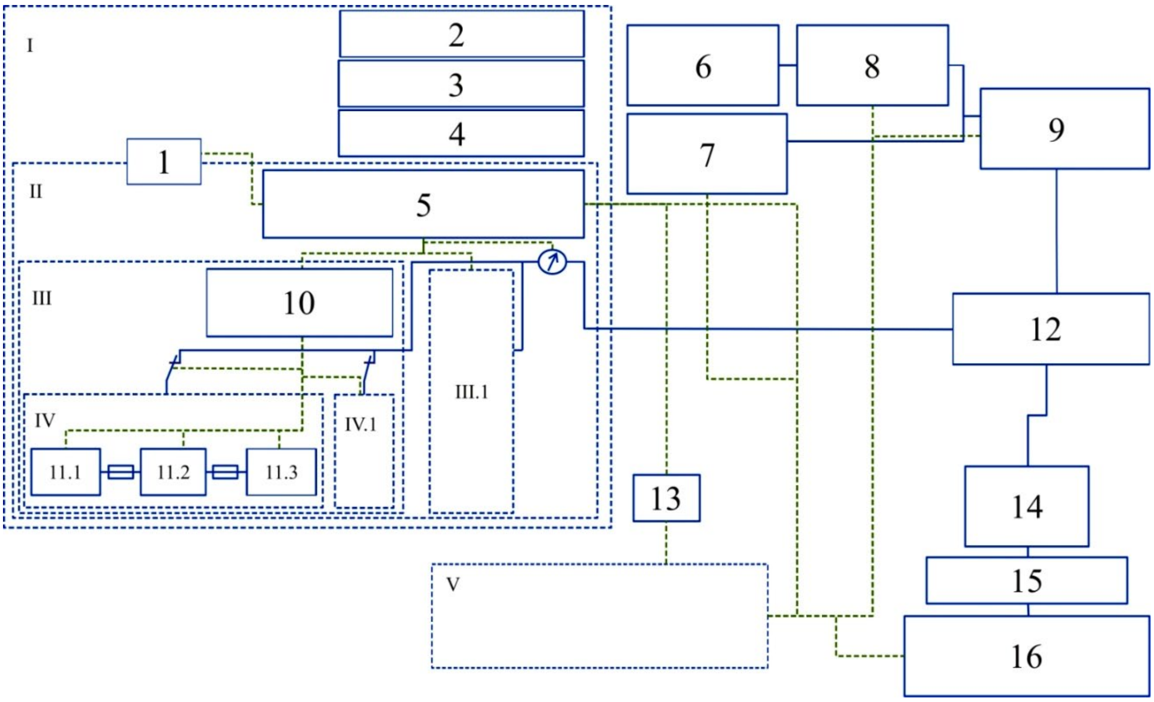

Fig. 2.7. Functional block diagram of hybrid DEPC with PVGS fragmentation: I – battery room with the system of air conditioning (2),ventilation (3) and fire-fighting (4); II – PVGS with temperature control device (1) and selective Battery management system (BMS) of Battery module assemblies (BMA – 5); III – BMA with the control system of voltage and temperature (10); IV – battery module (BM) with the parallel-series connection of Storage batteries (SB – 11); V – Electricity distribution control system (EDCS, PMS); 6 – land-based energy system; 7 – MSE; 8 – switchboard (SB) of land-based energy supply; 9 – charger, AC/DC converter; 12 – DC-link with AC/DC converter; 13 – CS of hybrid DEPC; 14 – VSI or CSI; 15 – HVSB; 16 – SPP with AC consumers, in particular – BEM, THR, LVSB

The variety of SPP CPC modes, when using LIB, determines not only more range of developed capacities and sizes of the batteries, but also a wide voltage range (from seven to several hundred volts) of the batteries based on them that are necessary for the implementation of certain powerful, energy and performance of PVGS [53, 88].

PVGS configuration is complicated in the presence of dangerous external influences, as well as in the case of powerful batteries (especially for hybrid DEPC) that demand an additional air or liquid cooling [161].

General requirements for all LIBs in the design of hybrid DEPCs are safety and ease of use, and full discharge of SB under cyclic mode, but do not work on schedule of weakest element. This is achieved by the introduction of the selective BMS of BMA in PVGS, which monitors the battery charge and protection from dangerous operating modes and provides information on its main parameters [109, 143, 163].

Given the high capacity and a large supply of energy and fire-danger of electrolyte in LIB, the main task of BMS of BMA is SB protection in the case of dangerous modes. These primarily include current overload and short circuit of the power circuits, SB overheating, excessive discharge and recharge of LIB. Protection of dangerous operation modes is done by leveling of LIBs voltage unbalance and formation of Control signals (CSg) to change the mode of external devices or to SB disable from external power circuits using switching equipment that is structurally located as a part of SBs and beyond them [49].

Given the above, we can conclude that DEPC development requires an additional research in improving energy processes involving the use of alternative energy sources in DEPC. The latter require the development of modern local CS from the point of view of their integration into CS of hybrid DEPC.

2.3. Improvement of the power processes control system in diesel-electric hybrid propulsion complexes of the ships made using alternative energy sources

Local CS performs voltage measurement of each element in LIB to protect of PVGS against overcharging and overdischarging. Measuring chains of all batteries in this case should be galvanically untied and are designed to operation at a voltage corresponding to the maximum PVGS voltage (Fig. 2.2). Precision of LIB voltage measurement for most applications should be no worse than ± 20 mV. With the CSg formation in terms of voltage LIB it is necessary to consider the voltage drop on their internal resistance and temperature.

ISBN 978-3-949059-43-8

LIB-element temperature control is necessary to protect ESS from overheating. Recently, for these purposes, temperature sensors with digital or analog output were commonly used. It is relatively easy to use, ensuring measurement accuracy ± (1-2) ºC. Thermistors or thermocouple are used today for a number of special applications related to ESS operation in extreme conditions or restrictions of use of imported components.

To measure a current in ESS, along with the shunt, Hall-effect current sensors are used. Their wide range allows to measure currents ranging from 10 to 1000 A with an accuracy ± 2 %. Except calculation of charging and discharging LIB capacities, current level is required to calculate the corrections to the measured LIB voltage values. Current sensors can also be used for protection against current overload of ESS power circuits near fusible inserts or fuses that self-renewing and protect LIB only from short circuit currents and not effective at relatively low (1,5÷2-time) current overload.

The most complex challenge in terms of implementation is to ensure ESS efficiency during failures (short circuit or open circuit) inside LIB. Open circuit in LIBs is most dangerous when they are in series connection in SEE, short circuit – for their parallel connection. In a parallel LIB connection for additional protection from the effects of the internal short circuits, fusible insert is installed in series with each of them.

To maintain SEE efficiency during a failure of one of the LIBs in their series connection it is necessary to exclude it from the power circuit, while maintaining its integrity. It uses electromechanical or electronic bypass device are used for this purpose. They are controlled by local CS and installed directly on LIB to remove of generated heat through them [109].

An important function of the local CS is a hardware leveling of charge (leveling voltage unbalance) for single LIB in ESS. The cause of voltage unbalance is the difference in SB charge rate due to differences in the rate of self-discharge that is defined as leakage currents through internal and external electrical circuits of SB and electrochemical processes occurring on their electrodes. The result of the voltage unbalance is SEE operation on the «worst» (the most discharged inside) LIB, even if it has the largest nominal capacity at all SBs in SEE.

Hardware methods for leveling voltage unbalance can be divided into the following:

1. Passive method that is the most simple to implement, when LIB of high voltage is discharged via the resistor connected in parallel to it.

2. Active methods that ensure SB voltage grading through redistribution of energy between them.

3. Systemic approaches that ensure the individual (independent) charging mode for each LIB.

The most simple, but very effective system method of leveling unbalance in LIBs of large and extra-large capacity is their charging by multi-channel chargers (AC/DC converter) (Fig. 2.2). For low-voltage portable LIBs are well established circuit solutions that provide an automatic LIBs swapping from the series circuit to parallel circuit in the case of connection of specialized charger to it [79].

Active methods implement transformer circuit of energy redistribution in LIBs and milking of «lagging» SBs is used from one or more DC sources, power supply of which is carried out form SB output or from an external power source (e. g. charger, ESS, another source of renewable energy). These devices provide great flowing currents and can not only to level the voltage imbalance of stresses in SBs, but also provide a complete discharge, rather than operate on schedule «of worse» LIB.

Information about SB condition for ease of use can be transmitted to an integrated CS of hybrid DEPC using a standard digital channel, displayed on the screen or displayed via LEDs using intuitive «traffic light» color symbols.

High-voltage high-capacity SBs are built in a modular approach based on the requirements to ensure electrical safety in the installation and repair as well as the possibility of their transportation and installation with minimum use of handling mechanisms (HM). They are used CSs that also built in a modular approach with 2-3 levels of control.

Safety requirements come to the fore when building powerful ESSs for hybrid

DEPCs during their installing, operating, maintenance and repair. An important requirement for reserve SBs is long-term preservation of specifications in the standby mode of connection to the load and ensuring a guaranteed discharging transition mode on a signal, the timing of which is uncertain. Standby time of the battery can vary from a few months to ten years or more. High-capacity SBs can be built in series-parallel or parallel-series circuits [148].

The specified lifetime and uninterruption of Large Scale Battery (LSB) operation are achieved: through the use of components and materials with appropriate terms of service; by structural redundancy in SB; through the use of chargers and continuous monitoring of their condition (Fig. 2.2), which allows for necessary maintenance or repair work on individual LIBs subsystems without removing all batteries from standby mode as soon as possible.

The algorithm of the SB operation provides periodically transition of the storage sections in the test mode in which they are connected to one of the regular loads. Discharge with a nominal current for 0,5 hours is conducted during the tests. According to a voltage magnitude in each LIBs at the end of discharge it is concluded about reduction of their nominal capacity and the possibility of further operation as individual LIBs and chargers as a whole. The test results and available information on the charger standby mode help to make decision about repair work on faulty sections. Defective chargers disconnected from the output ESS buses. All serviceable chargers after the end of test discharge are connected to charger of 4,2 V on any LIBs. A further charge to align the voltage on individual LIBs is performed using internal charging device from ESS.

For parallel LIBs connection in the power circuit of each must be provided protection against overcurrent (e.g. fusible insert) protecting charger from short circuit within individual LIBs and local CS must provide control of their condition.

 ISBN 978-3-949059-43-8

2.4. Determination of operating modes of hybrid DEPCs with AES in conditions of non-determined loads

Operating modes as DEPCs and SEEs are varying (Table 2.1). Examples of typical DEPCs operating loads are: dynamic positioning, passage narrow or shallow water at low speed, mooring operation with the loads on the power plant, which differ sharply from each other, working mode, towing and more.

Ship movement in conditions of significant loads is ensured by BEM that working and for SEE charge that can provide energy supply for less intensive load modes: electric propulsion at low speeds, electric lighting, energy supply of electronics and other low-voltage consumers.

Table 2.3.

Operating loads of DEPC and ESS in general

CEE	Component of hybrid DEPC
Disabling/enabling of various switches while checking or entry into service	Activation (excitation of the ship)
Disabling checking, monitoring and activation (start)	Full DEPC control in the mode of electric propulsion ship
Disabling, monitoring and setting equalizer devices	Hybrid control Disabling of the systems for service
Battery standby	Mooring – discharge Mooring – charge
Battery charge	Standby mode
battery discharge	Interoperating ship mooring

Reviewing the structures of all-electric and DEPC, the basic principle that is in research of operating modes remain a principle of fuel economy and uninterruptible power supply. All-electric propulsion complexes with SEE are very simple: BEM is driven by SEE, which can be recharged from the land-based network (ship mooring) or from ship AES (PVGS or wind turbines). Hybrid DEPCs may have a different structure.

In the serial hybrid DEPC screw drive is provided or by heat engine in its most efficiency modes, or when it stops for any reason, screw drive is provided by BEM from ESS. BEM in serial hybrid DEPC is operated directly on the screw, getting electricity or from SEEs, or from MSEs, which allows for movement of the ship, even if SBs are discharged.

Addition or power take-off from the propeller shaft are used in the parallel DEPC, providing a heat engine operation with the most efficiency, and when it stops, the screw drive may be from SEE. Propeller drive can be provided as from the heat engine and from BEM, which operates as a «motor/generator» and could either propeller screw, receiving power from SEE or used for SBs charging.

It is used the third type of system - a combination of serial and parallel systems.

Usually, at low loads, heat engine stopped and ship is provided with electric power from SEE, including to the propeller drive. SEEs may be charged from land-based sources, AES or heat engine, rotating propeller when the ship is moving.

DEPC with SEE, which is in continuous operating mode, must meet both cost considerations and environmental standards. Movement of the optimal speed is not always provided, and charging is performed in the final points during the stop. The probability of increasing economic efficiency increases with the installation of additional renewable energy sources, which combined with the existing (proposed) system.

2.5. Simulation of energy processes in hybrid DEPCs with AES in different operating modes for their parameterization and determination of boundary conditions for trouble-free operation

In this section, firstly, we will focus on determination of sizes for SEE, fuel and renewable energy elements and power converters. Then, based on the requirements to DEPC, the purpose of passive components of the converter is given, and, finally, the design process of electronic all-regime controllers is proposed.

The flow of power from DEPC power supply system, assuming n number of MSE, is characterized by the most efficiency of individual elements, namely: diesel – η_{eng}, generator – η_{gen} and SB – η_{batt}, η_{dc} – average efficiency of power converters,

$P_{eng,1}$ ... $P_{eng,n}$ and $P_{gen,1}$ ... $P_{gen,n}$ – power from each engine and generator, respectively. If SBs discharged, the power of SB $P_{batt} < 0$, if charged – $P_{batt} \geq 0$, measured in watts.

The total load consists of consumers of propulsion, auxiliary elements and their needs, and marked P_{load}, and should be provided by the energy from MSE and SBs. Considering the efficiency of the relevant components, we get the following equation:

$$P_{load} = \sum_{i=1}^{n} (P_{gen,i} \times \eta_{dc}) + (P_{batt} \times \eta_{dc} \times \eta_{batt}). \qquad (2.25)$$

Basic principles of simulation of the processes in SPP CPC under the influence of non-determined perturbation with several MSEs that working on complex load are considered in [26, 28].

Power supply is provided by the main MSEs and hybrid DEPC supports BEM and ESS in good condition to prepare for the unlikely emergency.

According to known principles of construction of dynamic models [26], decomposition [28] of investigated object – CPU CPC, in fact, is separation into interacting parts. Let’s present autonomous CPU CPC as a combination of two subsystems: «autonomous MSEs and ESSs – energy sources (ES)» and «consumers». With this, apparent partition, the input influence on consumers is generated voltage U, and output – load current I. Accordingly, for ES, input is load current I, and output – voltage U. Input and output effects of selected subsystems can be interpreted in different ways. For example, in the study of power supply mode from ESS, parameters U and I – average values of voltage and current are calculated taking into account the allowable pulsation factor kpuls_max. In the study of power supply mode from AC MSE, U and I – vectors of existing values of voltage and current, and the current vector I is characterized by the module I and argument φ, and waveform of voltage and current can be easily counted by total harmonic distortion (THD) when working under a load [114].

SPP CPC load is determined by the properties and parameters of individual consumers, especially for operation of energy sources at the consumer of commensurate capacity and also patterns of random processes of formation of group loads, which are the functions of a large number of random factors and their various combinations. Loads may take any values from limited known in advance ranges, and represented by any implementation of the class of functions specified by DEPC property. Therefore, when building a dynamic functional model for SPP CPC it is advisable to describe consumer subsystem by the range of admissible values and loads and by the classes of relevant functions $I(t)$.

In order to present a consumer subsystem in SPP DEPC research, it is necessary to describe its equivalent module – Dynamic functional analogue (DFA), through which it can reproduce the main operating modes of SPP CPC that are adequate to operating and emergency modes.

Obviously, that considered dynamic model is adequate for functioning of autonomous SPP DEPC in the time interval $t \leq t_0 \leq T$, there are such irregularities, where the index «m» are coordinates of dynamic model:

$$\left.\begin{array}{l} \left|I(t) - I^m(t)\right| \leq \varepsilon_I; \\ \left|U(t) - U^m(t)\right| \leq \varepsilon_U; \\ \left|\varphi(t) - \varphi^m(t)\right| \leq \varepsilon_\varphi; \\ k_{puls} \leq k_{puls\_\max} \text{ or } k_{puls} \leq k_{THD}. \end{array}\right\} \tag{2.26}$$

To inequalities $|I(t) - I^m(t)| \leq \varepsilon_I$ and $|\varphi(t) - \varphi^m(t)| \leq \varepsilon_\varphi$ performing in the specified time range $t \leq t_0 \leq T$, functional analogue must be a device that operated in directions $I^m(t)$ and $\varphi^m(t)$. And by providing a fairly small ε_U, we can assume that the simulation runs under the same loads of investigated energy sources (MSE and ESS), which in actual operating conditions and therefore, ensuring conditions $\varepsilon_U \approx 0$, $U(t) = U^m(t)$ is correct. Harmonic distortion and pulsation factors should be provided with appropriate choice of structural parameters of SPP DEPC model.

When ESS charge is started to its optimal capacity, CS of DEPC connects ESS to AES. At this time, the power of its own consumer subsystem needs should instantly connect to the DC-link, taking into account its dynamic performance, and AESs capacity increases slowly.

When ESS is discharged below the required voltage on the DC-link bus, it is connected to MSE through an appropriate converter to restore voltage to the required level.

Converters control using Pulse Width Modulation (PWM) is a means of pulsation smoothing because it is a component of DC-link, half voltage level is determined in which, for example, as follows [35]:

$$U_{dc\_N} = \frac{1}{\mathrm{mod}\,ind\_N} \cdot \frac{U^m \sqrt{2}}{\sqrt{3}} \ (\mathrm{V}), \quad (2.27)$$

where modind_N = 1,01 – value of random variable of optimal switching angles for power converter switches as a function of modulation index to eliminate 5th, 7th, ... 25th harmonics from the main.

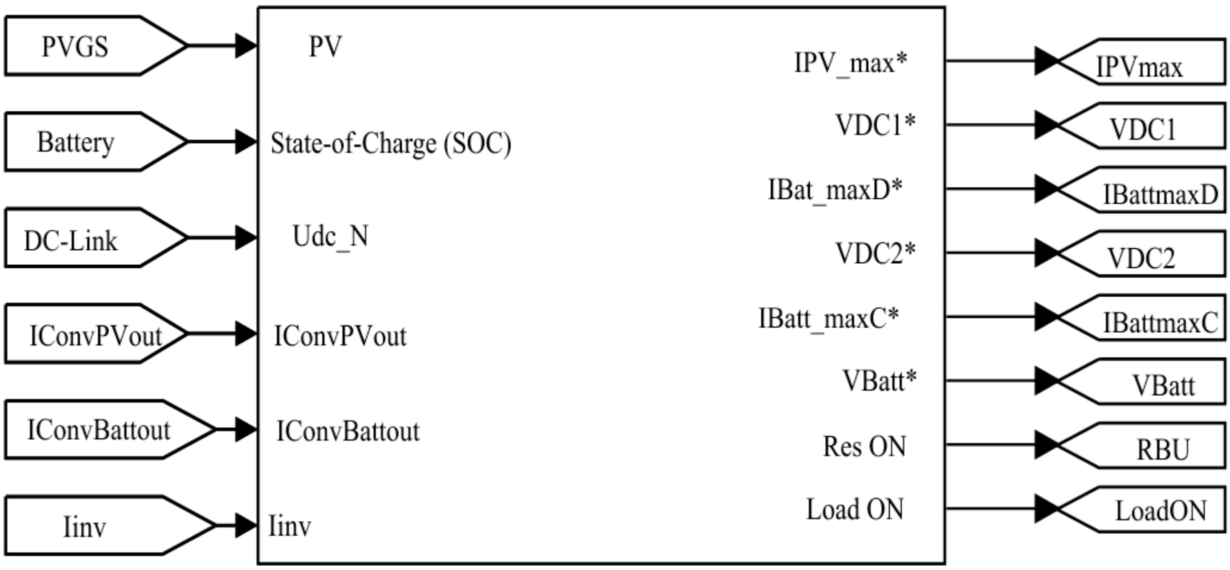

Fig. 2.8. EMS block diagram of hybrid DEPC: State-of-Charge (SOC) – ESS charge level, %; IConvPVout – output current of DC/DC (converter) of PVGS; IConvBattout – output current of DC/DC converter with ESS; Iinv – VSI; IPV_max – the maximum PVGS current; VDC1, VDC2 – voltage of DC/DC converter and ESS, respectively; IBat_maxD, IBat_maxS – the maximum current value of ESS charge and discharge, respectively; VBatt – ESS voltage; Res ON – resistor back unit (RBU); Load ON – load connection (consumers)

Then control pulse generation, in terms of getting harmonic voltage shape increases the efficiency of power transmission to consumers and out of the main waveform of output voltage and VSE controllers should operate in the power control mode, because in some cases there is its limitation. Input and output signals of Energy Management System (EMS) of hybrid DEPC, which block diagram is given in Fig. 2.1, are shown in Fig. 2.3.

The analysis of simulation method of different operating modes of SPP DEPC in terms of energy consumption allow to reveal the main criteria for comparing the performance of fuel consumption and state of ESS charge (voltage in the DC-link). The total system efficiency and voltage at each source of energy, which could affect the parameters of operating mode, will be evaluated using an approach based on the reverse wavelet transformation of their instantaneous power using SPP DEPC simulation model in MatLab/Simulink.

Fig. 2.4, Fig. 2.5, Fig. 2.6, Fig. 2.7, Fig. 2.8, shows the characteristics obtained during the simulation of energy processes in hybrid DEPC for 350 s in MatLab/Simulink environment. Load profile (consumer subsystem) was determined by equations (2.5) to $cos\varphi = 0,8$.

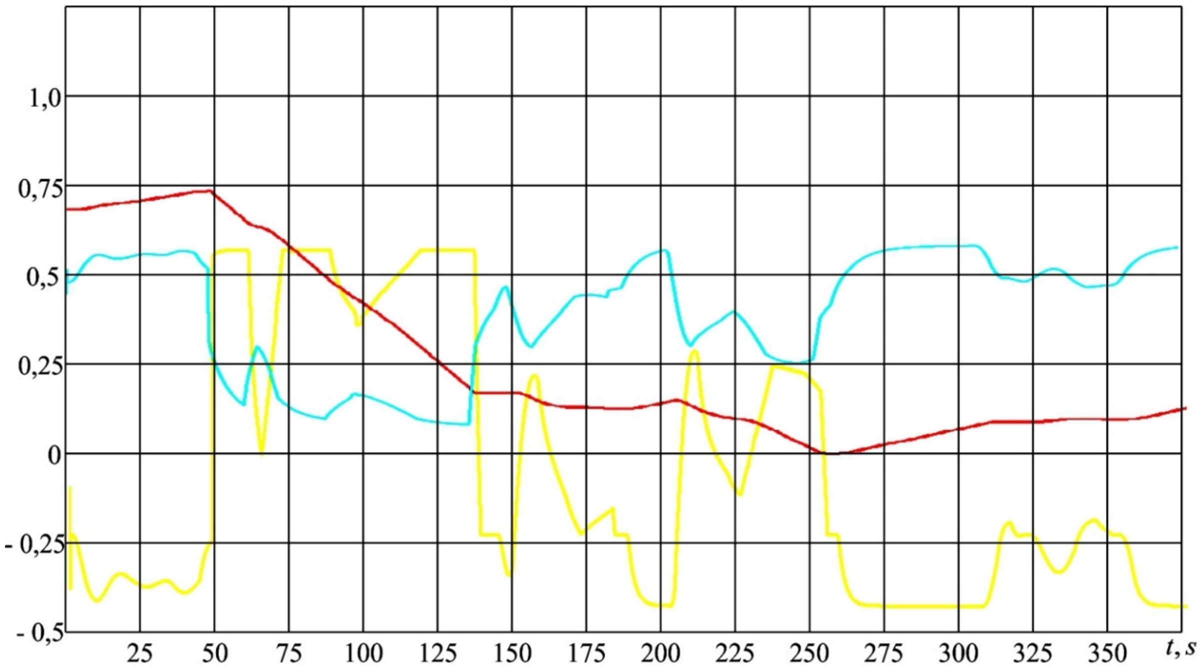

Fig. 2.9. ESS energy characteristics: —— – maximum current corresponds to the value of 400 A; —— – maximum voltage corresponds to the value of 48 V; —— – maximum level of charge corresponds to 100 %

 ISBN 978-3-949059-43-8

At the beginning of the simulation ($t = 0$ s), the load power is provided by basic MSEs and PVGSs of hybrid DEPC enable for ESS charging and prepare for an emergency.

At $t = 40$ s, there is a blackout of the ship. EDCS (PMS) switches power supply of the consumer to alternative sources. At that time, the extra power load instantly provided from the DC-Link, which «carried» dumping of energy from the main users, working in generator mode, because PVGS capacity increases slowly.

At $t = 45$ s, DC-Link voltage achieves a lower set point (270 V) and ESS begins recharge the DC-link bus to 450 V, the voltage at which at 47 seconds reaches the desired level and ESS can restrict its capacity slowly to zero. PVGSs provide total power load and continues to recharge DC-Link bus. Consumers of emergency mode connect to DC-link bus at 55 second. At $t = 62$ s, ESS is enabled to maintain the voltage of DC-Link bus to 450 V and help PVGS to provide the necessary extra power load.

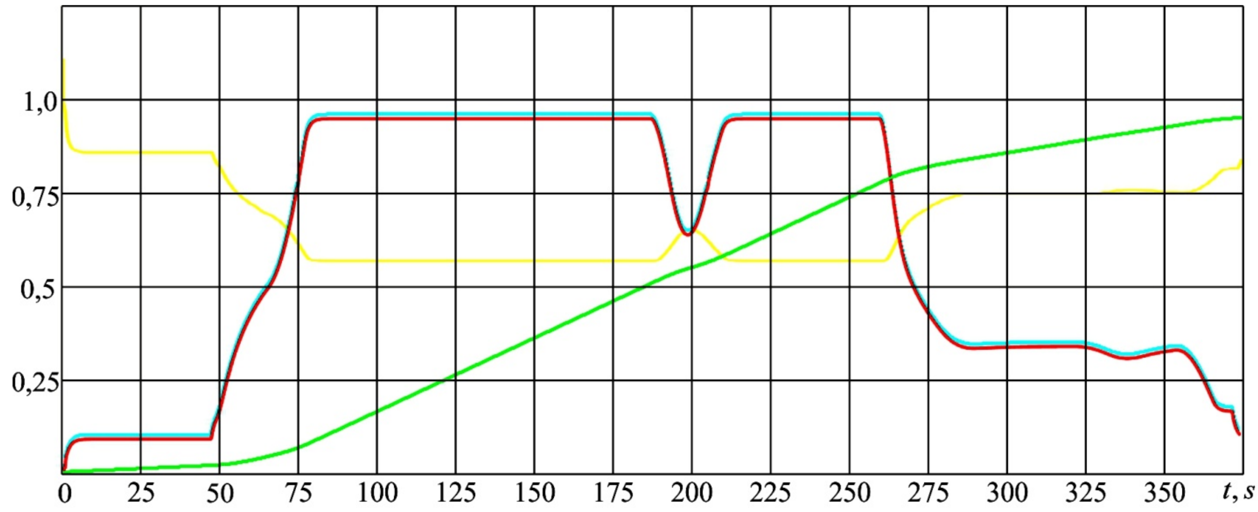

Fig. 2.10. PVGS energy characteristics: ——— – maximum voltage corresponds to the value of 170 V; ——— – maximum current corresponds to the value of 250 A; ——— – maximum level in relation of voltage in PVGS to idle voltage corresponds to the value of 1; ——— – PVGS maximum temperature corresponds to the value of 60 ºC.

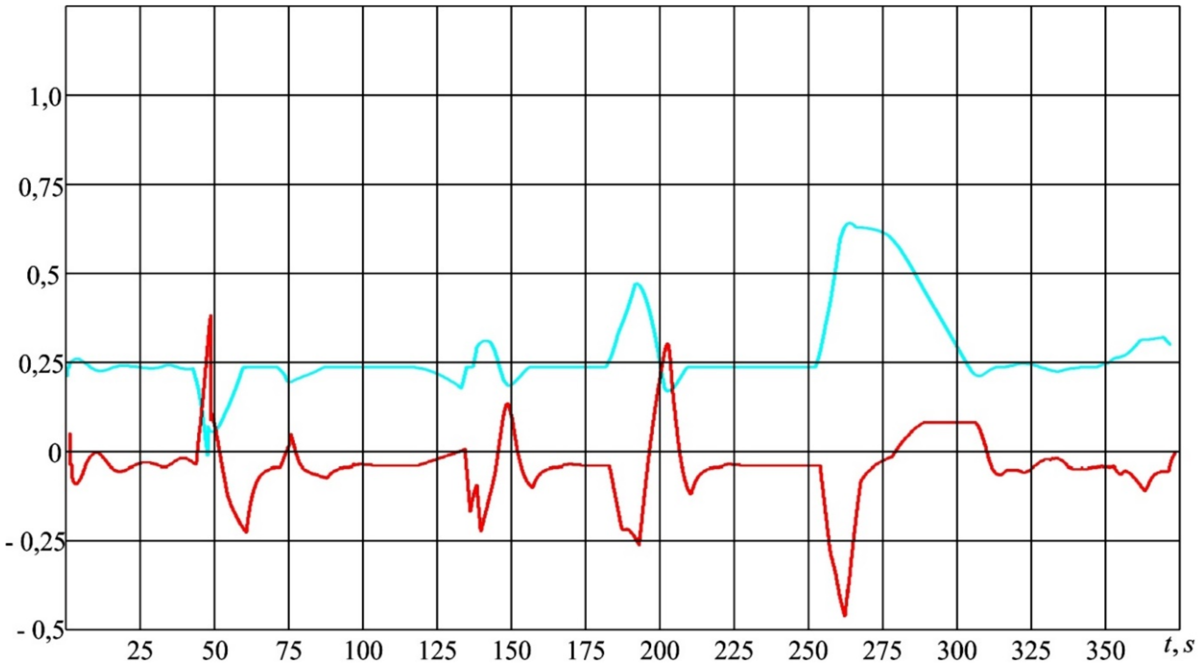

Fig. 2.11. Dependence of voltage and current in the DC-Link: —— – maximum voltage corresponds to the value of 450 V; —— – maximum current corresponds to the value of 1000 A.

At 80 seconds, PVGSs reach their maximum capacity, which is limited by the level of 10 kW because of range of input voltage DC/DC and the additional power load is provided by ESS, which maximum power is reached at t = 120 s (20 kW) and power supply of the load is provided via the DS-Link bus.

At 130 second, load power is reduced below the maximum PVGS capacity. Due to the low PVGS dynamic performance during transients, additional power supply of consumers with PVGS is switched to DC-Link bus. At t = 135 s, DC-Link bus voltage up to 450 V, and the charge of ESSs batteries reduces to zero. Consumers of emergency DEPC mode are enabled again at 140 second and EDCS (PMS) adjustment algorithm with providing the power for necessary consumers is similar to the first case, at t = 55 s.

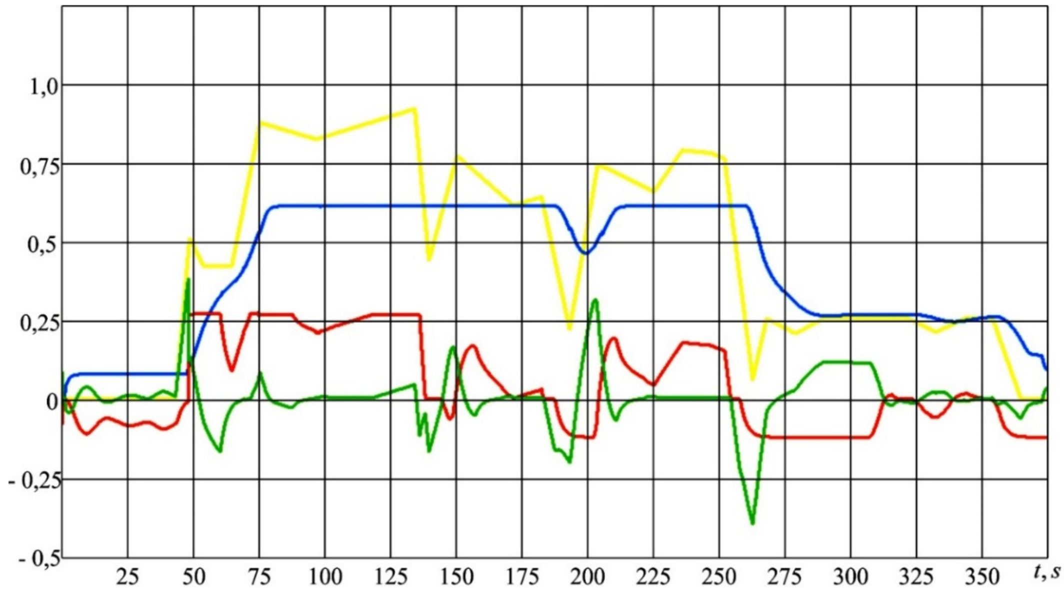

Fig. 2.12. Characteristics of capacities in different DEPC parts: —— – maximum load power corresponds to the value of 1000 kW; —— – maximum capacity in ESS corresponds to the value of 10 kW; —— – maximum capacity in ESS corresponds to the value of 20 kW; —— – maximum capacity in DC-Link corresponds to the value of 300 kW.

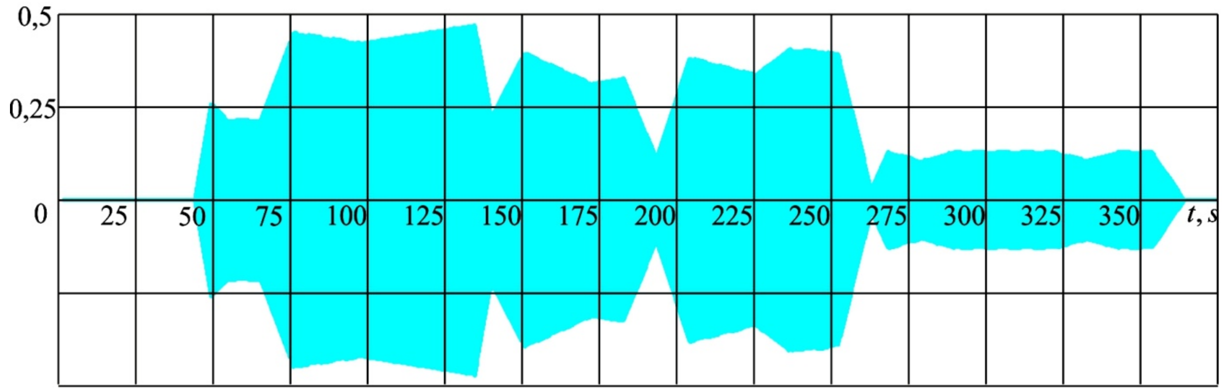

Fig. 2.13. Dependence of load current: the maximum current corresponds to the value of 3000 A.

At t = 165 s, load power reduces below PVGS maximum power and additional power is provided by ESS and DC-Link bus. At 190 second there is a sudden increase in load due connection of consumers, providing input of DEPC into action and EDCS (PMS) responds quickly, providing extra load power from DC-Link bus, to which PVGS batteries are connected at 195 second for voltage restoration and PVGS support with extra load power PVGS. The main MSEs of hybrid DEPC start at 250 second and additional ESS energy begin to accumulate in PVGS and DC-Link elements. At $t = 260$ s, DEPC require an additional capacity due to changes in operating conditions (e. g. – maneuvering of the ship) and PVGS energy is used again to support of the main MSEs. Ship enters the running mode at 330 second and load power decreases. PVGSs also slowly reduce their capacity to the optimum level and switch to ESS battery charge.

Table 2.2. shows comparative results of simulation of energy processes for power transmission in hybrid DEPC for two toughest operating modes: emergency operation mode and DP mode under conditions of use of various management strategies for EDCS (PMS).

Table 2.4.

Comparative results of simulation of energy processes for power transmission in hybrid DEPC

Name of element	Output data						DP					Emergency operation				
	Quantity	Installed capacity, kW	Efficiency	Power factor	Power consumption, kW		Diversity factor	Coefficient of loading	Power factor	Power consumption, kW		Diversity factor	Coefficient of loading	Power factor	Power consumption, kW	
					Single	Total				Active power, kW	Reactive power, kBAr				Active power, kW	Reactive power, kBAr
Hybrid Propulsion Complex																
PVGS	10	11,5	0,94	1,00	12,2	122,3	1,0	1,0	1,00	122,34	0,00	1,0	0,8	1,00	97,87	0,00
ESS	2	100,0	0,93	1,00	107,5	215,1	1,0	1,0	1,00	215,05	0,00	1,0	0,9	1,00	193,55	0,00
DC/DC converters	2	200,0	0,88	1,00	227,3	454,5	1,0	1,0	1,00	454,55	0,00	0,5	0,8	1,00	181,82	0,00
VSI	2	400,0	0,80	0,69	500,0	1000,0	1,0	1,0	0,69	1000,00	723,81	0,5	0,9	0,69	450,00	325,71
DC-Link	1	300,0	0,80	0,69	375,0	375,0	1,0	1,0	0,69	375,00	271,43	1,0	0,8	0,69	281,25	203,57
HVSB	2	611,5	0,88	0,43	694,9	1389,8	1,0	1,0	0,43	1389,77	1254,73	0,5	0,8	0,43	583,70	526,99
LVSB	2	1311,5	0,89	0,44	1473,6	2947,2	1,0	1,0	0,44	2947,19	2646,57	0,5	1,0	0,44	1414,65	1270,35
Load	2	1923,0	0,95	0,80	2024,2	4048,4	1,0	1,0	0,80	4048,42	2429,05	0,5	1,0	0,80	2024,21	1214,53
State machine control strategy							0,70			10552,3	7325,6	0,70			4022,6	3011,9
Classical PI control strategy with SOC's regulation							0,75			21104,6	14651,2	0,75			4847,9	3337,6
Frequency decoupling and state machine control strategy with SOC's regulation							0,80			16883,7	11720,9	0,85			4120,7	2836,9
Equivalent consumption minimization strategy							0,85			17727,9	12307,0	0,90			4326,8	2978,8
External energy maximization strategy with SOC's regulation							0,90			18614,3	12922,3	0,95			4543,1	3127,7
							SOC's reg.			yes	no	SOC's reg.			yes	no

2.6. Conceptualization of flexible multifunctional power generation systems

The above results of simulation of energy processes in hybrid DEPC make it possible to solve the problem of structuring of the last through the introduction of new types of power semiconductor technology and highly automated management technologies. The combination of these components allows to build flexible multifunction electricity generating system integrated into a hybrid DEPC as an integral part of it. But given the fact that the regulation of the battery charge level is incidentally impact on reducing consumption of reactive power (Table 2.2.) and power supply of inverters by unregulated rectified voltage creates a problem of energy recovery in the system of ship electricity consumers, we can conclude that the electromechanical compensation of reactive power of consumers mainly done using MSE that transferred by its Proportional–integral–derivative (PID)-controller in compensator mode. Further studies will be conducted to verify the obtained results on a physical model of multifunctional propulsive complex, which was created as a part of research work «Concepts, technologies and ways of improvement of ship power units (SPP) of combined propulsive complexes» (CPC) of the National University «Odessa Marine Academy» (state registration number 0114U000340) [21, 22, 24, 25, 26, 27, 28, 30, 31, 32, 33, 34, 35, 36, 108].

In particular, it is necessary to point out that the composition of DEPC includes auxiliary diesel or turbo-generators as the main source of heat and mechanical energy, the part of which is converted into electricity, and at other special conditions of utilization, in turn, must take into account the heat loss in their workflow. Particular attention in the development of block diagrams of hybrid DEPC should be paid to automate control of the entire energy complex, including subsystems of collection and processing of measurement data, coordinated control of individual power converters, generators and their excitation system, power semiconductor and switching devices, various mechanisms and their controllers interrelated to different hierarchical levels. In addition, the electricity generating system must satisfy often contradictory requirements arising from the appointment of the ship, divergent performance of the same equipment of different manufacturers, and features of its use, as well as being highly reliable with the necessary degree of redundancy and maintainability. It is established that improving the operating modes of hybrid diesel-electric propulsive complexes is possible through the use of modern energy storage systems using solar generating elements and optimal battery capacity. The dynamic performances of power transmission parameters in different parts of hybrid diesel-electric propulsive complex are obtained. They can work out the principles of the electric power distribution control systems management for different operating modes in terms of non-determined load. For example, analyzing the data in the Table 2.2, it can be concluded that the application of the classical PI control with adjustable degree of ESS battery charge decreases power consumption by consumers connected to the DC-link within 5÷7 % depending on the operating mode, and reactive power compensation is achieved within 2÷3 %. If to apply a control using the criterion of minimum power consumption, in this case there is an increase of pulsation factor of the output voltage within 1÷1,5 %, which can’t be offset without the support of ESS battery charge level at 85÷95 %. Energy processes in hybrid diesel-electric propulsive complex with alternative sources of electricity in the different operating modes of the ship are modeled. On the one hand, it provides a reasonable range of current-voltage characteristics of photovoltaic panels and the batteries of energy storage systems in terms of optimum charge/discharge cycles, on the other hand, allows to perform parameterization of the basic energy sources and to determine the boundary conditions of trouble-free operation. For example, analyzing dependences and data in Table 2.2, we can conclude that the control of frequency and MSE conditions with adjustable degree of ESS battery charge with all other equal conditions to operating mode can reduce the number or power of ESS modules by 7÷10 % and management for criteria to obtain a maximum of alternative energy and control of the charge degree of ESS battery allows to use batteries of smaller capacity within 6÷8 %.

 ISBN 978-3-949059-43-8

KAPITEL 3 / *CHAPTER 3*
MULTICRITERIA STRATEGY OF POWER MANAGING SYSTEM FOR SHIPS POWER PLANTS FOR COMBINED PROPULSION COMPLEXES

3.1. The basic principle of the proposed modifications

The development of the coastal shelf (the product of natural resources, the construction of wind and tidal power plants, pelagic fishing, etc.) involves the development of high-tech science-intensive sectors of the maritime industry, which involve the construction and operation of vessels for the provision of exploration, drilling, lifting and transport operations in various operating conditions (the so-called offshore fleet). Such vessels will be equipped with innovative CPCs with SPPs, which are built on the principle of unified electric power systems [15, 41].

The problems of increasing energy efficiency caused by energy shortages and the desire to improve the environmental performance of the SPP CPC are underpinned by the requirements established by the International Maritime Organization in Annex VI to the International Convention for the Prevention of Pollution from Ships (MARPOL) regarding the Energy Efficience Design Index (EEDI) and the Energy Efficiency Operational Index (EEOI) within the framework of developing and implementing an energy management plan SShip Energy Efficiency Management Plan (SEEMP) in the process of improving the operation and operation of the vessel.

Thus, it is possible to formulate the actual scientific and technical problem in the field of transport, transport technologies and related infrastructure development: research, development and forecasting of methods for improving the operational characteristics of the SPP of the CPC, which would ensure the efficiency of their operation is impossible without establishing the regularities of changing parameters and introducing methods and means of diagnosing and predicting the technical state of the SPP of the CPC during operation [51, 65].

Hybrid SPP CPCs with Alternative generating elements (AGE) that use the maximum efficiency of direct mechanical drive and the flexibility of combining the combustion power from the heat engine and the accumulated energy from the AGE are the most promising. At low power of a propulsion electric drive designed to bring the vessel in motion, Propulsion electric motor (PEM) provides the necessary power, and excess power of the thermal engine can be used as the power supply of its own needs from the booster. The typical SPP CPC architectures are shown in [28]: Anchor Handling Vessel – Fig. B.1; Multipurpose Offshore Vessel– Fig. B.2; Anchor Handling and Offshore Construction Vessel – Fig. B.3, Fig. B.4; Rescue, Rescue and Guard Vessels – Fig. B.5; Offshore Construction Vessel – Fig. B.6; Fig. B.7; Oceanographic Research Vessel – Fig. B.8; Fisheries research vessel – Fig. B.9; Diesel-electric Passenger Vessel – Fig. B.10; Fishing Trawlers – Fig. B.11; Fig. B.13; Pelagic Seiner/Pelagic Trawlers – Fig. B.12; Product/Chemical Tankers – Fig. B.14; Fig. B.15; Twin Marine Lifter – Fig. B.16; Small Waterplane Area Twin Hull – Fig. B.17; Cutter Suction Dredger – Fig. B.18; Seabed Logging Ship – Fig. B.19; Multipurpose Geotechnical & Soil Investigation Vessel – Fig. B.20; Offshore Subsea Construction Vessel – Fig. B.21; Multipurpose field & ROV Support Vessel, Multi-Purpose Vehicles (RV) – Fig. B.22; Cable laying vessel – Fig. B.23; Seismic Research Vessel – Fig. B.24; LNG Car Ferry – Fig. B.25; Roll-on/Roll-off ships – Fig. B.26.

Effective distribution of capacities between AGE, Battery storage power station (BSPS), SPP and other components of the SPP during the change of operating modes is possible due to the improvement of the strategy of controlling the hybrid SPP of the CPC on the criterion of minimum electricity consumption or by the criterion the maximum of obtaining alternative energy with the regulation of the charge level of batteries BSPS.

This can be accomplished by synthesizing a three-level multicriterion energy management strategy in the hybrid SPP CPC by integrating the classical power distribution control strategy with the Medium speed diesel-generator (MSDG) control strategy and the AGE BSPS charge rate, which will differ from the existing higher efficiency of detecting the risk of deenergizing the SPPs, with greater reliability and the accuracy of determining the need for reducing the load and is fully integrated with the intrinsic regulators of the frequency of rotation of the thrusters and the power supply system. The purpose of the work is to develop the theory, methodology and technology in the field of increasing the efficiency of the functioning of SPP CPC.

In order to achieve the certain goal, it will be necessary to solve the problem of increasing the efficiency of hybrid SPP CPC by combining the criteria of power management systems strategies.

Depending on the type of CPC, one or another of the three known methods of its dynamic hold over the drill point is used. This, in turn, predetermines the use of the Power Management System (PMS). SPP CPC usually consists 6÷10 different types motors for THR, depending on the positioning on the vessel for positioning, which feed on 4÷6 high-voltage MSDG.

MSDGs are distributed among the tires as the least two Main switchboards (MSB) connected to each other by means of an integral switch. PMS functions are implemented in three independent control systems, namely, Dynamic Positioning (DP), DC drilling (DC) and Data Management System (DMS).

In such projects, the power management functions of each system operate independently and have special inputs for sensors from main electrical chain [28, 81]. Systems calculate the total power, depending on the total load. If the system total load exceeds certain limits set in advance, they decrease. The system will also reduce the load if the load on any individual MSDG will exceed the preset limit. Such a structure allows not to exceed the load on a separate MSDG even when the reciprocating power is affected by any MSDG or the failure of the sensor component.

At the present stage of technical maintains and operation of such systems are the following problems:

- compliance DP systems to the requirements of Failure modes and effects analysis (FMEA), which are faced with the stage maintains and operation [153];
- unification of PMS in the combination of functions in relation to other similar [72, 84];

- the independence of the components of the PMS from each other even to the level of sensors [86, 100, 157];
- not only the reduction of power in terms of the total estimated load, but also the load of the detached MSDG [47, 89, 123];
- compliance of the system with the conditions for increasing the load in terms of sufficiency to ensure normal work, depending on any abnormal regime and not overloading the SPP in general [16, 97, 110, 127].

The development of strategies, methods and means for improving the efficiency of the SPP CPCs is limited to a substantial set of contradictory, conflict, and sometimes mutually exclusive factors and situations: the need to analyze the operation of the SPP CPC during exploration, drilling, hoisting and transport operations and loading different operating conditions; the need for analysis of processes at the intersections of energy flows in the SPP and the CPC with Thrusters (THR) and the lack of methods for recording degradation effects that have a significant effect on these processes; the need to improve the methods of computational hydrodynamics for tracking degradation effects on propeller flow lines and the lack of physical models of registration components of the monitoring system for degradation effects on shaft line lines; the need for the synthesis of mathematical models of intrinsic regulators of the revolutions of the THR with simultaneous improvement of the mathematical apparatus in the modeling of energy processes in the SPP CPC in different operating modes; formulation and association of criteria for choosing solutions based on the set of both SPP CPCs and operating modes in which they operate and the absence of formalized physical models of multifunctional SPCs taking into account situational environmental factors and identification factors of operating modes; the demand for power distribution management strategies in the SPP CPC and the lack of a methodology for the creation of mathematical models of Ship automated power plants (SAPP) with multi-constructions, taking into account the hydrodynamic properties of the vessel with the ability to assess their impact on energy processes; the development of technology for the implementation of the Decision Support System (DSS) for the SPP CPC and the presence of intellectual, behavioral and cognitive limitations of the Decision maker (DM).

3.2. Determination of criteria for applying energy management strategies

The control system (CS) of the SPP CPC distributes the power between the battery storage power station (BSPS), Photovoltaic (PV) generation system (PVGS) and SPP according to the chosen energy management strategy:

- with State machine control strategy (SMCS);
- with Classical PI control strategy with SOC's regulation of BSPS (CPICS);
- with Frequency decoupling and state machine control strategy with SOC's regulation of BSPS (FDSMCS);
- with Equivalent consumption minimization strategy (ECMS);
- with External energy maximization strategy with SOC's regulation of BSPS (EEMS).

Summary data on the analysis of advantages, disadvantages and criteria for the use of different types of SPP CPC are given in Table 3.1.

The disadvantages of the given functional diagram of the hybrid SPP CPC are:

- inconsistency of MSDG parameters with other components, which leads to uneven regulation of magnetic fluxes and voltage amplitudes, which causes an additional increase in voltage pulsations at the output of converters and the emergence of equalizing currents in synchronous operation;
- elevated level of harmonics in the current of consumers of energy;
- reduced reliability, efficiency, increased dimensions and mass, which arise due to the use of elements of increased power and equipment kits to them;
- the lack of the possibility of balancing the three-phase system of supply voltage with uneven loading of the phases.

Protection against the occurrence of hazardous operating modes is carried out by leveling the imbalance of LIB stresses and the formation of control signals for changing the operating mode of external devices or for switching off the battery from

Table 3.5.

Advantages, disadvantages and criteria of choice of engines and technologies of power supply SPP CPC

Techno-logy	Advantages	Disadvantages and selection criteria
Electromechanical CPC	Low losses at rated power	Low efficiency with partial and peak loads
	Low emissions of CO_2 and NOx at rated power	High NOx emissions when reducing load
	Low energy conversion loss	Low reservation
		Increased noise level
		Overload of diesel engines
CPC	Overload Capacity	MSDG rotation speed constant
	Consistency of load with MSDG	Losses at rated power
	High visibility	The risk of constant instability of load capacity
	Reduced NOx emissions at low speeds Potentially low noise level	
Hybrid CPC	Low losses at rated power	MSDG rotation speed constant
	Overload Capacity	
	Matching load and PEM at low power	The complexity of the system
	Potentially low noise level PEM	
Hybrid CPC with AGE	Independence from the state of air	Limited power
	Reduction of emissions into the air	Insecurity
	High efficiency and low noise	Ability to upgrade
Hybrid SAPP	Independence from the state of air	Limited power
	Reduced emissions into the air and low noise	Insecurity
CPC with hybrid SAPP	Leveling the load	MSDG rotation speed constant
	Zero noise and harmful emissions	The complexity of the system
	Storage of regenerated energy	Danger of battery maintenance
	Backup power efficiency	The cost of the bats
	Possibility of switching on pulse power	The need to control the state of each of the bacteria
	Reduced fuel consumption and emissions into the atmosphere	Ability to disable batteries as a result of recharging
	No increase of NOx during load increase	Difficulty monitoring the status of batteries

 ISBN 978-3-949059-43-8

Techno-logy	Advantages	Disadvantages and selection criteria
CPC with hybrid SAPP DC	Variable speed of PEM and load	The complexity of the system
	Optimal load PEM	Cost and loss in power electronics
	Reduced noise and vibration of the engine	Increase NOx due to variable power
	Reduced fuel consumption and CO_2 emissions	Need to introduce energy saving with power reduction
	Possibility of switching on pulse power	Management complexity

external power circuits with the help of switching equipment, which is constructively placed both within and outside battery [49, 163]. Taking into account the foregoing, one can conclude that the development of the SPP CPC requires additional research in the field of improving the energy processes associated with the use of alternative energy sources in the SPP CPC. The latter require the development of modern local CS from the point of view of their integration into the CS of hybrid SPP CPC.

To protect the BSPS from overcharging and overloading, the local CS measure the voltage of each element in LIB. In this case, the measuring circuits of all batteries must be galvanically solved and designed for operation at a voltage corresponding to the maximum voltage of BSPS (Fig. 2.2). Elemental temperature control of LIB is also required to protect the BSPS from overheating. Recently, for these purposes, temperature sensors with digital or analogue output are often used, relatively easy to use, providing accuracy of $\pm(1\div2)$°C. Thermoresistors or thermocouples continue to be used for a number of special applications related to the operation of BSPS under extreme conditions or with restrictions on the use of the imported elemental base.

For measure current in BSPS, along with shunts, current-type current sensors are used, the wide range of which allows measuring currents in the range from 10 to 1000 A with an accuracy of ± 2% accuracy. In addition to calculating the charge and discharge capacities of LIB, the value of current is necessary for the calculation of corrective corrections to the measured values of the voltage of LIB. Current sensors can also be used to protect against current overloads of the BSPS power circuits along with fusible inserts or fuses that self-repair and protect LIB from short-circuit currents only and are not effective at relatively small (1,5÷2-times) current overloads.

The most difficult, in terms of implementation, the task is to ensure the efficiency of BSPS with failures (short circuit or breakdown) within LIB. The breakthrough in LIB is most dangerous when they are connected in the consistent manner in the BSPS, short circuit – with their parallel connection. In the parallel connection of LIB in addition to protect from the effects of internal short circuit consistently with each of them installed melting insert. In order to maintain the efficiency of BSPS in the rejection of one of the LIB with their sequential connection it is necessary to withdraw it from the power circuit, while preserving its integrity. For this purpose, electromechanical or electronic bypass devices are used, which are controlled by the local CS, which are installed directly on the LIB for discharging the resulting heat.

An important function of the local CS is the hardware alignment of the charge level (leveling the voltage unbalance) of the individual LIB in the BSPS. The reason for the voltage disbalance is the difference in the degree of charge of batteries, which is due to differences in the rates of their self discharge, which is defined as leakage currents through external and internal electrical circuits of batteries, and electrochemical processes occurring on their electrodes. The hardware methods for leveling the voltage divergence, which are components of the DSS in the design of the SPP CPC, can be divided into the following: the most simple in implementation of the passive method, when the LIB with high voltage is discharged with the help of the resistor connected in parallel to it; active methods for balancing batteries voltage by redistributing energy between them; system methods that provide an individual (independent) charge mode for each LIB.

The simplest but fairly effective system method for leveling the imbalance in large and very large capacities of LIB is their charge with multichannel automatic chargers (AC/DC converter) Fig. 2.1. For low-voltage portable LIB, circuit-engineering solutions have been well-proven, providing automatic switching of LIB from the serial circuit to parallel with the connection to it of the specialized AC/DC converters [71, 109]. In active methods, transformer circuits of energy redistribution are implemented in LIB, or the "lagging" batteries is charged from one or more direct current sources supplied from the outlet of the batteries or from an external source of energy (eg, AC/DC converters, BSPS, other renewable energy source). Such devices, providing large flowing currents, allow not only to offset the imbalance of stresses in batteries, but also to provide their full discharge, and not to work according to the schedule of "worse" of LIB. High-voltage high-rise batteries are built on the modular basis, based on the requirements of providing electrical safety during installation and repair, as well as the possibility of their transportation and installation with minimal use of lifting-transport mechanisms. They use CS also built on the modular principle with 2-3 levels of control. During design of powerful BSPSs for hybrid SPP CPCs, the safety requirements for their installation, operation, maintenance and repair are on the forefront. For backup batteries, an important requirement is long-term maintenance of the technical characteristics in the standby mode of connection to the load, guaranteed transition and provision of a given mode of discharge by command, whose arrival time is uncertain. The battery life of the standby mode can range from a few months to ten years or more. High-energy capacitive batteries can be constructed in sequential-parallel or parallel-sequential circuits [73, 79, 140]. The specified lifespan and continuity of work of LIB are achieved: by means of the use of component parts and materials with appropriate service life; at the expense of structural redundancy in batteries; due to the use of AC/DC converters and continuous monitoring of their condition (Fig. 2.2), which allows to carry out the necessary regulatory and repair work on separate of LIB subsystems without removing the entire battery from the standby mode as soon as possible. At the magnitude of the voltage at each LIB at the end of the discharge, it is concluded that their nominal capacity is reduced and the possibility of further operation of both LIB and AC/DC converters as the whole. According to the results of testing and available information on AC/DC converters work in the standby mode, the decision is made to carry out repair and restoration work on faulty sections. Defective AC/DC converters are disconnected from the output bus of the BSPS. All normal AC/DC converters after the end of the test discharge are connected to the charge from the AC to the voltage of 4,2 V on any LIB. Further charge for leveling the voltages on individual LIB is carried out with the help of internal recharging devices from the BSPS. In the case of the parallel connection of LIB in the power circuit, each of them should provide an element of protection against overcurrent (for example, fuse-link), which protects the AC/DC converters from short circuit within individual of LIB, and the local CS should provide control over their state.

3.3. Method of design of mathematical models of power systems with multi-constructions

Depending on the connection point, the spatial vector of the consumed PEM (induction – IM or synchronous – SM) current will be rotated in *d*, *q* coordinates with the frequency determined by the load phase, which, in turn, depends on the impedance difference at the point of connection and the nearest high-voltage bus MSDG (Fig. 3.1).

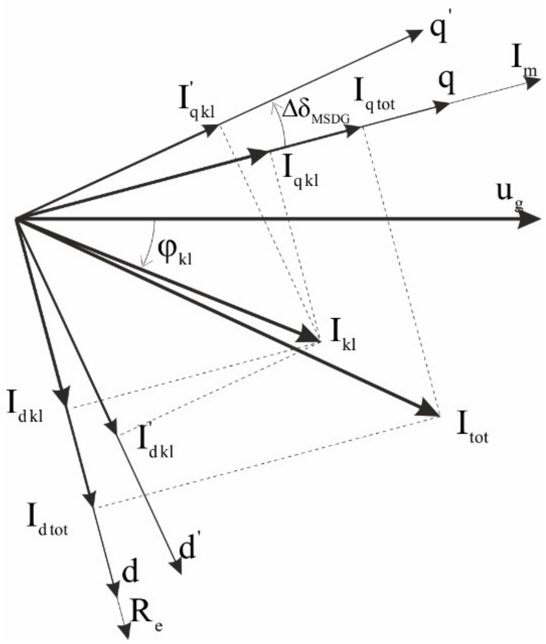

Fig. 3.14. Vector diagram for the area *kl* (*k*, *l* – natural number) of the high-voltage bus with connected to it IM and MSDG: u_g – voltage on the bus, [p.u.]; I_{tot} – total consumption current of IM, [p.u.]; $\Delta\delta_{MSDG}$ – load angle; φ_{kl} – current phase of the stator of IM.

The equation of the MSDG model connected to the bus can be described by the system of equations:

$$\begin{cases} \dfrac{d\overline{\Psi}}{dt} = (W(n) + FX^{-1})\overline{\Psi} + Nu_g + gu_f \\ \dfrac{dn}{dt} = \dfrac{1}{t}(t_{m\_msdg} - \overline{\Psi}^t (M^t KM) X^{-1}\overline{\Psi}) \\ \Delta\dfrac{d\delta_{MSDG}}{dt} = \omega_N (n - n_1), \end{cases} \tag{3.28}$$

where: $\overline{\Psi}$ – flux vector of the winding of the stator; u_f – excitation voltage, [p.u].; n – speed of rotation, [c^{-1}] shaft generator, [p.u.]; ω_N – nominal speed of rotation, [rad/s]; r_{ss} – resistance of the winding of the stator IM, [p.u.]; r_{lk} – resistance of the tire between points lk, [p.u.]; t_d, t_q – longitudinal and transverse components of the constant time of the damper winding of the MSDG, [s]; t_f – constant time of the winding of excitation, [s]; x_d, x_q – longitudinal and transverse components of the reactive resistance of the scattering of the windings of the stator, [p.u.]; $k_{\mu d}$, $k_{\mu q}$, $k_{\mu f}$ – longitudinal and transverse components of the coefficient of saturation of the damper and stator windings of the MSDG and the winding of excitation; μ_d, μ_f – coefficients of interinduction between the stator winding and the damping, between the winding of excitation and the damping.

$$W(n) = \begin{bmatrix} 0 & \omega_N n & 0 & 0 & 0 \\ -\omega_N n & 0 & 0 & 0 & 0 \\ 0 & 0 & 0 & 0 & 0 \\ 0 & 0 & 0 & 0 & 0 \\ 0 & 0 & 0 & 0 & 0 \end{bmatrix}; \quad N = \begin{bmatrix} \omega_N & 0 \\ 0 & \omega_N \\ 0 & 0 \\ 0 & 0 \\ 0 & 0 \end{bmatrix}; \tag{3.29}$$

$$F = \begin{bmatrix} \omega_N (r_{ss} + r_{kl}) & 0 & 0 & 0 & 0 \\ 0 & \omega_N (r_{ss} + r_{kl}) & 0 & 0 & 0 \\ 0 & 0 & -1/t_d & 0 & 0 \\ 0 & 0 & 0 & -1/t_q & 0 \\ 0 & 0 & 0 & 0 & -1/t_f \end{bmatrix}; \tag{3.30}$$

$$X=\begin{bmatrix} -x_d & 0 & 1 & 0 & 1 \\ 0 & -x_q & 0 & 1 & 0 \\ -(1-k_{\mu d})x_d & 0 & 1 & 0 & \mu_d \\ 0 & -(1-k_{\mu q})x_d & 0 & 1 & 0 \\ -(1-k_{\mu f})x_d & 0 & \mu_f & 0 & 1 \end{bmatrix}; \quad g=\begin{bmatrix} 0 & 0 & 0 & 0 & \dfrac{1}{t_f} \end{bmatrix}^t \tag{3.31}$$

Then, from expression (3.1), the vector of the flux coupling ψ MSDG is connected with the quantities that characterize the stator winding by the expression:

$$h(\bar{\Psi})=\bar{\Psi}_s^t K i_s=\bar{\Psi}^t(M^t KM)X^{-1}\bar{\Psi}, \tag{3.32}$$

where: $K=\begin{bmatrix} 0 & 1 \\ -1 & 0 \end{bmatrix}$; $M=\begin{bmatrix} 1 & 0 & 0 & 0 & 0 \\ 0 & 1 & 0 & 0 & 0 \end{bmatrix}$; $M^T KM=\begin{bmatrix} 0 & 1 & 0 & 0 & 0 \\ -1 & 0 & 0 & 0 & 0 \\ 0 & 0 & 0 & 0 & 0 \\ 0 & 0 & 0 & 0 & 0 \\ 0 & 0 & 0 & 0 & 0 \end{bmatrix}$ (3.33)

The common solution of (3.1), (3.2), (3.3), (3.4) allows us to determine the constant integration that characterizes the setpoint of the MSDG PID-regulators in their parallel work. The regulators are tuned so that one of the regulators controls the frequency and voltage, and the other for the supply of active and reactive power with the settings set for the power of the first generator. In this way, the uniform load distribution is achieved:

$$c=x_d(\mu_f(\mu_d+k_{\mu d}-1)-\mu_d+1-k_{\mu d}+k_{\mu f}(k_{\mu q}-1)).$$

If the properties of load are represented by the graphs in the form of the implementation of any stochastic process of changing the load of the MSDG during the change in the operating mode of the CPC $I_i(t)$ and $\varphi_i(t)$ for i = 1, 2, ..., then the functional analogue of the single operator of the E_F must be with two controllable coordinates $I^m(t)$ and $\varphi^m(t)$, whose values correspond to:

$$\dot{I}^m(t)=\left[-\boldsymbol{R}^m_{(\Psi)F}\cdot I^m(t)+E^m_F(t)+\beta_x\cdot\boldsymbol{X}_F(t)+\beta_\delta\cdot\delta_F(t)+\beta_\varphi\cdot\boldsymbol{Y}_F(t)\right]/\boldsymbol{L}^m_{(\Psi)F} \tag{3.34}$$

and
$$\dot{\varphi}^m(t)=c_I\cdot I^m_F(t)+c_U E^m_F(t)+c_{\varphi(U)}\cdot\delta_{(\varphi)F}(t)+c_{\varphi(I)}\varphi_F(t), \tag{3.35}$$

where: R_m and L_m are the matrices of the active and reactive components of the equivalent electrical circuits for the replacement of load; β_x, β_δ, β_φ – weighted average constant constructive coefficients of the self-excitation system of MSDG, shock absorbers and amplifier-phase transformer; c_I, c_U, $c_\varphi(U)$, $c_\varphi(I)$ – weighted average constant constructive coefficients of current, voltage and feedback sensors VSI or CSI (see Fig. 2.1, Fig. 2.2) by current and voltage respectively.

The values of the current of the stator, active (P) and reactive (Q) power are from the equation:

$$\begin{cases} i_s = MX^{-1}\overline{\Psi} \\ P = u_g^t i_s = u_g^t MX^{-1}\overline{\Psi} \\ Q = -u_g^t K i_s = -u_g^t KMX^{-1}\overline{\Psi}. \end{cases} , \qquad (3.36)$$

In the case of an increase in the total load, the generator connected to the parallel operation at an initial moment, proportional to the constant time of the MSDG, can automatically "take over" all the surplus demanded by power consumers. This is due to the fact that the rest of the generators operating in steady state will supply constant power depending on the settings, which can lead to an unexpected inconsistency of the load between the generators.

To avoid such inconsistencies, depending on the current consumption and the calculation of the difference between the power of the particular generator and the connected, the load distribution unit, by affecting the PID-regulators of the MSDG on the frequency of rotation and voltage, eliminates the inconsistency that arises.

3.4. Methodology of synthesis of multi-criterial strategies for managing power distribution

It is proposed to use an additional in the hybrid SPP CPC of the BSPS, which consists of Electric double-layer capacitor (EDLC). Block diagram of the classical strategy of controlling the hybrid SPP CPC using EDLC for the criterion of minimum electricity consumption is shown in Fig. 3.2.

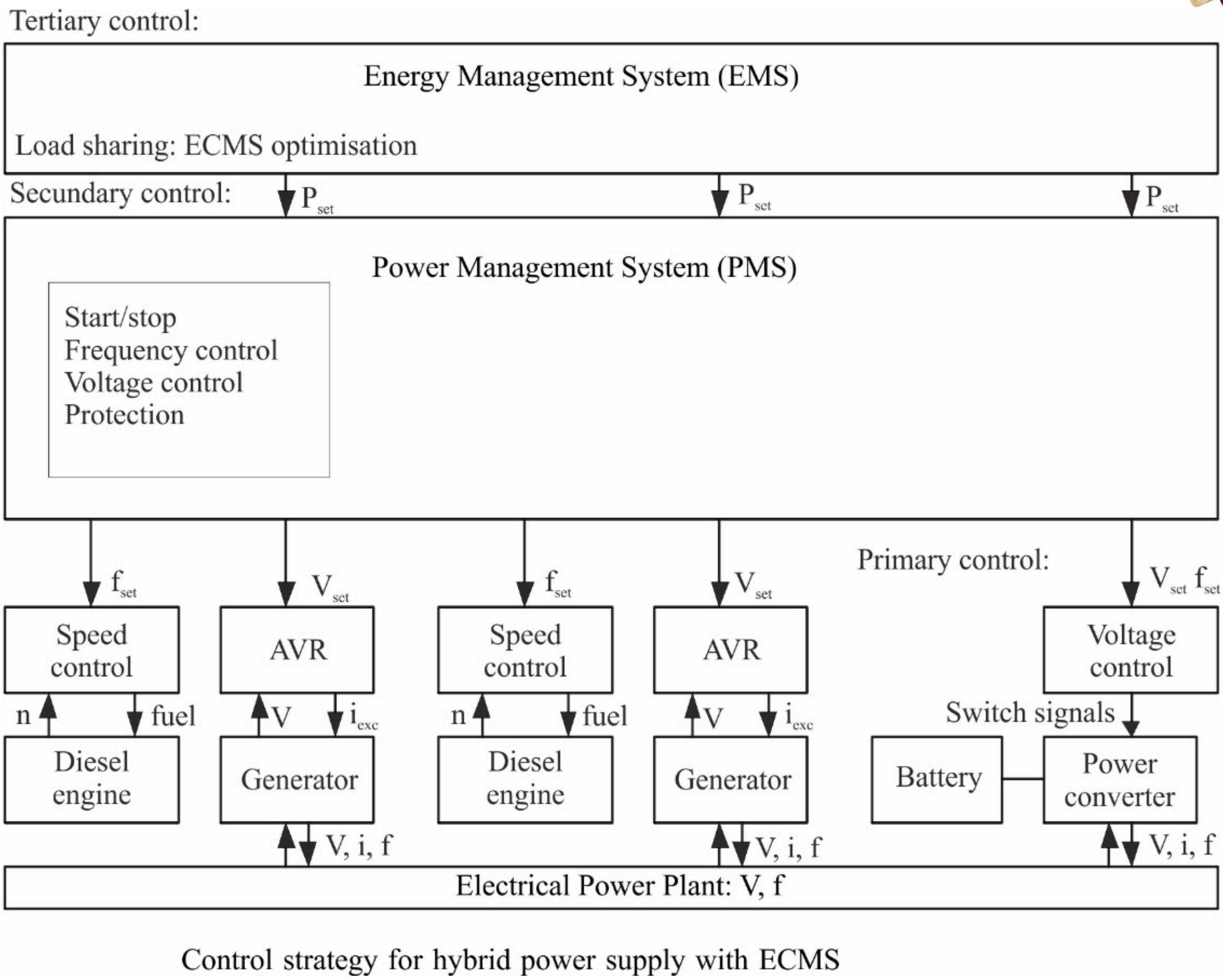

Fig. 3.15. Block diagram of control of hybrid SPP CPC for the criterion of minimum power consumption: AVR – Automatic Voltage Regulator; X_{set} – setting; P – power; f – voltage frequency; V – voltage; n – speed of rotation of MSDG; i_{exc} – current of excitation of generators; I – current of MSDG.

Based on the developed method, the strategy of controlling of the SPP CPC according to the criterion of the Equivalent Consumption Minimization Strategy (ECMS) has been improved by introducing the criterion for obtaining the maximum energy of alternatives (External energy maximization strategy with SOC's regulation – EEMS) and regulating the degree of charge of the battery of BSPS using PVGS to minimize fuel consumption. Observance of other criteria, such as noise, vibration, emissions to the environment or maintenance of MSDG, primarily depends on the operating point of the MSDG (Fig. 3.3) and PVGS [148] and is determined by the configuration of the electricity distribution control system.

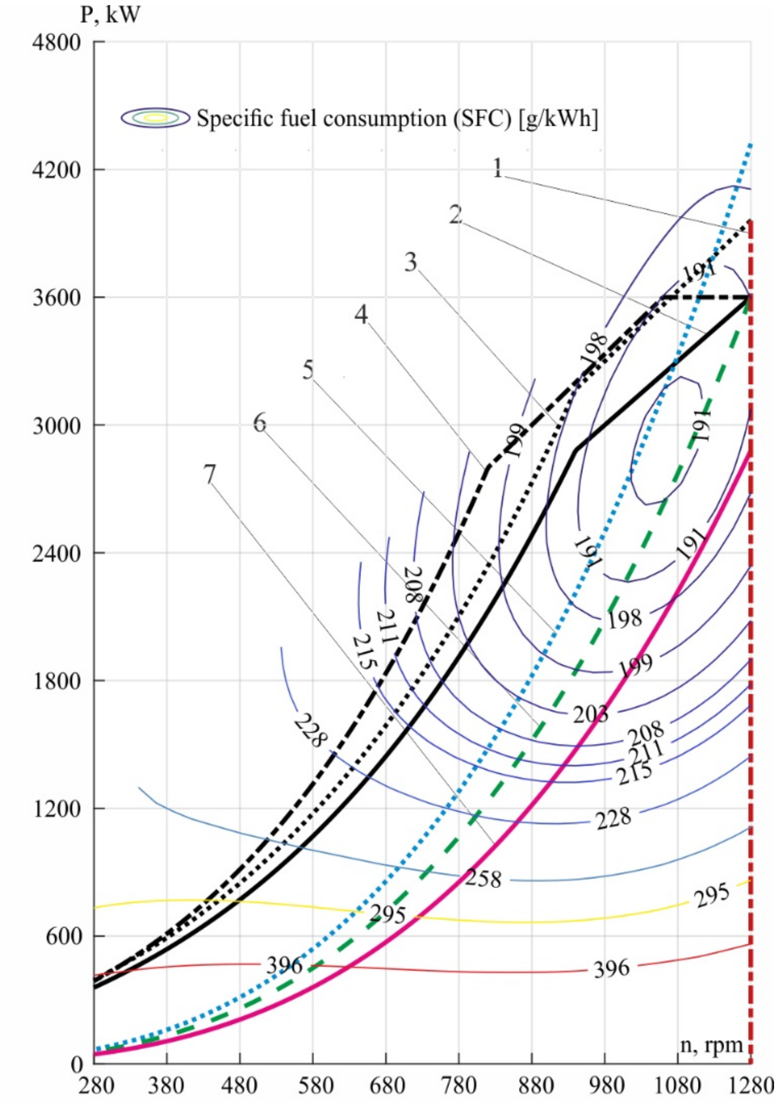

Fig. 3.16. Dependence of specific fuel consumption on load on MSDG and characteristics of propellers: 1-4 – characteristics of MSDG; 1 – barrier; 2 – loading; 3 – load bearing with high rating; 4 – load with sequential turbocharger; 5-6 – characteristics of propellers; 5 – settlement; 6 – on free water; 7 – test.

Thus, similar functions of costs depending on the mode of operation of MSDG can be obtained according to these criteria, and also the overall optimal power of the SPP CPC can be determined with the weighted function of costs for several criteria. Thus, improving the strategy by the criterion of obtaining the maximum energy of alternative energy and regulating the degree of charge of batteries of BSPS using PVGS becomes the promising approach to increase the efficiency of SPP CPC in comparison with many functions for future developments.

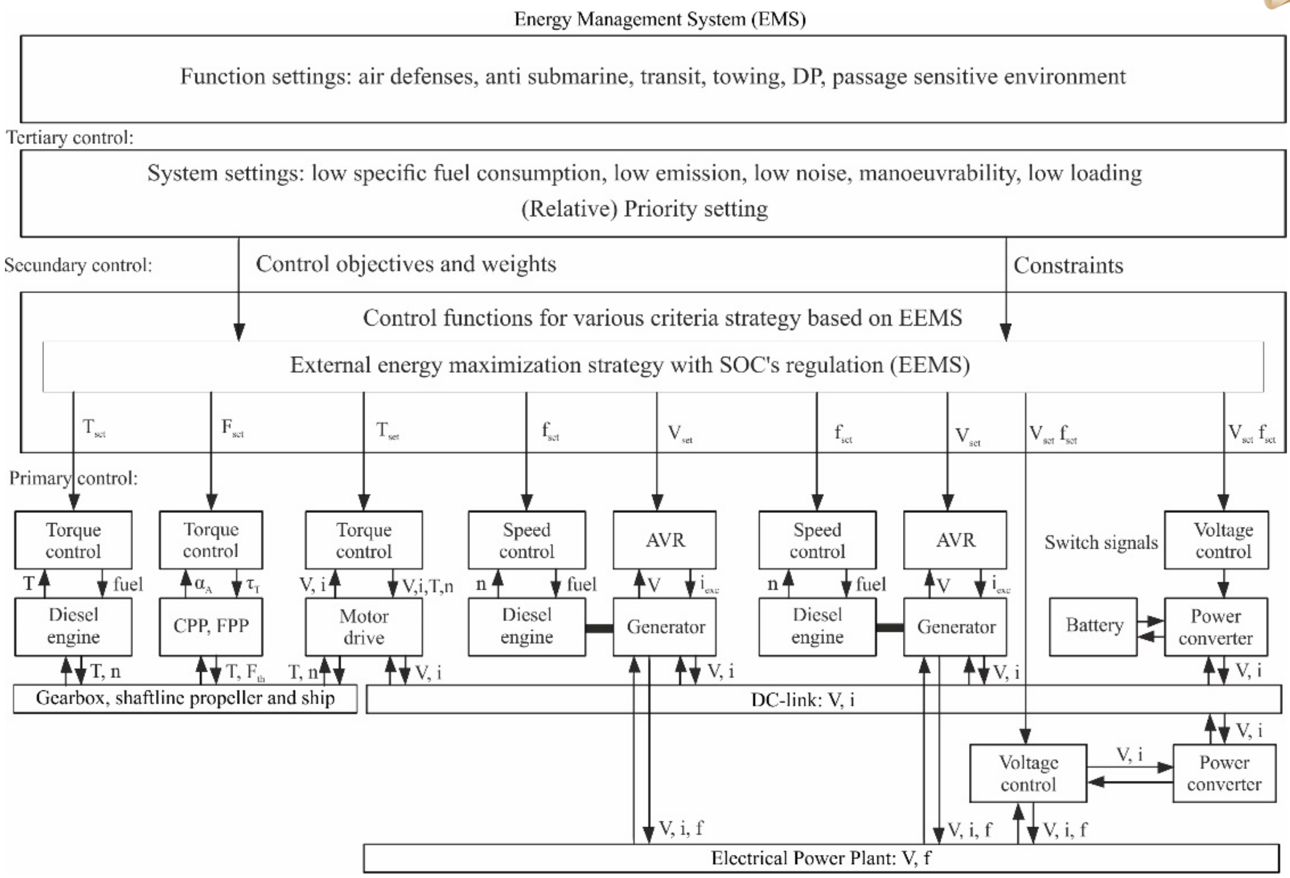

Fig. 3.17. Block diagram of the control strategy of the SPP CPC for the criterion of the maximum of alternative energy and the regulation of the battery charge level BSPS: X_{set} – setting; T – thrust (moment); F – force of propeller; f – voltage frequency; V – voltage; n – speed of rotation of MSDG; i_{exc} – current of excitation of MSDG; i – current; τ_T – resultant projection of the vector of effort on the plane of the vessel; α_A – angle of position of the THRs

Ultimately, further research should move through the integration of management strategies from the point of view of an integrated approach. The block diagram of one of the variants of the improved strategy of management of the integrated system with the hybrid SPP CPC and the so-called Western System Coordinating Council (WSCC) in Fig. 3.4.

The block diagram of the proposed system for monitoring the state of EDLC for one of the hybrid CPCs, strategy of controlling of which is given in Fig. 3.4, is presented in Fig. 3.5.

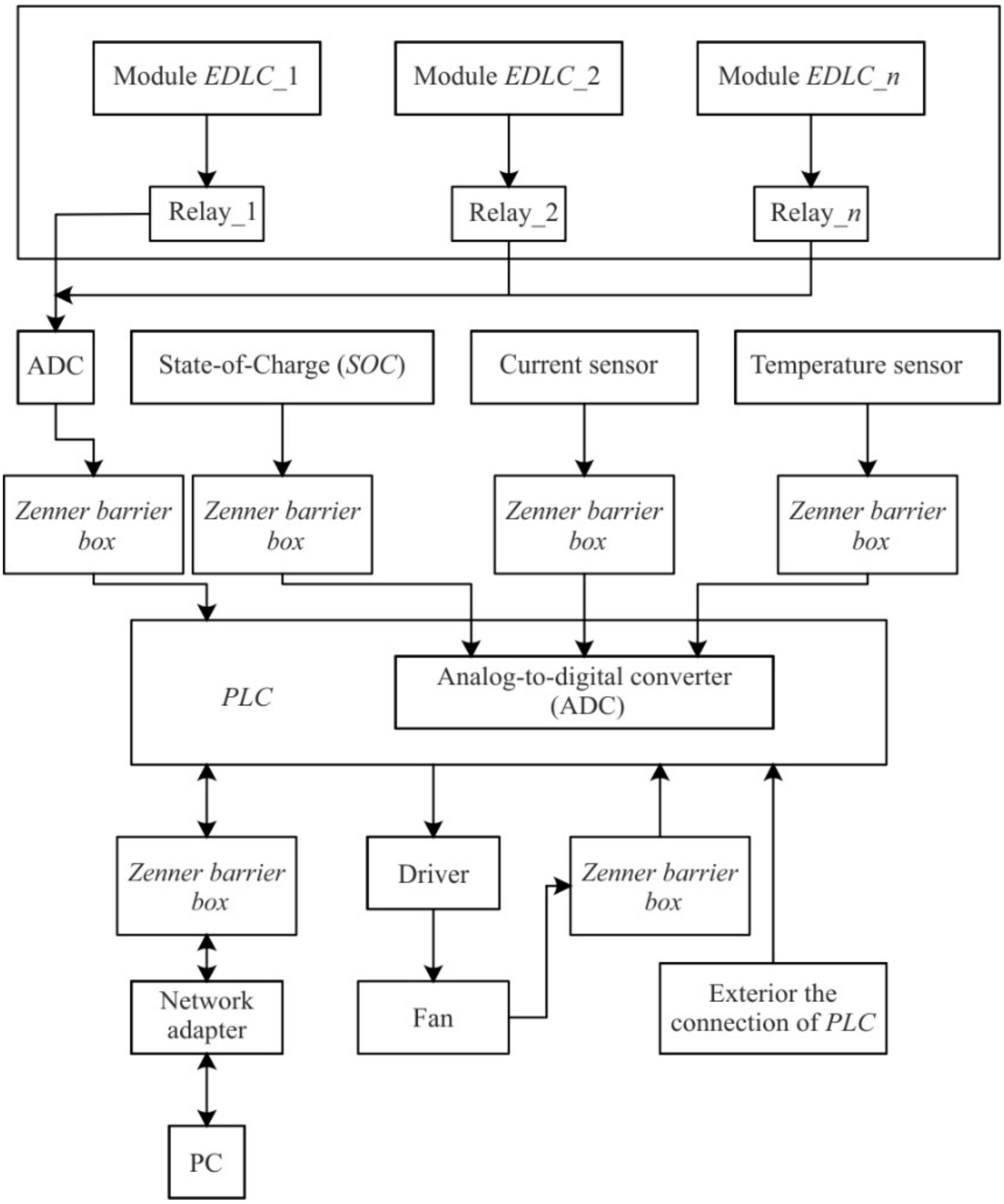

Fig. 3.18. Block-diagram of EDLC state monitoring system for hybrid CPC: ADC - analog-to-digital converter; PC - personal computer.

The energy of the discharge of condenser modules (Fig. 3.5) in the SPP of the CPC for the characteristics of the perturbing forces whose parameterization is determined by the equations (3.10) and (3.11), provided that all the thrusters in the coordinate plane of the direct control of the moment are determined by the (3.12) by estimating the integration of the total surface area of all EDLC modules under the galvanic discharge or charge curve.

$$\begin{cases} U_S(t) = I_S(t) \times Z_{SE} + t_{EM} \times \upsilon_S(t), \\ F_S(t) = I_S(t) \times t_{ME} + Z_{SM} \times \upsilon_S(t), \end{cases}, \tag{3.37}$$

where Z_{SE} – Impedance of the converter on the electric side; Z_{SM} – Impedance of the converter on the mechanical side; t_{EM} – constant time of electromechanical transformation; t_{ME} – constant time of mechanical-electrical transformation.

The general solution for the system of equations (3.10) will be to find the coefficients of the polynomial for the steady-state behavior of the disturbing forces determined by the flow quality according to the certain sensor provided that the operational mode of the SPP of the CPC remains unchanged beyond the calculation interval:

$$\begin{cases} \bar{U}_S(Z) = \bar{I}_S(t) \cdot Z_{SE} + t_{EM} \cdot \upsilon_S(t), \\ \bar{F}_S(Z) = \bar{I}_S(t) \cdot t_{ME} + Z_{SM} \cdot \upsilon_S(t), \\ (m_{cS} + m_{ncS}) \cdot \dfrac{d\bar{\upsilon}_S(t)}{dt} + \mu_S \bar{\upsilon}_S(t) + \mu_R \displaystyle\int_{\varepsilon_0}^{\varepsilon} \bar{\upsilon}_S(t)dt = \bar{F}_S(Z), \end{cases} \tag{3.38}$$

where $\boldsymbol{F}_S(\boldsymbol{Z}) = (\boldsymbol{F}_{S1}(\boldsymbol{Z}^1), \boldsymbol{F}_{S2}(\boldsymbol{Z}^2), \boldsymbol{F}_{S3}(\boldsymbol{Z}^3), \boldsymbol{F}_{S4}(\boldsymbol{Z}^4), \ldots, \boldsymbol{F}_{Si}(\boldsymbol{Z}^m))^{Tmatrix(i)}$; the complex impedance is determined by the matrices of the active and inductive components of the circuit for replacing the complex load $\boldsymbol{Z}^m = \boldsymbol{R}^m + p_i j\boldsymbol{L}^m$ (3.7), (3.8); $T_{matrix(i)}$ – matrix of the configuration parameters of the trimming devices, where ($i = 0 \ldots k$) is the number of the corresponding configuration CPC:

$$E_{\text{int/SOC}}(t) = I_{\text{EDLC}} \int_{U_{\text{EDLC\_max}}}^{U_{\text{EDLC\_min}}} U_S(t)dt \tag{3.39}$$

The following analysis of the method of different operating modes of the SPP CPC in terms of energy consumption, has allowed to identify the main criteria for comparing the fuel consumption and the state of the charge BSPS (voltage to DC-link). The overall efficiency of the system and the voltage at each source of energy that may affect the parameters of the operating mode was evaluated using an approach based on the inverse wavelet transformation of their instantaneous

ISBN 978-3-949059-43-8

capacities using the simulation model SPP CPC in MatLab/Simulink. On Fig. 2.4, Fig. 2.5, Fig. 2.6, Fig. 2.7, Fig. 2.8 shows the obtained characteristics during modeling of energy processes in the hybrid CPC for 350 *s* in the MatLab/Simulink environment. The load profile was determined according to the system of equations (3.7), (3.8) for cosφ = 0,8.

At the beginning of the simulation ($t = 0$ *s*), the power supply is provided by the main MSDG and PVGS of hybrid CPC is included for the charge of BSPS and preparation for emergency mode. At $t = 40$ *s*, there is the blackout of the vessel. PMS switches the load supply to alternative sources. At this time, additional load power is instantly secured from DC-link, where "realized" the reset of energy from the main consumers who worked in the generator mode, since the power of the PVGS is increasing slowly.

3.5. Results of simulation of energy processes in the hybrid CPC using of multi-criterial strategies for managing power distribution

In the chapter, further development of resource-saving ecologically clean technologies of operation of the SPP CPC through the use of alternative generating elements in designing power supplies and increasing their speed when changing operating modes, which allowed to improve the strategy of controlling the hybrid SPP CPC in terms of power distribution between BSPS, PVGS, SPP and other components of the SPP in accordance with the chosen energy management strategy. Namely: in the state machine control strategy; with PI-control and state-of-charge regulation (SOC), the classical PI-control strategy with the SOC regulation; with control of the frequency and state of the MSDG and frequency decoupling and state machine control strategy with SOC regulation (FDSMCS); equivalent consumption minimization strategy (ECMS); based on the criterion of obtaining the maximum of alternative energy and regulating the degree of charge of batteries. For the first time, a three-level multi-criteria strategy for managing energy distribution in the hybrid SPP CPC was synthesized by combining the classical power management control strategy with the control strategy for the MSDG state and the charge level of the PVGS of BSPS, which allows the design of flexible multifunctional power systems that integrate into the hybrid SPP CPC as an capacitive component, as well as parametrization of propulsion and power characteristics depending on the change of operating modes, hydrodynamics characteristics and environmental conditions. Important is the possibility of iterative optimization of the parameters of the SPP, which allows using the developed method as the means of intelligent design, the result of which is the improved performance of the SPP CPC. The proposed strategy compared to existing systems has the higher efficiency of detecting the risk of blackout of the SPP, greater reliability and accuracy in terms of determining the need for the reduction in load (within 150 milliseconds). The new concept is the fully integrated system with intrinsic controllers of the speed of rotation of the THRs and the power supply system.

For example, analyzing the obtained dependencies and the data in [31], we can conclude that the control of the frequency and state of the SODG with the regulation of the charge level of batteries BSPS , with all other equal conditions for operating mode, allows to reduce the quantity or power of the modules of the PVGS for 7 ÷ 10%, and management by using the criterion of obtaining the maximum of alternative energy and adjusting the level of the battery's capacity to use low-capacity rechargeable batteries in the range of 6 ÷ 8%. The concept of constructing the mathematical model of the SPP CPC [23, 24, 27, 30, 33], which takes dynamics of all its objects, including vessels in the transmission modes of power from MSDG to propellers, is proposed, confirmed its working capacity with the help of DSS Ships_CPC [21].

The comparative analysis of simulation results can only be carried out for similar strategies. Since today the proposed strategy is original, it is not possible to perform such an analysis. The indirect indicators of the benefits of the proposed strategy are, above all, to exclude blackout of the SAPP.

The researching of the influence of the parameters of the main regulators of the control system on energy processes in the SPP of CPC, confirmed the wide possibilities for the development and application of various effective strategies for the operation of the MSDG voltage stabilization systems. DSS Ships_CPC was developed using the Open System technology, which means its ability to reorganize, reconfigure and integrate into the technological processes of managing the energy system of the vessel of any complexity with the prospect of completion in the form of the universal structure.

KAPITEL 3 / *CHAPTER 3*
FORMALIZATION OF DEVELOPMENT OF PHYSICAL MODEL OF THE AZIMUTH THRUSTER BY THE METHODS OF COMPUTATIONAL FLUID DYNAMICS

4.1. Statement of the problem and analysis of the current level of technology development

The development of coastal shelf of the world's ocean, from the point of view of extraction of natural resources, the use of wind energy and current, has been going on at the very high rate. Carrying out drilling operations is one of the most important components of these processes.

In contrast to drilling on land, functional drilling schemes of marine drill-holes are complicated by the behavior of water between the wellhead and the drilling unit. Among the variety of technological processes employed in these operations, commonly used are, in particular, the stationary self-lifting tower (SLDR) and the semi-submersible self-propelled drilling rigs (SSDR), as well as drilling ships (Fig. 4.1). The main factor that influences the choice of the type of floating drilling facilities is the depth of sea at the location of drilling.

The drilling ships, due to better maneuverability and motion speed, better autonomy in comparison with SSDR, are used when drilling the prospecting and exploration wells in remote areas at the depths of water areas up to 3000 m. As opposed to SSDR, the drilling ships have considerable constraints for their operations depending on the sea state. Thus, during drilling, vertical pitching of the drilling ships must not exceed 3,6 m, while for SSDR – up to 5 m. The shortcomings of the latter include the low speed of motion.

The azimuthal thruster with the azimuth propeller-steering column (APSC) was developed and implemented in 1950. Over the subsequent period, these installations have gained positive reputation on the ships, which require high maneuverability under conditions of limited space. In 1990, the firm ABB Group (Sweden) put the high-torque electric motor inside the shell of APSC gondola and installed it on the tug Seilin (Finland), having registered it under the brand name Azipod®. Since then, this type of installations has been widely used on other types of ships. At present, APSC of power up to 20 MW is the remarkable propulsive solution for the wide range of ships [10, 11].

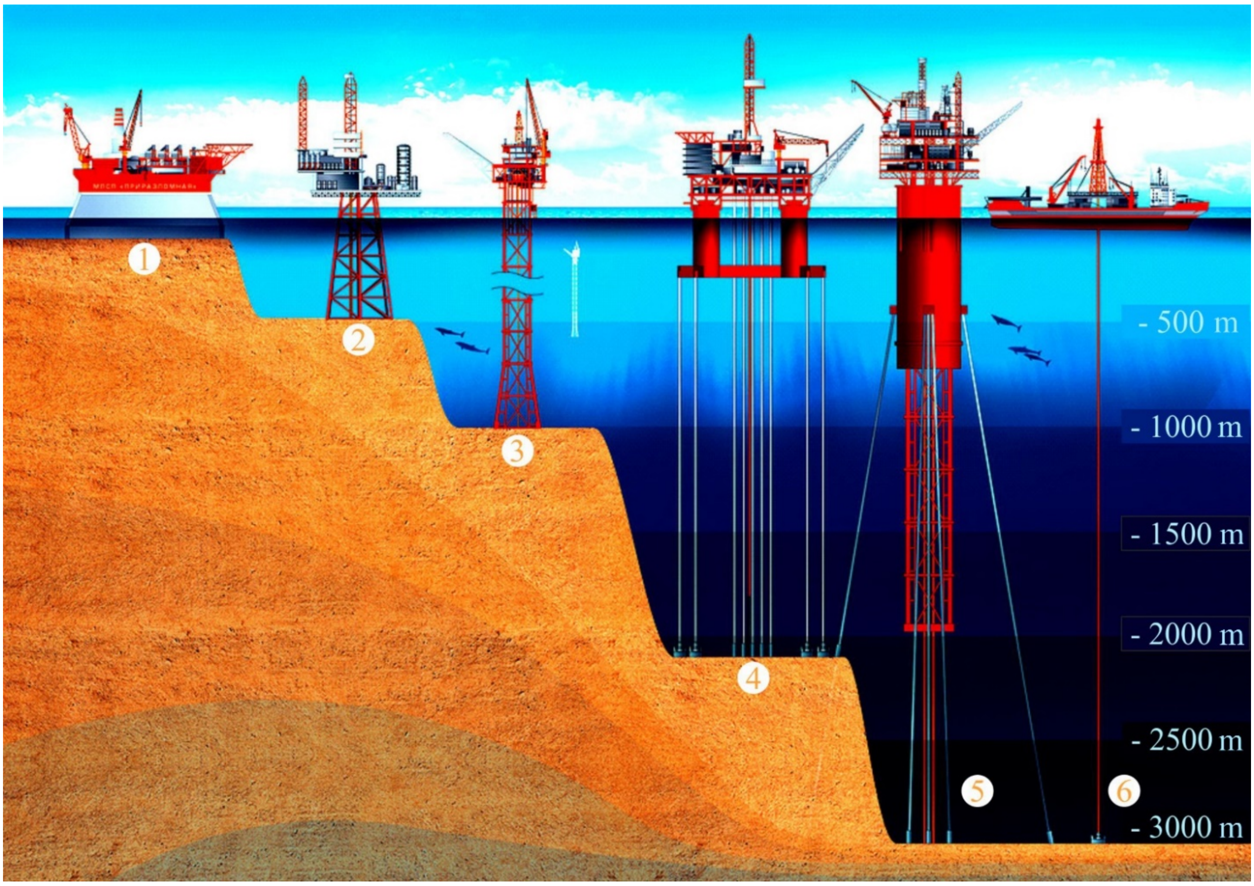

Fig. 4.19. Types of marine drilling means: 1, 2 – stationary drilling platforms; 3 – stationary self-lifting tower (SLDR) or the flexible tower; 4 – semi-submersible self-propelled drilling rigs (SSDR) of the type TLP (tension-leg platform); 5 – platforms of the type SPAR (Single Point mooring And Reservoir); 6 – drilling ships.

Recently, given the development of technology and more strict requirements for the precision of DP mode of ships, as well as to simplify maneuvers under conditions of limited operation space, ships are more and more equipped with APSC, which can be installed both as an optional and as the main propulsion units [11]. The main task is to ensure the stability of the ship and manageability in the wide range of these types of ships.

However, during the APSC operation, the situations occur when their safe and efficient work deteriorates [83]. Thus, one variant is the case of slow motion on course by ships that lay the cables and fixing the position for SSDR and other types of ships. In order to maintain the object in the position, APSC directs the water flow under the bottom of the ship and in this case there is the probability of occurrence of the Coanda effect when the flow "sticks" to the bottom of the ship [45]. In this ase, the force acting on the propeller leads to the deviation of the rowing shaft, which entails an increased wear of deadweight, propulsive and supporting bearings. Due to the design feature that locates the APSC below the waterline under the bottom of the ship, the access to diagnosis, routine maintenance and repair is hampered. The work of drilling ships is based on the dynamic positioning mode and premature failure of one of the APSCs may lead to tragic consequences, multi-billion dollar losses and technogenic disaster [57].

Unfortunately, predicting and calculating the process with detailed outline of all parameters is not possible because the occurrence of the Coanda effect is influenced by many factors, such as:

– the ship velocity, the speed and direction of propellers rotation;

– condition of the environment, chemical composition and the depth of water surface;

– the speed and direction of water flows from other APSCs that work together and are included in the system of dynamic positioning.

These factors do not make it possible to accurately predict the time of occurrence of this effect.

Depending on the technique of transferring the power to the propeller and its required need, APSC are divided into nine basic types (Fig. 4.2, *a–i*).

Standard modules Z-Drive made by Rolls-Royce company with input power from 250÷3700 kW (Fig. 4.2, a) to install on the tows, starting from 11 to more than 120 tonnes. Modular design allows changing the configuration, size and type of installation, in order to better satisfy the requirements of the user. These designs are available with reverse rotation of propellers to ensure high efficiency of engine with small subsidence, or with fixed pitch/controllable pitch (FPP/CPP) propellers, open or duct, with diameter matching the displacement.

APSC of the type Azippul (depending on the type of the ships) are characterized by low resistance and high efficiency that combines the advantages of thrust of the propeller with the flexibility of using the drive of capacity from 900÷5000 kW (Fig. 4.2, *b*).

Such steering propeller (SP) are designed for velocities of up to 24 knots while maintaining excellent maneuverability, hydrodynamic and fuel efficiency, low level of noise and vibration. Large area of rudder provides excellent course stability; in terms of minimizing the degradation effects, the units also enable the optimization of the stern part of the hull for minimum resistance and simplified design.

APSC Contaz® (Fig. 4.2, *c*) with the reverse rotation of propellers provides high efficiency of the engine and reduce vibration of ships with small subsidence. Efficiency can be improved in the range of 10÷15 percent compared to conventional azimuthal thrusters.

The stern FPP return the part of energy losses in the flow, as well as significant losses in rotation, which is why they are promising in terms of reducing the lower limit of power. APSC Contaz® have the wide range of the length of the stem and are ideal for passenger/car ferries and ships that operate in areas with limited terms of operating modes.

Reliable ultra-strong standard modules L-Drive (Fig. 4.2, *d*) are APSC designed specifically for long and reliable operation under DP modes for drilling ships and offshore drilling rigs. Compact design allows for easier installation and maintenance. There are two ways to connect the lifting actuators: flange from the middle of the ship to SP or external at the engine flange. SSC are controlled by the tools of hydraulic type.

Retractable structures of APSC models of the type UL ensure the rapid hydraulic lifting and lowering of the unit (Fig. 4.2, *e*) that allows reducing resistance to the motion of the ship. The UL models are designed for the horizontal drive with automatic system of disconnecting the shaft. The ULE models are designed for the vertical drive. Both are available with FPP or CPP.

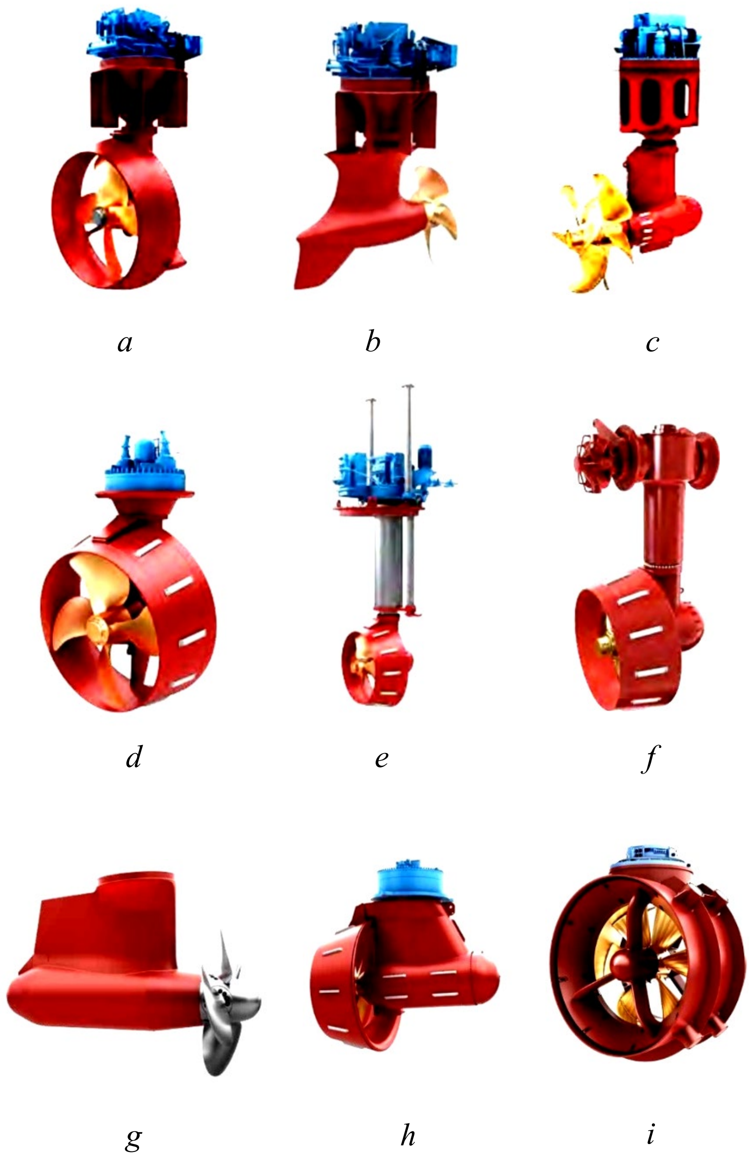

Fig. 4.20. Basic types of APSC: *a* – standard modules Z-Drive with power of 250÷3700 kW; *b* – modules Azippul with power of 900÷5000 kW; *c* – modules Contaz® with power of 2200÷3700 kW; *d* – standard modules L-Drive with power of 3000÷6,500 kW; *e* – models UL/ULE with power of 580÷3800 kW; *f* – model of the type Swing-UP with power of 736÷2000 kW; *g* – model of the type ICE/HICE of ice class with power of 4000÷18000 kW; *h* – model of the type PUSH with power of 4000÷12000 kW for ships operating on small speeds; *i* – model of the type TT-PM with power of 1000 and 1600 kW.

APSC of the type Swing-UP (Fig. 4.2, *f*) in submersed position act as azimuthal engines with thrust vectoring in any required direction to propel the ship or maintenance the position. In an elevated position, with special structures located in the hull, it can function as the tunnel motor (TH of tunnel type). APSC Rolls-Royce of the type Mermaid™ (Fig. 4.2, *g,e*) provides flexibility in the design of the ship and layout of equipment. Such designs combine the functions of propulsion engine, main propeller, steering unit and the stern thruster in one block. Ice-strengthened structures of the type ICE/HICE are specifically designed for all variants of equipment of SPP of CPC. These ships can operate under the most severe arctic conditions with the range of power from 4000 to 18000 kW (Fig. 4.2, *g*).

The models of the type PUSH (Fig. 4.2, *h*) with power from 4000 to 12000 kW are intended for operation at lower speeds, high loads and strict requirements to the control quality under an assigned operating mode. Equipped with hydrodynamically optimized nozzles to achieve maximum efficiency, such models of thrusters (THR) enable the operators to make the most of all the benefits of energy saving. THR based on APSC of the type TT-PM (Fig. 4.2, *i*) is the latest design of THR by Rolls-Royce. The design uses AC electric motors with permanent magnets with power of 1000 and 1600 kW, designed for the DP modes. Sensitivity of SPP CPC to various losses depends on the types of propellers and engines, the use of various stabilizers in the design of the ship hull and the principles of change in control algorithms. Thus, we can state that the principles of formalization in the development of physical models of THR of CPC SPP are the relevant issue. This is especially true for the process of selection and improvement of different designs of CPC and the adjustment of chosen regulators. All propulsion engines can operate under modes of regulating the moment (thrust) or rotation speed but each type of the SP has its own special features. Some important parameters will have slightly different values for different types of SP. Fig 4.3, *a-c* shows the schematic overview of action of thrusts of various types of engines of SP.

The losses of propellers, caused by the axial influx of water, depend on the following effects that will contribute to the reduction of thrust of the propeller and the torque:

– arrival of water perpendicular to the axis of the propeller caused by the current from the ship speed or flows from other engines with the force in the direction of flow through the deviation of propeller flow. It is often referred to as the cross-combination of thrusts [112];

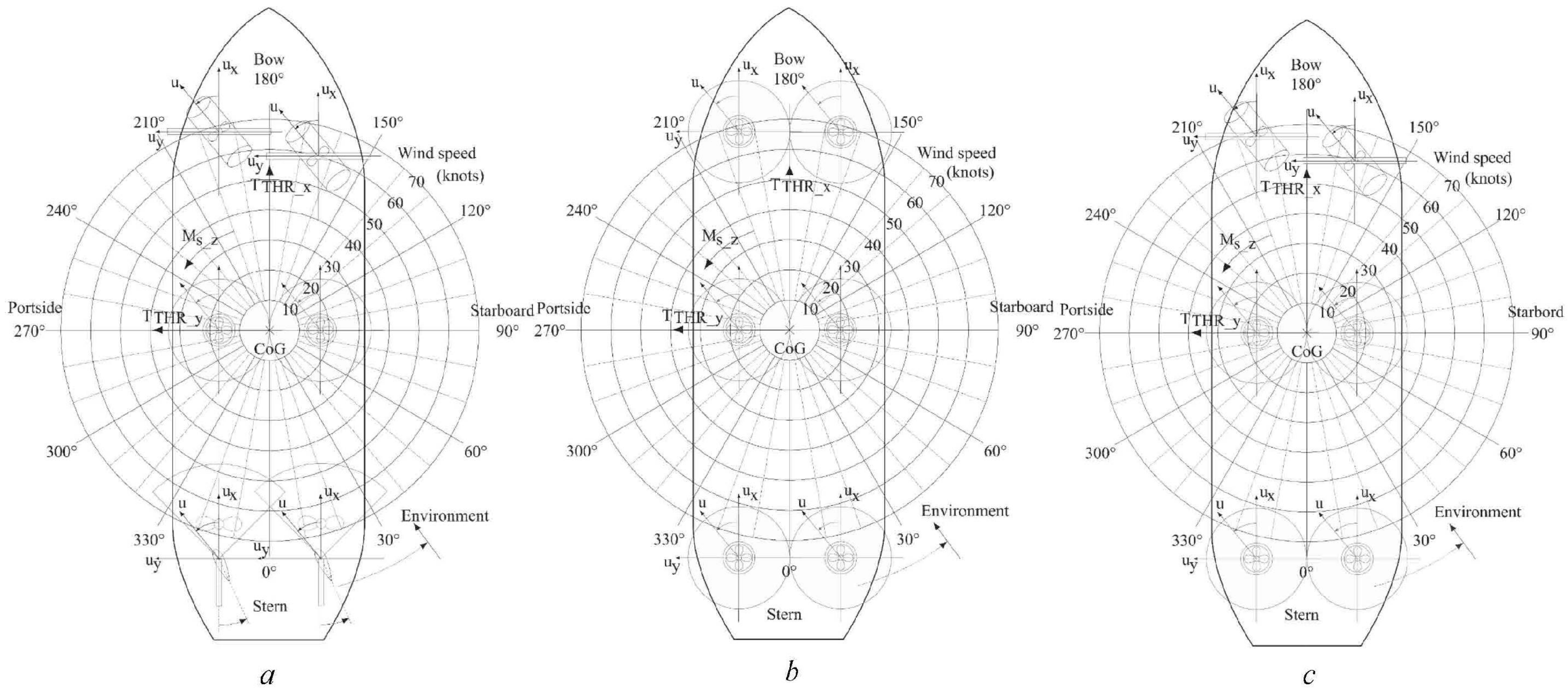

Fig.4.3. Action zones of thrusts of SP on different types of assembly of ship power plants of combined propulsive complexes: *a* – action zone of thrust of devices with the classical ship power plant in the stern of the ship and tunnel thrusters in the bow; CoG is the center of gravity; T_{THR_y}, T_{THR_x} are the thrusts of the SP along their respective axes; M_{S_z} is the ship's turning point; *b* – Action zones of thrusts for the ship power plant of combined propulsive complex with full assembly of thrusters of the azimuthal type; *c* – Action zone of thrusts for the ship power plant of combined propulsive complex with the partial assembly of thrusters of the tunnel and azimuthal types.

ISBN 978-3-949059-43-8

– the presence of cavitation for heavy loads on propellers (intake of air) leads to the decrease in pressure on the propeller blades and can occur at low immersion of the propeller due to the motion of ship across the waves [131];

– extreme conditions with large amplitudes of the motion of the ship perpendicular to the surface of water leads to the sudden drop in thrust and torque with the hysteresis effect [74];

– simultaneous reduction of thrust and reverse thrust can occur due to the interaction between the flow from SP and the hull, caused by the effects of pressure, when the small thrust of SP passes along the hull. This is referred to as the Coanda effect [7, 35, 126];

– loss of thrust of SP can be caused by the influence of the rowing flow from one engine on the neighboring engines, and lead to the significant decrease in thrust, if appropriate precautions are not taken in the algorithm of distribution of thrusts on SP [108].

The main losses when main propulsion motor (MPM) CPC SPP operate under the influence of non-determined loads is the interaction of flows of propellers (thruster-thruster interaction) and the interaction of flows with the hull (thruster-hull interaction). These effects have gained the general name in studies – degradation effects on the lines of propellers flows.

In order to evaluate and examine such phenomena, along with experimental data, the results of computation by the methods of Computational Fluid Dynamics (CFD) are employed.

The research base in the field of calculating the hydrodynamic processes on the propellers lines of MPM of SP of CPC SPP is the Navier-Stokes equations:

$$\frac{\partial \vec{\upsilon}}{\partial t} = -(\vec{\upsilon}\nabla)\vec{\upsilon} + v_w \nabla \vec{\upsilon} - \frac{1}{\rho}\nabla P_v + \vec{f}_m, \quad \nabla \cdot \vec{\upsilon} = 0, \tag{4.40}$$

where ∇ is the Nabla operator; Δ is the Laplace vector operator; t is the time [*s*]; v_w is the coefficient of kinematic viscosity, $\times 10^{-6}$ [m^2/s]; ρ is the medium density [kg/m^3]; P_v is the flow pressure, [Pa]; $\vec{\upsilon} = (\upsilon^1, \ldots, \upsilon^n)$ is the vector velocity field; $\vec{f}_m$ is the vector field of mass forces.

For the turbulent flows of water from the propellers of MPM of SP of CPC SPP it is based on the generalized equation of Navier-Stokes (4.1), which holds for both laminar and turbulent fluid flow mode. However, using the given equation for the turbulent motion regime is almost impossible. In it, the input instantaneous values of velocity and pressure of the flow are the pulsating magnitudes, which is why for the turbulent regime, the task is to find the time-averaged velocities and pressures. For this purpose, they apply the Reynolds equations received based on the Navier-Stokes equation, whose all terms undergo the operation of averaging over time [99].

To obtain adequate results of dependence at the levels of flows from the propellers, the operations of averaging must take place. These operations are based on the assumption that the averaging performed on it for any turbulent flow yield the magnitude of invariables during repeated averaging [152].

Pulsating variable components are characterized by frequency and amplitude, while the mean amplitudes of pulsation are characterized by appropriate coefficients of pulsations [104]. For example, for the Reynolds-averaged Navier-Stokes (RANS) equation, the method of averaging is to replace the flow characteristics (velocity, pressure, density) with totals of the averaged and pulsating components that randomly change. In the case of stationary flow of an incompressible Newtonian fluid, the Reynolds equation are written in the form:

$$\rho \frac{\partial \bar{u}_j \bar{u}_i}{\partial x_j} = \rho \bar{f}_{mi} + \frac{\partial}{\partial x_j}\left[-\bar{P}_{\nu}\delta_{ij} + \mu_R \left(\frac{\partial \bar{u}_i}{\partial x_j} + \frac{\partial \bar{u}_j}{\partial x_i} \right) - \rho \bar{u}'_i \bar{u}'_j \right]. \tag{4.41}$$

Variables averaged over time are marked in this equation with the line atop; the pulsation components – with an apostrophe. The left side of the equation (non-stationary term) describes the change in the volume of water flow motion from the propeller, due to the change over time in the averaged component of its velocity. This change is compensated for by the averaged external forces of perturbation $\rho \bar{f}_{mi}$, averaged by pressure forces $\bar{P}_{\nu}\delta_{ij}$ and viscosity forces:

$$\mu_R \left(\frac{\partial \bar{u}_i}{\partial x_j} + \frac{\partial \bar{u}_j}{\partial x_i} \right),$$

where μ_R is the medium viscosity coefficient or the coefficient of viscous friction.

Under certain operating modes, the medium viscosity coefficient defines assigning the limits to the Reynolds number. To achieve formalization of the physical model of the multifunctional combined propulsive complex, it is necessary to consider situational factors of the environment and identifying factors of operating modes.

The right side of equation (4.2) includes the set voltages $\rho \overline{u'_i} \overline{u'_j}$, which take into account additional losses and the redistribution of energy in the turbulent flow at the boundary with the laminar flow. The losses are caused by the emergence of the so-called degradation effects [125].

4.2. Formalization of the physical model of the azimuthal steering propeller with two degrees of freedom

The application of computational fluid dynamics in order to analyze the effects of degradation of flow from the propeller of azimuthal engine is still, to the large degree, is an unexplored area. These effects are important for the design of ships, especially for those that operate under the mode of dynamic positioning. Testing the real models is relatively expensive and in general become affordable at the later stages in the process of designing the technical tool. As an alternative, by using computational fluid dynamics of various designs of ships and engines at an early stage of design process, the effects of interaction can be explored in an economical fashion.

The aim of present research is to develop principles of applying the methods of computational fluid dynamics for the formalization of physical models of azimuthal SP in terms of tracking the degradation effects on the flow lines of propellers.

To accomplish the set aim, the following tasks are to be solved:

– at the preparatory stage, to form the geometry of the model and to formulate required physical conditions;

– discretization of the geometry and setting the initial and boundary conditions of differential equations;

– at the stage of calculation, according to the assigned algorithm, to solve basic equations in terms of fundamental physical parameters, as well as the arrangement of results of the solution;

– to represent the results of solutions in the form of graphs, tables, as well as outline/vector diagrams, related to the original geometry.

A physical model of SP with two degrees of freedom, the outer view of which is shown in Fig. 4.3, was developed taking into account the most important properties of SP, parameters of operational modes and situational factors.

Authors of article [92] used as software for computational fluid dynamics the package Marin ReFRESCO (Reliable&Fast Rans Equations (solver for) Ships, Cavitation (and) Offshore, Netherlands) which is widely employed for the visualization of flows around different objects. ReFRESCO solves the RANS equations (averaged Reynolds Navier-Stokes equations) for multiphase non-stationary incompressible flows. The system is supplemented with the models of turbulence and volumetric-fractional equations of convective diffusion for each phase. The equations are discretized employing the method of finite volumes in physical space. Implementation is surface-oriented, which makes it possible to generate grids with arbitrary number of faces or locally cleaned grids with hanging nodes.

In order to visualize the flow of azimuthal engine of SP of CPC SPP, we accepted the model in which the propeller is represented as an Actuator Disk (AD) [136]. The model of AD replaces propeller blades by the equivalent force distribution over the entire volume of the propeller. Such model is the application of the RANS equations on the model of propeller with the possibility of obtaining the results of modeling the flow from the engine in the open water, under the hull and on the end of the hull.

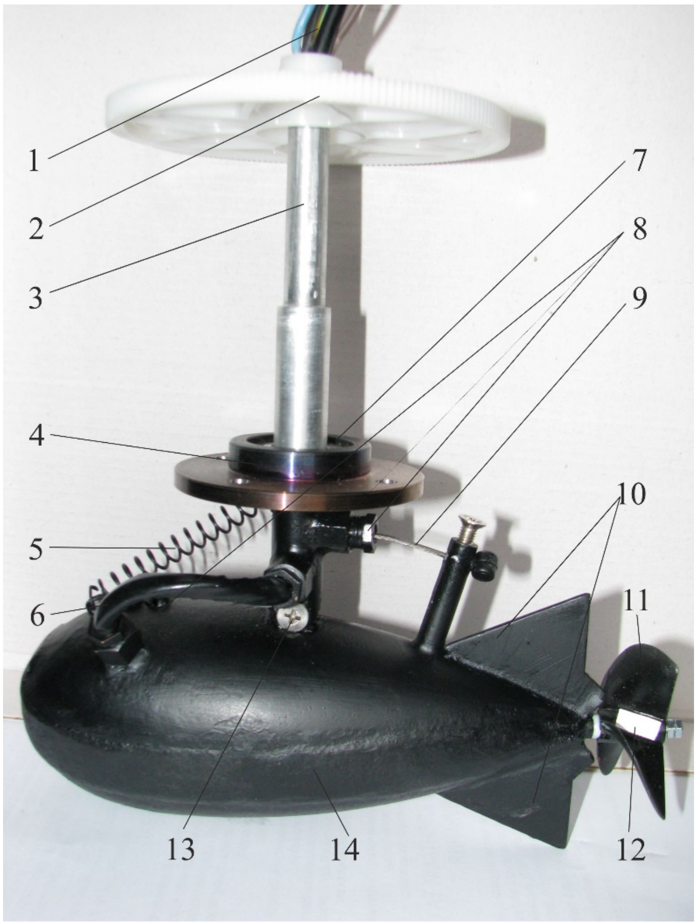

Fig. 4.21. Physical model of the thruster with two degrees of freedom: 1 – power cable of the propulsion asynchronous motor and the drive to change the sloping angle; 2 – anchor gear of the drive of rudderstock turning; 3 – rudderstock; 4 – bearing shield; 5 – feedback spring of the drive to change the sloping angle; 6 – power cable; 7 – supporting bearing; 8 – gland inputs; 9 – the rope of the drive to change the sloping angle; 10 – stabilization wings; 11 – screw of the fixed step; 12 – fluorescent label for the remote measurement of rotation frequency of the screw of fixed step; 13 – place of connecting the rudderstock to the body of the thruster; 14 – body of the thruster with an induction motor located inside

According to an analysis of information about the ship, the types of propeller are applied, as well as the modifications of SP, schemes of location of medium speed diesel engine (MSDE) of SPP and their structures. The indicated schemes are the multi-bus structures with the non-uniform distribution of impedance [32]. Such uniform electrical power systems are built by the technology of Flexible Alternative

Current Transmission Systems – FACTS. The application of methods of computational fluid dynamics to track the degradation effects on the flow lines of propellers is preceded by the systematization of required identification parameters and situational factors.

Calculation of effective traction efforts on propellers is the complicated condition. Iterative procedure for the solution of nonlinear equations (4.1), (4.2) are unstable for sustainable modes as there is no priority direction of flow in the larger part of the region. That is why it is necessary to apply the approach in which the action of the flow of SP is imposed in the direction of low velocity of the motion of the ship, thus bringing the active traction effort to the assigned boundary numerical conditions. For this purpose, thrust coefficients of propellers K_T and coefficients of the torque of propellers K_F for the current velocity of the ship υ_i will be defined equal to the corresponding coefficients for absolute velocity of the ship and the speed of inflow of water. The coefficients have to be formalized in accordance with the equations of similarity for the determined Reynolds and Froude numbers and coefficient of the favorable flow w_s: $\upsilon_a=(1-w_s)\upsilon_s$, where, as the rule, $0<w_s<0.4$:

$$F_p = \frac{\upsilon_i}{n \cdot D_p}, \tag{4.42}$$

where n is the rotation frequency of propeller, [rev/s]; D_p is the diameter of propeller, m. Relative step of propeller and its effectiveness in the open water are defined as the ratio of the actual work of propeller to obtain the force of traction to the work required to overcome the torque of thrust on the shaft. The values of Reynolds and Froude numbers for the limits of boundary conditions must be such that the flows of function and the force acting on SP are not under the influence of perturbing forces.

Fig. 4.4, a-*d* shows characteristics of the flows, and the components of *x*-velocities of SP for the model UL/ULE (Fig. 4.2, *e*) of power 1500 kW. The figures display significant recirculation zones near the stern stanchion that causes an increase in the load on the rotating axis (rudderstock) and external nozzle. This fact confirms the necessity of application of complex functions for calculating the energy indicators in the intersections of energy fluxes from MSDE to the engines of SP of CPC SPP.

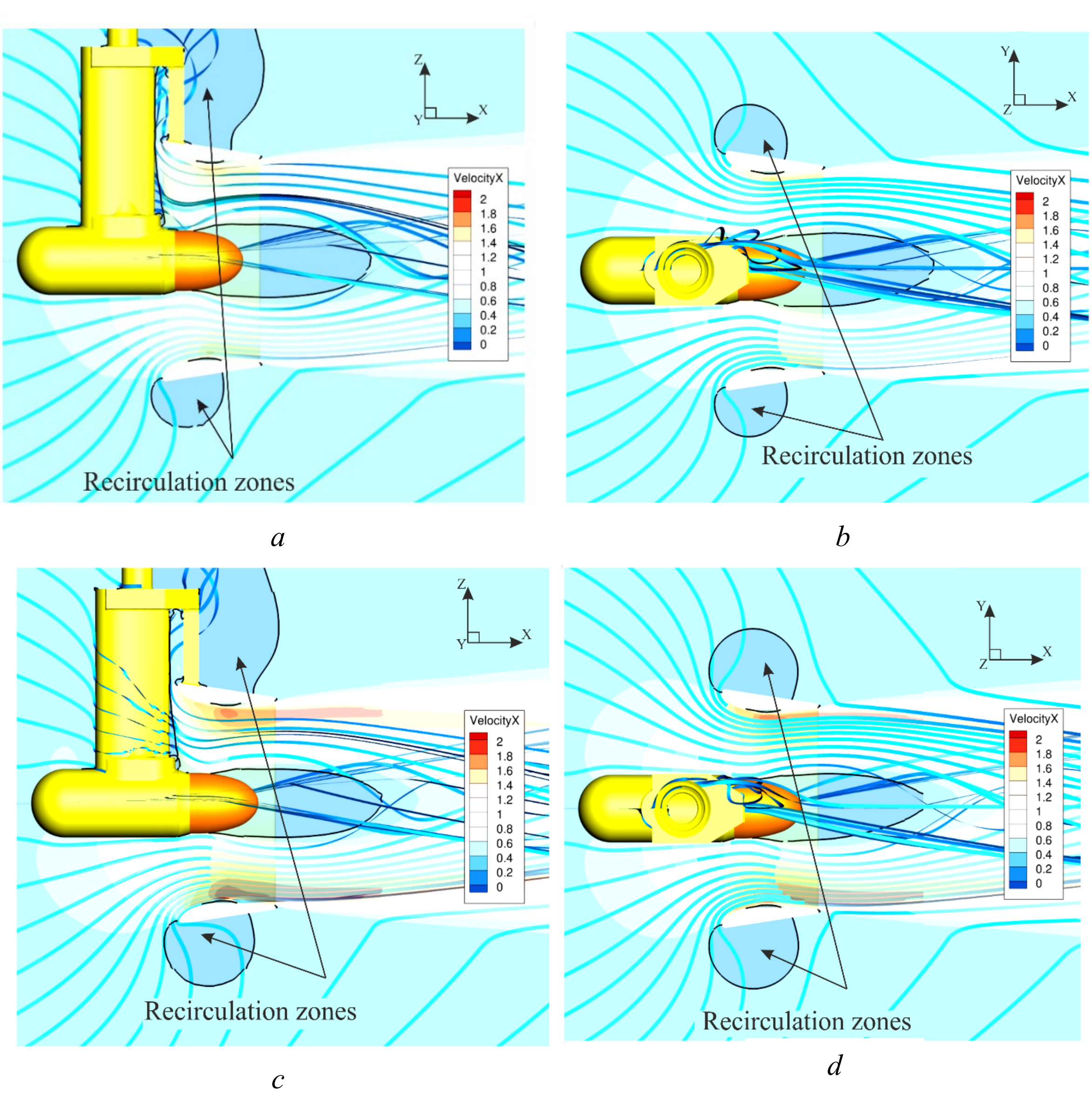

Fig. 4.22. Characteristics of flows and components of *x*-velocities of the thruster of the model UL/ULE with power of 1500 kW: *a, b* – for 70 % of the rated power on propeller shaft (side view and top view, respectively); *c, d* – for 100 % of the rated power on propeller shaft (side view and top view, respectively).

The corresponding (4.3) force of propeller thrust (CPP or FPP) of SP will be calculated based on the values of two radii (radius along the edge of propeller R_p and radius of intersection of the propeller blade r_p and thickness of the propeller blade b_p. These parameters can be unambiguously determined as the axial characteristics of blades from their intersection. Axial and tangential forces will be determined based on the thrust and torque of the propeller that is simulated. Axial forces F_x, F_y, F_z – as algebraic distribution that is scaled and integrated to the required thrust (4.3). The tangential force is determined by the actual value of propeller thrust T_d [29] taking into account properties of feeding voltage [18] and it is interrelated to such properties of propellers as the step ratio of propeller p_D (H_P/D_p). That is, all preliminary calculations of torques acting on the lines of propeller shafts of SP of CPC SPP will be carried out in the way given below:

$$\frac{F_x(\hat{r}), F_y(\hat{r})}{F} = \left(\frac{a+\hat{r}}{a+1}\right)^m \left(\frac{b+1-\hat{r}}{b+1}\right)^n,$$

where

$$\hat{r} = \frac{r - r_p}{R_p - r_p}, \quad (r_p \le r \le R_p), \tag{4.43}$$

$$T_p = \int_{-\pi}^{\pi} \int_{0}^{1} F_x(\hat{r}), F_y(\hat{r}) d\hat{r} d\theta. \tag{4.44}$$

Distribution of axial forces (4.3) is parameterized according to the values of identification coefficients a, b, m, n, or the so-called characteristic markers of energy flux (situational factors) characterize the particular operational mode. The nonzero distribution of axial component of the force can be established over the entire range ($r_p \le r \le R_p$) by careful selection of parameters a and b. The values of integral components correspond to the selected direction of propeller thrust T_p.

In turn, tangential components of thrusts and torques are calculated as follows:

$$\frac{F_\theta}{F_x, F_y}(\hat{r}) = \frac{{}^{H_P}\!/\!{}_{D_p} \times R_p}{\pi \times r}, \tag{4.45}$$

$$M_p = \int_{-\pi}^{\pi} \int_{r_p}^{R_p} r \times F_\theta(\hat{r}) d\hat{r} d\theta. \tag{4.46}$$

Fig. 4.5, *a-d* shows the visualization of force flows from an azimuthal engine of SP of SPP CPC executed by the above technique. The flows are represented as AD, where it is visible (Fig. 4.5, c). One can see that along the rotating guides there occurs the capturing of output flow to the lines of the recirculation zone. This effect leads to the emergence (Fig. 4.5, *d*) of recirculation zones on the y-plane and identification of turbulent areas with relative coefficients of vortex viscosity $\mu_{t/}\mu_w$.

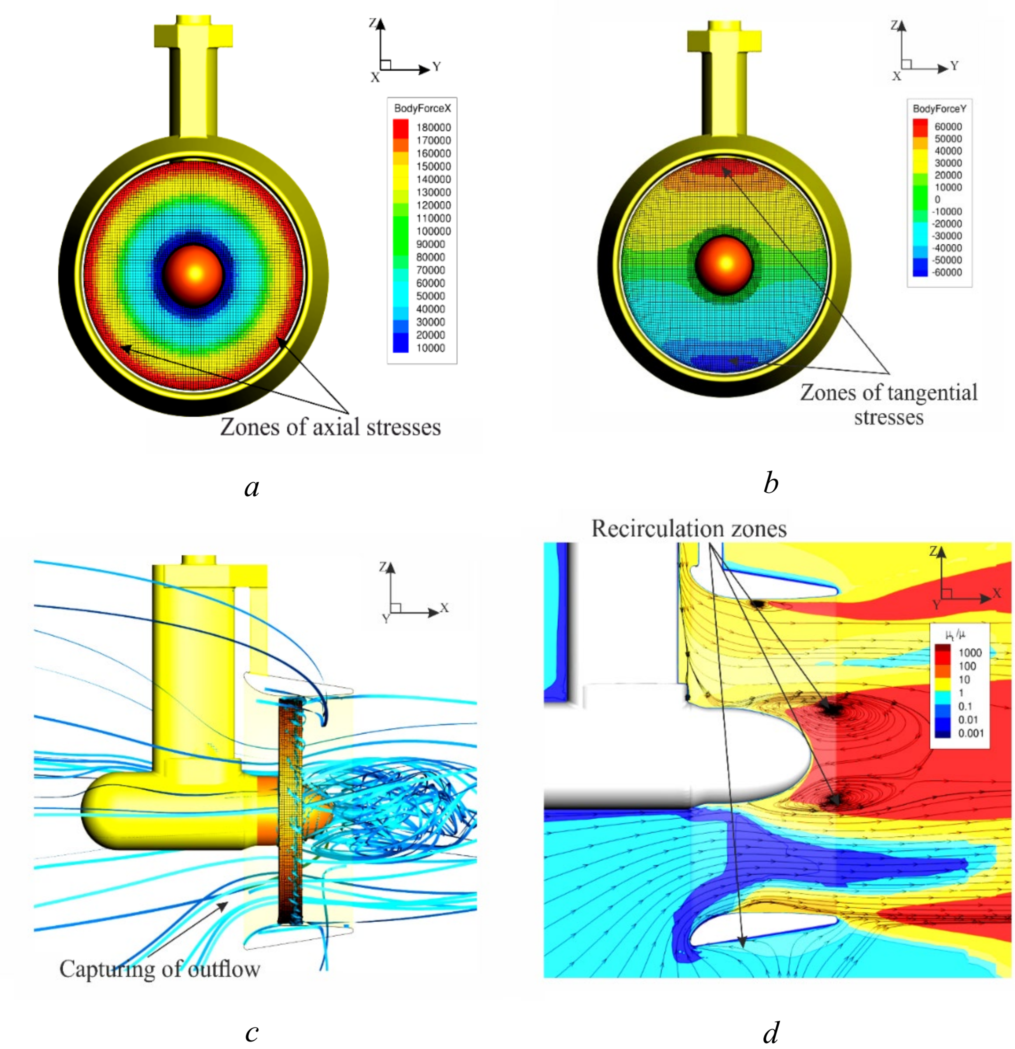

Fig. 4.23. Visualization of flow from azimuthal engine of SP of CPC SPP in the form of actuator disk (AD): *a* – axial and *b* – tangential components of force flows with identified zones of stress; *c* – capturing of the outflow to the lines of recirculation zone on rotating guides; *d* – recirculation zones on the y-plane and identifications of turbulent regions with relative coefficients of vortex viscosity $\mu_{t/}\mu_w$.

On the other hand, the above recirculation zones give rise to degradation effects. Fig. 4.7, *a-d* shows comparative analysis of trajectories of components of x-velocities of the propeller flow of SP. The measurements were carried out in the intersection of the flow of azimuthal propeller along the axis of rotation with dimensions in units of the propeller diameter D_p.

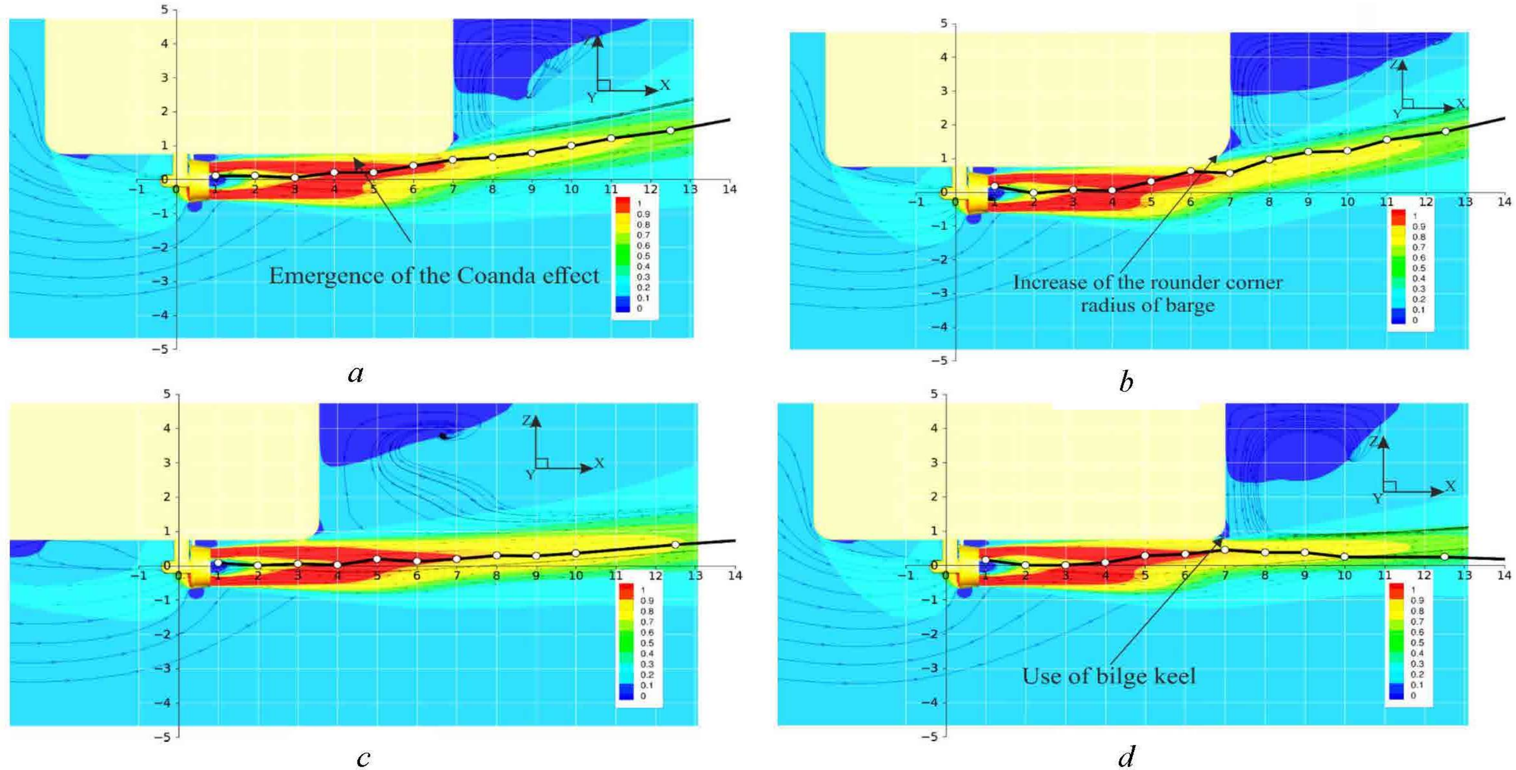

Fig. 4.7. Comparative analysis of trajectories of components of x-velocities of the propeller flow of the thruster by measurement results: emergence of the Coanda effect: *a* – standard radius of rounding the hold hull; *b* – increased radius of the rounded hold hull; *c* – reducing the sticking of flow by moving the fastening point of rudderstock of the thruster closer to the edge of the hull; *d* – use of hold keel on the envelope line of the hull.

 ISBN 978-3-949059-43-8

As the summary, it should be noted that notwithstanding the possibility to increase the number of intersections of measurements, some points along the trajectory remain inaccessible, which makes it impossible to fully analyze effectiveness of the proposed methods of dealing with the above mentioned effects. That is why preliminary results of formalization of the physical model of the thruster come down to determining the Reynolds and Froude numbers (4.3) for the zero-velocity model of the ship.

4.3. Results of calculating the power components of radial distribution of thrusts in the physical model of thruster

Fig. 4.7, Fig. 4.8 show comparative results of the two sets of parameters for power components of radial distribution of SP thrusts in the moving coordinate system. The values of the components of forces are not given on graphs because the distribution is scaled for the assigned thrust and torque.

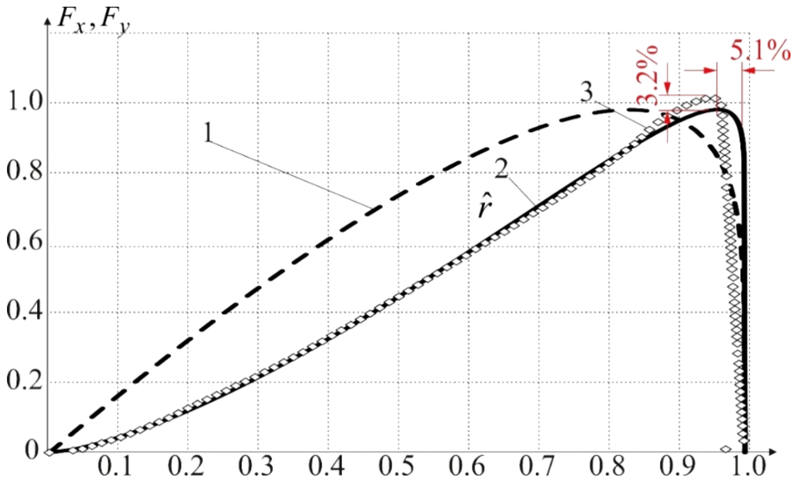

Fig. 4.7. Components of axial forces, proportional to the radius of the envelope line of propeller blades: 1 – initial parameters according to the boundary conditions of operating mode and situational factors (Table 4.1); 2 – selected parameters; 3 – according to pre-set specifications

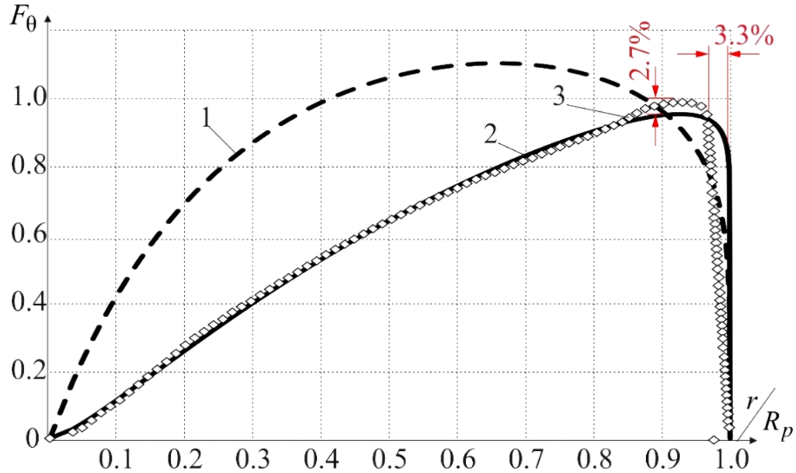

Fig. 4.8. Components of tangential forces, proportional to the radius of propeller: 1 – initial parameters according to the boundary conditions of operating mode and situational factors (Table 4.1); 2 – selected parameters; 3 – according to pre-set specifications

Data were calculated for the model of SP whose identification parameters and situational factors of CPC SPP are given in Table 4.1. The initial selection of parameters of axial forces of the model was conducted according to equation (4.4), and then, taking into account the data received in [36] for the model of SP AD, these initial assumptions were refined. By analyzing results for the open water at 100 % propeller rotation velocity, we found the following set of identification parameters of the physical model of SP for maximum thrust:

$$(a, b, n, m)^{*}=(0; 0; 1{,}45; 0{,}06). \qquad (4.47)$$

Iteration solution (4.3), (4.4), (4.5), (4.6), (4.7) for the found parameters (4.8) and corresponding coefficients of similarity allows us to formalize the Reynolds and Froude numbers for zero velocity of the model of the ship: R_n=4,405×10^6; F_r=3,124. In this case, the ratio between propeller diameters of the model and an actual ship should be such as to ensure maintaining the similarity of appropriate thrusts (4.6) and torques (4.7).

Fig. 4.7, Fig. 4.8 illustrate that the proposed method allowed us to specify the components of axial and the tangential forces of radial distribution of SP thrusts within the limits of 2,7÷5,1 %. According to (4.8), the largest deviation of similarity coefficients occurs in the region of 85÷100 % of the rated propeller thrust. The value of corrective factors depending on the propeller flow direction relative to the plane of motion of the ship is within the few hundredths of the percent.

Table 4.6.

Identification parameters and situational factors of CPC SPP of the model of the ship of the type Supply Ship

Parameter (factor)	Characteristic of parameter (factor) in accordance with the operating mode
D_p	Propeller diameter
λ (H_P)	Propeller relative step
K_T	Propeller thrust coefficient
t_s	Horizontal retention ratio
n	Rotation frequency
n_N	Rotation speed
P_v	Flow pressure
H_P/D_p	Propellers constructive step
T_p, T_{THR}, T_d	Propellers thrust, thrust of thruster, real value of propeller thrust
R_p	Propeller radius
R_n	Reynolds numbers
M_p	Propeller torque
υ_a	Water inflow rate on the propeller plane
υ_s	Ship absolute velocity
υ_i	Current ship velocity
F_l, F_x	The force acting on the ship lengthwise l_s
F_h, F_y	The force acting on the ship widthwise h_S that predetermines the appropriate angle of heel
F_z	The force acting on the ship in the direction of motion that predetermines the appropriate yaw angle
l_S, l_M	Length, respectively, ($_S$) – of the ship (to be assigned), and ($_M$) – of the model of the ship (to be calculated)
b_S, b_M	Width, respectively, ($_S$) – of the ship (to be assigned), and ($_M$) – of the model of the ship (to be calculated)
h_S, h_M	Subsidence, respectively, ($_S$) – of the ship, and ($_M$) – of the model of the ship
υ_{sx} (u_s)	Velocity of longitudinal motion of the ship in the Cartesian coordinate system
υ_{sy} (v_s)	Velocity of lateral motion of the ship in the Cartesian coordinate system
υ_{sr} (r_s)	Velocity of yaw of the ship in the Cartesian coordinate system

 ISBN 978-3-949059-43-8

υ_{saxi}	Axial component of velocity of the motion of the ship in the cylindrical coordinate system
υ_{stg}	Tangential component of velocity of the motion of the ship in the cylindrical coordinate system
μ_w	Dynamic viscosity coefficient
ν_w	Kinematic viscosity coefficient of turbulent flow
ρ	Water density
τ_T	Vector of thrust and torque
Ω	Rotation frequency

When analyzing preliminary results of an analysis, we see that on the flow line from SP propeller there are significant tangential forces. There is also the "sticking" of the flow to the ship hull, which creates the degradation of thrust, reduction in the coefficient of useful action of propeller η_{pF} for the given value of K_F and increase in the coefficient of relative vortex viscosity $\mu_{t/}\mu_w$. This leads to excessive stress on the suspended structure of SP, which creates mechanical stresses that damage the most critical design details: bearings, seals, and shaft. In addition, it worsens such operating regime of the ship as the dynamic positioning. Results of the analysis and practice of manufacturing such units reveal that the most common technique for eliminating these effects is the use of nozzles, tilted relative to the plane of the hull bottom at about 7 degrees. This solution does not avoid such effects either, and significantly reduces the efficiency of the unit, which is associated with increased consumption of fuel and pollution of the environment.

The major unexplored problem in that direction is how to impede the free fluid coming from one side of the flow. The turbulence created in the region of low pressure contributes to the emergence of significant tangential forces that act on the rudderstock of SP perpendicular to the flow direction. They do not completely solve the problem on increasing the radius of rounding the hold hull, moving the point of fixing the rudderstock of SP closer to the edge of the hull and use of hold keel on the envelope line of the hull. Results of the study are protected by appropriate patents on useful models [113, 114, 115], and implemented in the developed decision support system when designing and examining the CPC SPP.

4.4. Systematization of parameters and factors according to the operating mode

We calculated the geometry of physical model of the thruster with two degrees of freedom and specified the required physical conditions for its implementation. For the zero-velocity model of the ship: Reynolds number $R_n = 4{,}405 \times 10^6$; Froude number $F_r = 3{,}124$. We formalized geometric parameters of the model, assigned the initial and boundary conditions of differential equations that describe behavior of flows of propellers in the recirculation zones and coefficients, which take into account the existence of degradation effects. Components of the axial and tangential forces of the radial distribution of SP thrusts are refined within the limits of 2,7÷5,1 %. According to the assigned algorithm, we obtained solutions to basic equations in terms of fundamental physical parameters, as well as arranged the results of solutions. The largest deviation of similarity coefficients is in the region of 85÷100 % of the rated propeller thrust. We received dependences of adjustment factors that affect the components of thrusts and torques proportional to the radius of the model and the actual SP, related to the original geometry. The value of corrective factors depending on the propeller flow direction relative to the plane of motion of the ship is within the few hundredths of the percent. We systematized and compiled in the table the list of parameters (factors) according to the operating mode of the ship, which are required for solving the basic equations in the formalization of physical models of thrusters.

KAPITEL 4 / *CHAPTER 4*
THEORETICAL-APPLIED ASPECTS OF THE COMPOSITION OF REGRESSION MODELS FOR COMBINED PROPULSION COMPLEXES BASED ON DATA OF EXPERIMENTAL RESEARCH

5.1. Quality assessment of design of marine power plants of combined propulsion complexes

This condition arises at the early stages of designing long before the construction and making technical decisions to improve performance efficiency of SPP CPP. For this purpose, models of the processes in CPC SPP and in the systems, described by mathematical dependences, which is of interest to designer, characteristics of operating conditions and parameters of CPC SPP devices are used. In the process of designing any CPC SPP, including the control system (CS), various types of models at different stages are employed. Initially, if it is possible, analytical models for control problems are compiled, for example, in the form of systems of differential equations or logical-algebraic expressions [59]. Then the algorithms are selected that make it possible to bring solutions to the problems to numerical values. For this purpose, numerical methods of solution and numerical models of problems are widely applied. To conduct the study using an electronic computer (EC), it is necessary to translate numerical models into programs and information arrays, that is, to create informational and software models [87].

Such the research path, based on the application of analytical models, is often inadequate due to the large dimensionality and complexity of the models obtained. Therefore, man-machine methods for simulation modeling of complex systems have become widespread [29].

Simulation models are implemented on EC using universal high-level algorithmic languages or system modeling languages, as well as Decision Support System (DSS) [22]. Simulation modeling implies carrying out experiments with the model represented in the form of the set of algorithms describing behavior of CPC SPP. The simulation process is executed by running the multitude of sets of experimental data according to the operating mode and situational factors of the programs based on them [21, 22, 62]

The main advantage of simulation modeling is its universality and the possibility of ensuring high adequacy of the examined model of CPC SPP to the actual object. This is achieved through the deep elaboration of the algorithmic description, which is impossible during study conducted by analytical methods that are associated with the simplification of processes and strict restrictions on the conditions of using the model.

Thus, for example, in analytical study of the transfer of power to propellers, an attempt at taking into account the influence of random factors of the operating mode for the model of CPC SPP leads to significant difficulties which sometimes are impossible to overcome. In the study of CPC SPP, simulation modeling under conditions of random environmental effects is not difficult and it is currently the most effective one. Moreover, at the design stage, this method is practically the only available means of obtaining information about the behavior of CPC SPP. In summary, one can say that the modeling of processes in CPC SPP during the transfer of power to the propellers is the major design problem of any CS. Models and methods of optimization used in the design of CS of SPP CPP are determined by the content of specific control tasks, research tools, and by the technical implementation of the components of CPC SPP and are the relevant problem. This specifically concerns decision-making process on the selection and improvement of SPP structure and CPC design, as well as adjustment of all-mode controllers of propulsion devices CS.

5.2. The distribution of models according to the purpose of the study when designing

The models of CPC SPP that are used in the process of their design, can be divided into classes, each of which corresponds to the certain purpose of research in designing within the framework of the developed DSS.

The class of dynamic models includes models that represent mathematical description of the processes of transfer of power to the propellers of CPC. These models are widely used in the design of CS for thruster drives (TDs) and power distribution systems. Mathematical forms of models depend on the accepted method for measuring coordinates of the object's state and time. In connection with the digital implementation of CS, discrete-continuous models (DCM), which represent the processes in discrete time in the form of differential equations, acquire an increasingly specific weight.

Methods of classic and extended variation calculus have been widely used in the analytical design of all-mode controllers. Many tasks on determining the optimal values of control parameters can be solved using the Pontryagin maximum principle [9]. This method, for example, can solve the problem on the construction of the multi-level operating strategy of CPC SPP, optimal by speed. Such strategies ensure the transition from one ship's operational mode to another under conditions of existing restrictions on activities.

Given the application of DSS, models and optimization methods based on the principles of mathematical programming have been widely developed. Thus, in various DSS, algorithms for optimizing the energy processes in CPC SPP, which are under position keeping mode, and based on the principles of dynamic programming, have high efficiency. Objectives and methods of optimization have been widely covered in the scientific literature. In [124], for example, the author developed the fuzzy-probabilistic model for risk assessment of complex technical systems and its schematic structure. An analysis of various modeling techniques depending on the architecture of intelligent control strategies of CPC SPP was considered in [60]. And in [135], an attempt was made to categorize safety indicators of CPC SPP with their further implementation into mathematical models of energy processes.

The use of probabilistic models is predetermined by the necessity to account in the process of designing CPC SPP for various random factors and situational factors of operating modes, which in many cases have the decisive influence on the characteristics of CS.

Thus, for example, consideration of the random nature of incoming requests from numerous devices of CPC SPP is necessary when determining productivity of the multilevel CS over power distribution. Random values of the magnitudes measured in the process of control are the cause of the nondeterministic number of operations performed by CS during implementation of control algorithms.

When substantiating the chosen control strategy for the allocation of power, models of energy processes in CPC SPP are particularly important. Such models make it possible to determine the required efficiency of information processing devices and the throughput of communication channels, rational sequence of CS functioning, as well as develop algorithms to control resources of CPC SPP.

The discrete models include graph and algebraic models designed to develop the complete model of functioning of CPC SPP during simulation modeling in the framework of the developed DSS.

Control complexes of CPC SPP consist of the large number of different devices and systems and are characterized by the presence of numerous external and internal random effects. These are environmental perturbations, changes in the hydrodynamic characteristics of CPC associated with the hull fouling, the occurrence of failures in the elements of systems that require localization of malfunctions to prevent emergency situations, etc. In connection with this, the needs to resolve certain problems of information processing and the time of actually solving these problems are also of random character.

Many tasks in information processing, related to controlling and managing technical means of CPC SPP, are of cyclic nature. However, in general, the accidental impact of the environment on CPC generates irregularity in the use of devices that perform various control and operational functions. The random magnitude is also the time spent by CS on processing the information during control process since the algorithms for solving problems possess ramifications, and contain cycles. The number of operations performed during implementation of such algorithms depends on the random values of the measured parameters.

All this necessitates employing probabilistic models in the design of CPC SPP.

Such models are necessary both for describing the processes of performing individual tasks by algorithms and for describing systems that perform the certain set of control and operational tasks. In [141], the author presented results of simulation modeling of the fuzzy controller with the fuzzy dynamic correction for the nonlinear control of objects with variable parameters. The methods that were applied by the author were used in the fuzzy proportional-differential (PD) controller, which made it possible to reduce overtime of the task and shorten the time needed for the controlled parameters to return to an equilibrium. For the ships that is in the ice region, two probabilistic data-driven models were devised [105] that take into account the stop mode of rowing electric motors under current. Two full-scale datasets were utilized to design the models. First, the set of navigation data of the selected ship in the "heavy" water obtained using the system of automated identification. Second, the data set obtained from the numerical model of "heavy" water of Helsinki Multi-category sea-ice model (HELMI), developed by Finnish Meteorological Institute. The new approach to the systematization of construction of mathematical models of the medium surface fluctuation is presented in [6]. Based on the Markov models chain, cross-correlations were drawn between successive wave heights and periods. In addition, by employing the Karhunen-Loève theorem, the distributions of probabilistic transitions were obtained; continuous analogues of discrete heights, periodic fluctuations were constructed; groups of waves were derived for assessing the condition of ships under irregular environment. In paper [56], the authors proposed the methodology for optimizing the design of CPC SPP by solving two objective functions. The first objective function is an extended fuel consumption; the second one is the cost function that takes into account traction, torsion torque, propeller's characteristics in free water, as well as coefficients of deviation from circulation. The obtained results failed to solve the problem of simultaneous design of the structure of CPC and the choice of types of screw propellers.

DSS with mass service models can be used as models of functioning of CS of CPC SPP intended to solve the certain set of computational problems in the process of managing power distribution. In [55], on the example of automation of cargo handling works, the authors proposed the matrix-geometric method for their improvement. Paper [75] addresses solution to the problem of developing the two-dimensional model of cargo handling, which makes it possible to confirm the minimality of two indices of optimal efficiency of ship's functioning. The two-objective model for developing the reliable two-directional motion of ships in the logistic service network under conditions of uncertainty of their technical condition is proposed in [138]. The objectives of this modeling are to minimize the overall and expected costs for the transportation of the ship after the breakdown.

Such studies are the complicated labor-intensive process, which requires the development of specialized software for simulation on EC. Simulation modeling is typically carried out when designing CPC SPP whose structure can vary in certain specified limits. More accurate estimates of the characteristics of CS of SPP CPC are obtained by the simulation modeling employing the method of statistical tests and construction of CPC SPP models based on data obtained during experimental research.

5.3. Fundamentals of the construction of models of ship power plants in the combined propulsion systems based on experimental data

The objective of present study is to develop principles for the construction of regression models of ship power plants for combined propulsion complexes based on data obtained during experimental research data. This will make it possible to study internal properties of CPC SPP with determining the laws that describe their behavior depending on the situational factors, which correspond to the certain operational mode.

To achieve the set objective, the following tasks have to be solved:

– to study internal properties of the components of CPC SPP and to define fundamental laws that describe behavior of certain classes of these components;

– to determine the function that connects the input variables and the output variable based on experimental data and which contains N common observations of

ISBN 978-3-949059-43-8

input and output magnitudes;

– to verify adequacy of the model obtained using data from experimental tests.

Distinctive features in the construction of equations that characterize energy processes in the specific SPP of the specific CPC are the problem of mutual implementation of spatial vectors, taking into account certain situational factors in accordance with the change in the operational mode.

For example, for stepwise relations $p_{Di}=H_P/D_{pi}$, the magnitudes of thrusts and torques of CPC that operates under mode of dynamic positioning, the process of maintaining the ship at the given point is determined by the vector of effort τ_T, which is described by equation (1.14), where u_T is the vector of variable thrusts of TD applied to the ship (1.15); $K_{Tmatrix}$ is the matrix of coefficients of propellers' thrusts (1.16); T_{matrix} is the matrix of TD configuration (1.17).

The forces of thrusts of TD, which are determined by vector (1.14), are divided into continuous, transverse, and angular (dislocation) components by the matrix of TD configuration. For example, the ship of the Supply Vessel type has four azimuthal and one bow tunnel TDs installed. The azimuthal TDs are located between the diametrical plane and the bow and can rotate at any angle α_A relative to the diametrical plane of the ship: two main azimuthal TDs and two auxiliary ones, which extend from the ship's hull. Given this, we have the following configurations of thrusts that are applied to the ship: $u_{T1,2}$ are the thrusts of the main azimuthal TDs; $u_{T3,4}$ are the thrusts of the auxiliary azimuthal TDs, u_{T5} is the thrust of the bow TD.

On the other hand, the algorithm for the formation of controlling influences g_i and ε_i according to the operational mode of CPC of the ship taking into account (1.14), (1.15), (1.16), (1.17), consists in solving the problem on the mutual implementation of spatial vectors of energy processes in SPP and CPC by using representation operator $\boldsymbol{R}_{(\Psi)F}$: $(\overset{U}{x_i}, \overset{U}{\delta_i}, \overset{U}{y_i}) \xrightarrow{R(\Psi)F} i, \overline{I}_i$, which connects dependences of change in voltage U on current I of the load. Controlling influences g_i and ε_i can be formed to provide medium speed diesel-generator (MSDG), as energy sources, with the properties of the single operator $\boldsymbol{E}_F$: $\boldsymbol{I}=\boldsymbol{E}_F\times\boldsymbol{I}$ i $\varphi=\boldsymbol{E}_F\times\varphi$.

In this case, the component-wise composition of vectors of the x_i, δ_i, y_i variables can be different for the stated task, and represent the certain subset $\bar{I}_i$ of the set of the whole set of variables $\bar{I}$. Components of vectors x_i, δ_i, y_i , selected in such the way, are the most effective in the given situation.

If the properties of SPP and CPC are represented by charts in the form of the implementation of any stochastic process of the change in the load of MSDG when changing the operating mode of CPC $I_i(t)$ and $\varphi_i(t)$ at i = 1, 2, ..., then the functional analogue of single operator $\boldsymbol{E}_F$ must have two controlled coordinates $I^m(t)$ and $\varphi^m(t)$, whose values correspond to (3.7) and (3.8).

Thus, it can be stated that the traditional use of classic method of the least squares (MLS) for estimating the parameters of regression equations characterizing energy processes in CPC SPP will run into objective obstacles due to the fact that the number of observations may turn to be less than the number of internal degrees of freedom of the observed models.

In this case, in order to construct an empirical model that connects energy processes in SPP and CPC and is based on determining function $y=\varphi\ (x_1, x_2, \ldots, x_n)$ by experimental data, which contains N common observations of the input and output magnitudes, it is necessary to perform identification of characteristics:

$$\varphi(x_1, x_2, ..., x_n) = \beta_0 + \sum_{(i=1)}^{n} \beta_i x_i + \sum_{(i,j=1)}^{n} \beta_{ij} x_i x_j + ..., \tag{5.48}$$

where $\beta_i=\partial\varphi/\partial x$; $\beta_{ij}=\partial^2\varphi/\partial x_i \partial x_{ij}$; i, j=1, 2,…, n.

Based on (1.17), we choose the structure of the model of CPC SPP. We determine the number of counted terms of the power series, the number of required identifications and the weight of coefficients. The model is constructed in the form of the polynomial with the number of terms, restricted by the linear part of the identified characteristics.

At certain statistical properties of vectors of variables x_i, δ_i, y_i, applied to SPP and CPC, coefficients of the model will be evaluated by experimental data using the regression analysis procedure. Having experimental data in N points in the region of determining independent variables, and having the matrix of observations X and output vector Y, the empirical regression model of CPC SPP is constructed in the form of the regression equation:

$$X = \begin{bmatrix} x_{11} & x_{12} & \cdots & x_{1n} \\ x_{21} & x_{22} & \cdots & x_{2n} \\ .. & .. & .. & .. \\ x_{N1} & x_{N2} & \cdots & x_{Nn} \end{bmatrix}; \; Y = \begin{bmatrix} y_1 \\ y_2 \\ . \\ . \\ . \\ y_N \end{bmatrix}, \tag{5.49}$$

$$\hat{y} = b_0 + \sum_{(i=1)}^{n} b_i x_i + \sum_{(i,j=1)}^{n} b_{ij} x_i x_j + ..., \tag{5.50}$$

where b_0, b_1, b_{ij} are the sample estimates of coefficients from equation (5.1); $\hat{y}$ is the estimation of mathematical expectation of random variable y. In this case, the MLS criterion takes the form

$$Y = \min \sum_{k=1}^{N} \left(y_k - \sum_{i=0}^{t} b_i x_{ki} \right)^2 . \tag{5.51}$$

In order to calculate coefficients of the regression equation that provide the minimum value of criterion (5.4), it is necessary to solve the system of equations derived by zeroing the time derivatives from the residual sum from unknown variables $b_0, b_1, \dots, b_t$:

$$\frac{\partial \sum_{k=1}^{N} \left(y_k - \sum_{i=0}^{t} b_i x_{ki} \right)^2}{\partial b_i} = 0; \quad i = \ 1, \ 2, \dots, t.$$

The equations thus obtained are close to the normal MLS equations, which should be appropriately solved, representing them in the matrix form:

$$\left(X^T X \right) B = X^T Y, \tag{5.52}$$

where X is the matrix of observations of independent variables; X^T is the transposed matrix X; Y is the vector-column of observations of dependent variable; B is the vector-column of coefficients of the regression equation.

Coefficients of regression model B and the y values calculated using it are the random variables, but in order to estimate model's errors and its suitability for the description of the examined SPP and CPC, it is necessary to repeat statistical processing of the results of the experiment as many times as it took for the identification procedures to be carried out.

Therefore, for the system of random variables $b_0, b_1, \ldots, b_t$ with theoretical mean values $\beta_0, \beta_1, \ldots, \beta_t$ we shall compile the matrix of other central moments defining all the statistical properties of coefficients B, and hence the regression equation $\hat{Y}=XB$. We obtain the matrix of variations-covariations M^{-1}, along the main diagonal of which the variation estimates are located, while the remaining places are taken by estimates to the variations of coefficients of the regression equation:

$$M^{-1} = \begin{bmatrix} s^2\{b_0\} & \text{cov}\{b_0 b_1\} & \cdots & \text{cov}\{b_0 b_m\} \\ \text{cov}\{b_1 b_0\} & s^2\{b_1\} & \cdots & \text{cov}\{b_1 b_m\} \\ .. & .. & .. & .. \\ \text{cov}\{b_m b_0\} & \text{cov}\{b_m b_1\} & \cdots & s^2\{b_m\} \end{bmatrix}.$$

Hence, we obtain the ratio for the estimates of variations and covariances of the coefficients of regression equation $s^2\{b_i\}=c^2_{\text{ij}}\{y\}$; $\text{cov}\{b_i b_j\}=c_{ij}s^2\{y\}$.

The evaluation of variation of reproducibility $s^2\{y\}$ is determined from formula

$$s^2\{y\} = \frac{\sum_{k=1}^{N} \sum_{q=1}^{m_k} (y_{kq} - \bar{y}_k)^2}{\sum_{k=1}^{N} (m_k - 1)},$$

where $\bar{y}_k$ is the mean value of magnitude y_k determined based on data from m_k repeated experiments. The magnitude $f_y = \sum_{k=1}^{N} (m_k - 1)$ is the number of degrees of freedom of variation in the reproducibility of the entire experiment. The estimation of variations in coefficients of the regression equation allows us to determine significance of the coefficients, that is, to refine the structure of the CPC SPP model. For this purpose, we shall employ the Student t-criterion to determine the confidence interval

$$\Delta b_i = \pm t(\alpha, f_y) s^2\{b_i\}, \qquad (5.53)$$

where $t(\alpha, f_y)$ is the tabular value of t-criterion for the chosen level of significance α and the number of degrees of freedom f_y.

In order to determine suitability of the model obtained, we shall estimate variation of the predicted value of the output magnitude in point k $s^2\{\hat{y}_k\}$ and the variation in adequacy s^2_{ad}, which characterizes spread of experimental results in relation to the predicted regression equation values.

The estimation of variation in the predicted value of response $s^2\{\hat{y}_k\}$ at each point of the experiment is determined based on the error summation rule

$$s^2\{\hat{y}_k\} \approx \sum_{i=0}^{n} \left(\frac{dy}{db_i}\right)_k^2 s^2\{b_i\} + \sum_{i=1}^{t} \sum_{j=0}^{t} \left(\frac{d^2 y}{db_i db_j}\right) \operatorname{cov}\{b_i b_j\},$$

or in the matrix form

$$s^2\{\hat{y}_k\} = X_k^T (X^T X)^{-1} s^2\{y_k\} X_k = X_k^T M^{-1} X_k,$$

where X_k is the coordinate vector of the k-th experiment point. The estimation of variation in adequacy is determined from expression

$$s^2_{ad} = \frac{1}{N-L} \sum_{k=1}^{N} (\bar{y}_k - \hat{y}_k)^2,$$

where L is the number of coefficients included in the regression equation after the removal of insignificant coefficients. The magnitude $f_{ad} = N–L$ is called the number of degrees of freedom in the variation of adequacy.

In order to check the statistical hypothesis about the homogeneity of variations, we employ the Fisher’s F-criterion:

$$F_e = \frac{s^2_{ad}}{s^2\{y\}}.$$

If the obtained model is not adequate, then it is necessary to include additional terms in the equation, to reduce the region of change of independent variables, or to increase the number of identification procedures, so that the modules of vectors (1.14), (1.15), (1.16), (1.17), (3.7), (3.8) and (5.1) are equal to the single value.

5.4. Results of constructing the empirical model of CPC SPP in accordance with the goal of functioning

Here are the results of determining the dependence of thrust moment M_c on the shaft of TD CPC SPP with the FPP on the number of shaft rotations n_s and the step ratio H. The shape of static characteristic of plant $M_c=f(n_s,H)$ is influenced by various external factors (environment condition, fouling of the propeller, change in draught, etc.). Therefore, in order to provide the optimal operating conditions for SPP in the process of dynamic positioning, it is necessary to adjust this dependence, that is, to perform the identification of characteristics. Table 5.1 gives results of measuring the moment on the shaft of the engine M_s under steady-state conditions (at $dn/dt=0$) when $M_s=M_c$ for different values of shaft rotations n_s and the step ratio of propeller H. All values are given in relative units: $m_c=M_c/M_n$; $n=n_s/n_n$; $h=H/H_m$, where M_n, n_n are the nominal values of moments and engine rotations; H_m is the step ratio that corresponds to the maximum thrust of FPP.

Table 5.7

Values of shaft rotations, step ratio of the propeller, and the moment of thrust in different points of the experiment

Parameter	1	2	3	4	5	6	7	8	9	10	11	12	13	14
n_s	0,32	0,44	0,49	0,57	0,63	0,68	0,73	0,77	0,81	0,86	0,91	0,95	0,96	1,0
H	0,6	0,95	0,01	0,3	0,6	0,01	0,95	0,96	0,3	0,6	0,95	0,01	0,3	0,6
m_c	0,16	0,34	0,06	0,11	0,38	0,07	0,66	0,74	0,21	0,55	1,08	0,10	0,30	0,76

Dependence $M_c=f(n_s,H)$ is essentially nonlinear, which is why we give regression equation in the following form

$$m_c=b_0m_0+b_1n+b_2h+b_3nh+b_4n^2+b_5h^2.$$

We shall introduce fictitious variable x_0=1 and denote $x_1=n_1$; $x_2=h$; $x_3=nh$; $x_4=n^2$; $x_5=h^2$; $y=m_c$. Then the regression equation will take the form

$$\hat{y}=b_0+b_1x_1+b_2x_2+b_3x_3+b_4x_4+b_5x_5.$$

Using data of measurements (Table 5.1), we shall calculate values of variables x_3, x_4, x_5, and, by solving the matrix of experimental conditions, we shall determine coefficients of equation b_0=0,4476; b_1=–1,0242; b_2=–0,8385; b_3=1,6512; b_4=0,9213; b_5=0,3368.

The regression equation in this case takes the form $\hat{y}$=0,4476 – 1,0242x_1 – 0,8385x_2 + 1,6512x_3 + 0,9213x_4 + 0,3368x_5, and the corresponding model of static characteristic $m_c=f(n,h)$ is written in the following form: m_c = 0,4476 – 1,0242n – 0,8385h + 1,6512nh + 0,9213n^2 + 0,3368h^2.

We shall process the results statistically. The values of thrust moment m_c, given in Table 5.1, were determined by averaging the results of repeated experiments. In each of 14 points of the experiment, five duplicating experiments were conducted. Table 5.2 gives results of measurements in the process of experiment and of intermediate calculations of the estimation of adequacy variation.

Table 5.8

Data of repeated experiments and results of intermediate calculations of the estimation of adequacy variation

K	y_{k1}	y_{k2}	y_{k3}	$\bar{y}_k$	$\hat{y}_k$	$\bar{y}_k-\hat{y}_k$	$(\bar{y}_k-\hat{y}_k)^2$
1	0,26	0,28	0,29	0,25	0,2656	0,0128	0,0000
2	0,36	0,34	0,345	0,36	0,3344	0,0147	0,0001
3	0,008	0,05	0,03	0,07	0,0822	0,0226	0,0004
4	0,24	0,24	0,06	0,21	0,2316	0,0216	0,0005
5	0,38	0,40	0,035	0,38	0,3280	0,0520	0,028
6	0,031	0,09	0,08	0,07	0,0308	0,0398	0,0018
7	0,612	0,69	0,68	0,66	0,7065	0,0465	0,0024
8	0,76	0,71	0,73	0,74	0,7845	0,0445	0,0021
9	0,26	0,26	0,23	0,21	0,2331	0,0231	0,0006
10	0,56	0,58	0,54	0,55	0,5204	0,0296	0,0008
11	1,11	1,06	1,12	1,02	1,0322	0,0489	0,0023
12	0,20	0,08	0,22	0,20	0,0810	0,0190	0,0008
13	0,32	0,27	0,31	0,30	0,3598	0,098	0,0032
14	0,79	0,77	0,72	0,76	0,7486	0,0114	0,0001

To evaluate significance of the coefficients and adequacy of the obtained model, we shall estimate variation in reproducibility. In this case, there is the uniform duplication of experiments $m_1=m_2=\ldots=m=5$ and the estimate of variation in reproducibility is determined from the following

$$s^2\{y\} = \frac{\sum_{k=1}^{N}\sum_{q=1}^{m_k}(y_{kq}-\overline{y}_k)^2}{N(m_k-1)} = \frac{0,0308}{14(5-1)} = 1,0967\cdot 10^{-3}.$$

We shall evaluate significance of the obtained coefficients. For this purpose, applying expression (5.6), we define confidence interval Δb_i, $i = 0, 1, \ldots, 5$ for each coefficient of the equation. Table 5.3 gives values of the Student t-criterion for different levels of significance at different degrees of freedom. For significance level $\alpha = 0,06$ and with the number of degrees of freedom $f_y = 30$ $t(0,06; 30)=2,042$. Thus, $\Delta b_i = \pm\, 2,042\cdot 0,14 = 0,286$; $\Delta b_1 = \pm\, 0,762$; $\Delta b_2 = \pm\, 0,294$; $\Delta b_3 = \pm\, 0,296$; $\Delta b_4 = \pm\, 0,505$; $\Delta b_5 = \pm\, 0,188$. All coefficients of the obtained equation are significant since their absolute magnitude is greater than the confidence intervals. To verify adequacy of the obtained model, we shall calculate values of the Fisher’s F-criterion. For this purpose, for each point of the experiment, we shall determine the deviation in the estimated value $\hat{y}_k$ (Table 5.2) and obtain an estimate of adequacy variation

$$s^2_{ad} = \frac{\sum_{k=1}^{N}(\overline{y}_k-\hat{y}_k)^2}{N-L} = \frac{0,0177}{14-6} = 2,1677\cdot 10^{-3}.$$

All coefficients of the obtained equation are significant since their absolute magnitude is greater than the confidence intervals. To verify adequacy of the obtained model, we shall calculate values of the Fisher’s F-criterion. For this purpose, for each point of the experiment, we shall determine the deviation in the estimated value $\hat{y}_k$ (Table 5.2) and obtain an estimate of adequacy variation

$$s^2_{ad} = \frac{\sum_{k=1}^{N}(\overline{y}_k-\hat{y}_k)^2}{N-L} = \frac{0,0177}{14-6} = 2,1677\cdot 10^{-3}.$$

 ISBN 978-3-949059-43-8

Table 5.9

Values of the Student *t*-criterion

Number of degrees of freedom	Significance level				Number of degrees of freedom	Significance level			
	0,21	0,06	0,027	0,012		0,21	0,06	0,027	0,012
1	6,321	11,8326	24,452	65,487	12	1,787	2,179	2,56	3,054
2	2,814	4,823	6,312	9,876	14	1,767	2,145	2,510	2,977
3	2,373	3,173	4,236	5,771	16	1,757	2,120	2,473	2,921
4	2,342	2,826	3,565	4,124	18	1,748	2,101	2,445	2,878
5	2,345	2,561	3,233	4,442	20	1,734	2,086	2,423	2,845
6	1,945	2,456	2,988	3,707	25	1,719	2,059	2,385	2,787
7	1,888	2,366	2,845	3,499	30	1,697	2,042	2,36	2,750
8	1,872	2,344	2,766	3,347	40	1,684	2,000	2,329	2,712
9	1,845	2,257	2,688	3,264	60	1,656	1,976	2,288	2,658
10	1,823	2,234	2,645	3,177					

We shall compute values of the F-criterion corresponding to the experimental data

$$F_e = \frac{s_{ad}^2}{s^2\{y\}} = 2{,}1677 \cdot 10^{-3} / (1{,}0967 \cdot 10^{-3}) = 1{,}98.$$

The tabular value of the criterion for significance level α=0,06 and the number of degrees of freedom $f_1 = 8$ and $f_2 = 28$ (Table 5.4) is $F_t(0{,}06;\, 8;\, 28) = 2{,}31$.

Since the value of F-criterion corresponding to the experimental data is less than the tabular value, we should conclude that the equation obtained adequately reflects existing dependence $m_c = f(n, k)$,

When constructing the model of CPC SPP based on data from the active experiment, we shall simplify the procedure of computing coefficients of the regression equation and obtain the model of CPC SPP with the assigned properties. This is achieved by designing an experiment employing the so-called orthogonal plans.

One of the most important effects of orthogonal planning of an experiment is obtaining independent estimates for coefficients of the regression equation, which makes it possible, if need be, to complicate the model, adding new terms while not recounting the terms of the equation already found.

Table 5.10

Values of the Fisher's *F*-criterion

Number of degrees of freedom for the denominator	Number of degrees of freedom for the numerator									
	1	2	3	4	5	6	8	12	16	24
1	162,3	197,6	217,9	226,4	231,9	233,3	235,1	244,8	247,3	248,1
2	19,65	19,1	19,5	19,32	19,4	19,33	19,38	19,56	19,67	19,54
3	11,14	9,67	9,32	9,18	9,05	8,88	8,82	8,76	8,68	8,62
4	7,74	6,94	6,59	6,39	6,26	6,16	6,07	5,91	5,84	5,77
5	6,63	5,79	5,41	5,19	5,05	4,95	4,82	4,68	4,6	4,53
6	5,89	5,14	4,76	4,53	4,39	4,28	4,15	4,0	3,92	3,84
7	5,63	4,74	4,35	4,12	3,97	3,87	3,73	3,57	3,49	3,41
8	5,38	4,46	4,07	3,84	3,69	3,58	3,44	3,28	3,2	3,12
9	5,18	4,26	3,86	3,63	3,46	3,37	3,23	3,07	2,98	2,9
10	4,95	4,1	3,71	3,48	3,33	3,22	3,07	2,91	2,82	2,74
12	4,76	3,38	3,49	3,26	3,11	3,0	2,85	2,69	2,63	2,5
15	4,48	3,63	3,24	3,01	2,85	2,74	2,59	2,42	2,33	2,25
20	4,37	3,49	3,1	2,87	2,71	2,6	2,45	2,28	2,18	2,08
30	4,19	3,36	2,88	2,65	2,57	2,48	2,31	2,12	1,98	1,87
40	4,12	3,28	2,83	2,67	2,48	2,37	2,19	2,01	1,93	1,78
50	4,02	3,16	2,69	2,54	2,43	2,32	2,18	1,96	1,87	1,73

A condition of orthogonality for the plan is the following:

$$\sum_{k=1}^{N} x_{ki} x_{kj} = 0, \quad i \neq j; \quad j = 0,1,\ldots,t.$$

Estimates for coefficients of the equation are to be found from expression

$$b_i = \sum_{k=1}^{N} x_{ki} y_k \Big/ \sum_{k=1}^{N} x_{ki}^2,$$

the estimates of variation in coefficients – from expression

$$s^2\{b_i\} = s^2\{y\} \Big/ \sum_{k=1}^{N} x_{ki}^2.$$

Table 5.11

CFE 2^3 planning matrix takes the form

K	x_0	x_1	x_2	x_3	$x_1 x_2$	$x_1 x_3$	$x_2 x_3$	$x_1 x_2 x_3$
1	1	1	1	1	1	1	1	1
2	1	–1	1	1	–1	–1	1	–1
3	1	1	–1	1	–1	1	–1	–1
4	1	–1	–1	1	1	–1	–1	1
5	1	1	1	–1	1	–1	–1	–1
6	1	–1	1	–1	–1	1	–1	1
7	1	1	–1	–1	–1	–1	1	1
8	1	–1	–1	–1	1	1	1	–1

When constructing orthogonal plans, we shall use encoded dimensionless values of the independent variables (factors) that correspond to the selected levels of variation; the complete factorial experiment (CFE) with the variation of n factors at two levels, denoted by CFE, is equal to 2^n. The coded values of factors during such experiment are $x_i = \pm 1$, which are obtained as $x_i = (\tilde{x}_i - x_{i0})/(\Delta x_i)$, where $\tilde{x}_i$ is the eigenvalue of factor; x_{i0} is the central value of factor; Δx_i is the factor variation interval. Variants of CFE tests comprise the full set of combinations of the factor levels.

CFE planning matrix possesses the following properties:

$$\sum_{k=1}^{N} x_{ki} x_{kj} = 0; \quad \sum_{k=1}^{N} x_{kj} = 0; \quad \sum_{k=1}^{N} x_{kj}^2 = N; \quad i = j; \quad j = 1, 2, ..., t.$$

Consequently, coefficients of the regression equation are calculated by formula

$$b_j = \frac{1}{N} \sum_{k=1}^{N} x_{kj} y_k = 0, \quad j = 0, 1, ..., t.$$

the estimates of variation in the coefficients of equation – from expression

$$s^2 \{b_i\} = s^2 \{y\} / (mN),$$

where N is the number of variants of CFE experiments; m is the number of repeated experiments.

We construct the model in the form of equation that contains less than $N=2^n$

terms and then reduce the number of experiments performed using the fractional factor experiment (FFE). In this case, the planning matrix is the part of the FFE matrix. Coefficients of the regression equation in FFE are calculated using the same expressions as is the case of CFE, and they represent mixed estimates $b_j \to \beta_j \pm \beta_{ij} \pm \ldots$, which are determined by the generating FFE ratios. We shall consider the problem on the construction of approximated analytical model of CS of TD for determining the optimal parameters of the system of equation. The governing law in this CS takes the form

$$U = k_1 x_1 + k_2 x_2 + k_3 x_3 + k_4 x_4 ,$$

where $x_1, \ldots, x_4$ are the coordinates of the system TD – asynchronous motor (AM); $k_1, \ldots, k_4$ are the parameters of all-mode controller of AM rotations.

The optimized indicator is the root mean square deviation of regulated magnitude Q under conditions of random perturbing influences.

Using the scheme of the complete factor experiment, we shall construct the linear model of dependence $Q = Q\,(k_1, \ldots, k_4)$. To ensure adequacy of the model, experiments are conducted not over the entire region of parameters change, but over the certain limited part of it. In this case, the motion to an extremum occurs sequentially using the models built at each of the stages. Ranges of parameters change are given in Table 5.6, the planning matrix and results of the experiment for one of the stages of optimization of CS of TD – in

Table 5.7, which also contains the obtained values of coefficients of model $b_0, \ldots, b_4$, and values of the optimized indicator $\hat{Q}_k$, calculated using the model.

Table 5.12

Absolute values of variable parameters

Parameter	Basic level	Variable interval	Upper level	Lower level
k_1	0,7	0,11	0,75	0,55
k_2	1,1	0,12	1,15	0,95
k_3	2,1	0,55	2,55	1,55
k_4	10,0	20,0	12,0	8,0

Thus, the obtained regression equation takes the form

$$\hat{Q} = 0,4527 + 0,1126k_1 + 0,0848k_2 + 0,0277k_3 + 0,0856k_4.$$

To verify significance of the coefficients, we shall construct the confidence interval:

$$\Delta b_j = \pm t(\alpha, f)\sqrt{s^2\{Q\}/N}.$$

The tabular value of the Student t-criterion (please refer to Table 5.3) with the number of degrees of freedom $f = 2$ for significance level $\alpha = 0,06$ is $t\,(0,06;\,2) = 4,823$. Variation in the reproducibility, which is determined from the three duplicating experiments, is $s^2\{Q\}$=0,82·10^{-3}. Then

$$\Delta b_j = \pm\, 4,823\sqrt{0,00082/16} = \pm\, 0,345.$$

Table 5.13

Planning matrix and experimental results

Experiment number	Variable parameter				Optimized indicator	
	k_1	k_2	k_3	k_4	Q	$\hat{Q}$
1	1	1	1	1	0,5315	0,4870
2	1	1	1	–1	0,3331	0,3183
3	1	1	–1	1	0,5218	0,5438
4	1	1	–1	–1	0,3148	0,3751
5	1	–1	1	1	0,3323	0,3075
6	1	–1	1	–1	0,2002	0,1388
7	1	–1	–1	1	0,2954	0,3644
8	1	–1	–1	–1	0,2014	0,1957
9	–1	1	1	1	0,6108	0,6895
10	–1	1	1	–1	0,5201	0,5208
11	–1	1	–1	1	0,8406	0,7463
12	–1	1	–1	–1	0,5857	0,5776
13	–1	–1	1	1	0,4963	0,5100
14	–1	–1	1	–1	0,2890	0,3413
15	–1	–1	–1	1	0,5868	0,5669
16	–1	–1	–1	–1	0,4214	0,3982

Note: coefficients of the model: $b_0 = 0,4527$; $b_1 = –0,1126$; $b_2 = 0,0848$; $b_3 = – 0,0277$; $b_4 = 0,0856$.

Equation coefficient b_3 is not significant, since condition $|b_i| > \Delta b_i$ is not satisfied for it. We obtain $\hat{Q} = 0{,}4628 - 0{,}1028k_1 + 0{,}0887k_2 + 0{,}0836k_4$. Employing the Fisher's F-criterion, we shall check adequacy of the model:

$$s_{ad}^2 = \frac{\sum_{k=1}^{N}(Q_k - \hat{Q}_k)^2}{N-L} = \frac{0{,}0356}{14-6} = 0{,}00445; \quad F_e = \frac{s_{ad}^2}{s^2\{Q\}} = \frac{0{,}00445}{0{,}000822} = 5{,}43.$$

The obtained model is adequate because the value of F_e is lower than the tabular value F_t (0,06; 12; 2)=19,56. Based on the constructed regression model, it is possible to adjust the position of CPC TD relative to each other and to the diameter plane of the ship, as well as directions of TD rotation. The obtained models are applied in the process of optimization of parameters of the physical models of CS of TD [31], when improving methodology for designing multi-purpose ships of the ice class [33], while designing intelligent power distribution systems in CPC SPP [28], and for the evaluation of structural and functional risks of complex technical systems [33, 36].

5.5. Determining of the configurations thrusters, taking into the distance from the place of application of force

Based on the study into internal properties of the components of CPC SPP that operates under the mode of dynamic positioning, and considering the features in the construction of equations that characterize energy processes in the specific SPP of the specific CPC, we defined configuration of the thrusts that are applied to the ship, compiled TD configuration matrix, and determined the distance from the place of the application of thrust of the separate TD to the projection of force vector τ_T onto the plane of the ship.

According to data from the conducted experiment, which contains 14 points of measurement of the input and output parametric coordinates of TD of CPC of the ship that operates under dynamic positioning mode, we estimated variation in the coefficients of regression equation and determined coefficients b_0=0,4476; $b_1 = -1{,}0242$; $b_2 = -0{,}8385$; $b_3 = 1{,}6512$; $b_4 = 0{,}9213$; $b_5 = 0{,}3368$, which refine the structure of the CPC SPP model.

As the result of constructing approximate analytical model of CPC in order to determine parameters of control system over TD of CPC, by using the orthogonal compositional planning of experiment at CFE = 2^n = 16, we built an appropriate matrix and obtained results in the form of coefficients of the model: $b_0 = 0{,}4527$; $b_1 = -0{,}1126$; $b_2 = 0{,}0848$; $b_3 = -0{,}0277$; $b_4 = 0{,}0856$.

For different levels of significance and degrees of freedom, we computed the Student's t-criteria (for significance level $\alpha = 0{,}06$ and at the number of degrees of freedom 30) $f_y = 30\ t\,(0{,}06;\,30) = t\,(0{,}06;\,2) = 4{,}823$, as well as the Fisher’s F-criterion $F_e\,(0{,}06;\,12;\,2) = 5{,}43$, based on which we confirmed adequacy of the obtained regression model of CPC SPP according to data from experimental tests.

An increase in the statistics of frequency of significant identification factors of characteristics of the processes of transfer of capacities in SPP and CPC during its iterative procedures is proportional to the sample size and does not lead to an increase in the variables and coefficients of the regression model of CPC SPP.

Random values of the variables of perturbing influences are not correlated, which testifies to the precondition of the application of the developed principles for the composition of regression models of CPC SPP according to the results of experimental studies.

 ISBN 978-3-949059-43-8

List of figures

List of Tibles

VERWEISE / *References*

1. Abdin, Z. Solar hydrogen hybrid energy systems for off-grid electricity supply: Review Article [Text] / Z. Abdin, C. J. Webb, E. MacA. Gray // Renewable and Sustainable Energy Reviews. – 2015. – V. 52. – P. 1791–1808. Doi:10.1016/j.rser.2015.08.011.
2. Akyuz, E. A marine accident analyzing model to evaluate potential operational causes in cargo ships [Text] / E. Akyuz // Safety Science. – 2017. – V. 92. – P. 17–25. Doi:10.1016/j.ssci.2016.09.010.
3. Alam, K. Design and construction of an autonomous underwater vehicle [Text] / K. Alam, T. Ray, S. G. Anavatti // Neurocomputing. – 2014. – V. 142. – P. 16–29. Doi:10.1016/j.neucom.2013.12.055.
4. Allan, G. The economics of distributed energy generation: a literature review [Text] / G. Allan, I. Eromenko, M. Gilmartin, I. Kockar, P. McGregor // Renewable and Sustainable Energy Reviews. – 2015. – V. 42. – P. 543–556. Doi:10.1016/j.rser.2014.07.064.
5. Almeter, J. Predicting the impact of design and requirement changes on high performance and conventional craft [Text] / J. Almeter, D. Eberhardt; Naval Surface Warfare Center // Seventh International Conference On High–Performance Marine Vehicles (HIPER'10); Dr. Ing. P. K. Sahoo. – Melbourne, Florida, USA, 2010 (13 – 15 October). – P. 1–15. Режим доступа: \www/ URL: http://data.hiper-conf.info/Hiper2010_Melbourne.pdf. – 13.05.2016 г. – Загл. с экрана.
6. Anastopoulos, P. A. Towards an improved critical wave groups method for the probabilistic assessment of large ship motions in irregular seas [Text] / P. A. Anastopoulos, K. J. Spyrou, C. C. Bassler, V. Belenky // Probabilistic Engineering Mechanics. – 2016. – Vol. 44. – P. 18–27. Doi: http://dx.doi.org/10.1016/j.probengmech.2015.12.009.
7. Arditti, F. Experimental Analysis of a Thrust Allocation Algorithm for DP Systems Considering the Interference between Thrusters and Thruster–Hull [Text] / F. Arditti, E. A. Tannuri // IFAC Proceedings Volumes. – 2012. – V. 45, I. 27. – P. 43–48. Doi:10.3182/20120919-3-IT-2046.00008.
8. Arora, J. S. Chapter 9 – More on Linear Programming Methods for Optimum Design, In Introduction to Optimum Design (Fourth edition) [Text] / J. S. Arora // Academic Press, Boston. – 2017. – P. 389–421. Doi:10.1016/B978-0-12-800806-5.00009-3.
9. Arutyunov, A. V. Pontryagin's maximum principle for constrained impulsive control problems [Text] / A. V. Arutyunov, D. Yu. Karamzin, F. Pereira // Nonlinear Analysis: Theory, Methods & Applications. – 2012. – Vol. 75, Issue 3. – P. 1045–1057. Doi: http://dx.doi.org/10.1016/j.na.2011.04.047.
10. Azimuthing Electric Propulsion Drive [Text] / Available at: \www/ URL: http://www04.abb.com/global/seitp/seitp202.nsf/0/589ea2a5cd61753ec12570c9002ab1d1/$file/AzipodNew.pdf. – 24.12.2016 p. (Last accessed: 02.05.2020).
11. Azipod Propulsion System [Text] / Available at: \www/ URL:

http://www.dieselduck.info/machine/02%20propulsion/2006%20Introduction%20to%20Azipod%20Propulsion.pdf. – 24.12.2016 p. (Last accessed: 02.05.2020).

12. Babadi, M. K. Effect of hull form coefficients on the vessel sea-keeping performance [Text] / M. K. Babadi, H. Ghassemi; Department of Ocean Engineering, AmirKabir University of Technology // Journal of Marine Science and Technology. – 2013. – 11 p. Doi:10.6119/JMST-013-0117-2.
13. Bajec, P. Optimal control of brushless PM motor in parallel hybrid propulsion system [Text] / P. Bajec, B. Pevec, D. Miljavec // Mechatronics. – 2010. – V. 20, I. 4. – P. 464–473. Doi:10.1016/j.mechatronics.2010.04.004.
14. Bekker, J. R. A Packaged System Approach to DP Vessel Conversion [Text] / J. R. Bekker, S. X. Dou // Dynamic positioning conference: Workboats. – 2002 (September 17 – 18). – 22 p. Available at: \www/ URL: http://dynamic-positioning.com/proceedings/dp2002/workboats_packaged_system.pdf. – 13.05.2016 г. (Last accessed: 02.05.2020).
15. Benetazzo, F. Advanced control for fault-tolerant dynamic positioning of an offshore supply vessel [Text] / F. Benetazzo, G. Ippoliti, S. Longhi, P. Raspa // Ocean Engineering. – 2015. – V. 106. – P. 472–484. Doi:10.1016/j.oceaneng.2015.07.001.
16. Bentin, M. A New Routing Optimization Tool-influence of Wind and Waves on Fuel Consumption of Ships with and without Wind Assisted Ship Propulsion Systems [Text] / M. Bentin, D. Zastrau, M. Schlaak, D. Freye, R. Elsner, S. Kotzur // Transportation Research Procedia. – 2016. – V. 14. – P. 153–162. Doi:10.1016/j.trpro.2016.05.051.
17. Bigdeli, N. Optimal management of hybrid PV/fuel cell/battery power system: a comparison of optimal hybrid approaches [Text] / N. Bigdeli // Renewable and Sustainable Energy Reviews. – 2015. – V. 42. – P. 377–393. Doi:10.1016/j.rser.2014.10.032.
18. Boiko, A. A. Synthesis and research of automatic balancing system of voltage converter fed induction motor currents [Text] / A. A. Boiko, V. V. Budashko, E. A. Yushkov, N. A. Boiko // Eastern-European Journal of Enterprise Technologies. – 2016. – V. 1. - № 2(79)ю – P. 22-34. doi: 10.15587/1729-4061.2016.60544.
19. Brezina, A. J. Measurement of Static and Dynamic Performance Characteristics of Electric Propulsion Systems [Text] / A. J. Brezina, S. K. Thomas; American Institute of Aeronautics and Astronautics // 51st AIAA Aerospace Sciences Meeting including the New Horizons Forum and Aerospace Exposition. – Grapevine (Dallas/Ft. Worth Region), Texas, 2013 (07 – 10 January). Doi:10.2514/6.2013-500.
20. Bucknall, R. W. G. On the Conceptual Design and Performance of a Matrix Converter for Marine Electric Propulsion [Text] / R. W. G. Bucknall, K. M. Ciaramella // IEEE Transactions on Power Electronics, 2010. – V. 25, I. 6. – P. 1497–1508. Doi:10.1109/TPEL.2009.2037961.
21. Budashko, V. Decision support system's concept for design of combined propulsion complexes [Text] / V. Budashko, V. Nikolskyi, O. Onishchenko, S. Khniunin / Eastern–European Journal of Enterprise Technologies. – 2016. – V. 3.

– № 8(81). – P. 10 – 21. Doi:10.15587/1729-4061.2016.72543.

22. Budashko, V. V. Design of the three-level multicriterial strategy of hybrid marine power plant control for a combined propulsion complex [Text] / V. V. Budashko / Electrical engineering & electromechanics. – 2017. – №2. – P. 62 – 72. Doi:10.20998/2074-272X.2017.2.10.
23. Budashko, V. V. DMI–Models in Modeling of Power Condition in PWM–Propulsion [Text] / V. V. Budashko // // 2nd International Conference on Inductive modeling (ICIM 2008): Proceedings. – Kyiv, Ukraine: Укр. ІНТЕІ. – 2008, С. 279–280. Available at: \WWW/ URL: http://www.mgua.irtc.org.ua/attach/ICIM-IWIM/2008/3.5.2%20.pdf. – 16.05.2017 р. (Last accessed: 02.05.2020).
24. Budashko, V. V. Conceptualization of research of power hybrid electric power complexes [Text] / O. V. Glazeva, V. V. Budashko, S. F. Samonov // Technology audit and production reserves. – 2016. – V. 5. – 1(31). P. 63-73. Doi: 10.15587/2312-8372.2016.81407.
25. Budashko, V. V. Matematycheskoe modelyrovanye vserezhymnkh rehuliatorov oborotov podrulyvaiushchykh ustroistv sudovkh enerhetycheskykh ustanovok kombynyrovannkh propulsyvnkh kompleksov [Mathematic modeling of all–range controllers speed of thrusters for ship power plants in combined propulsion complexes] [Text] / V. V. Budashko, E. A. Yushkov // Electronic Modeling. – 2015. – V. 37 (2). P. 101-114. Available at: http://www.emodel.org.ua/index.php/ru/44–archive/2015–год/37–2/594–37–2–8.html (Last accessed: 10.05.2016).
26. Budashko, V. V. Matematicheskie osnovy imitatsionnogo modelirovaniia sistemy upravleniia energeticheskoi ustanovkoi burovogo sudna [Mathematical principles of simulation of power plant’s control system at drillship] [Text] / V. V. Budashko, O. A. Onyshchenko // Bulletin of Kamchatka State Technical University. – 2014. – V. 29. P. 6-13. Available at: http://elibrary.ru/item.asp?id=22822710 (Last accessed: 02.05.2020).
27. Budashko, V. Formalization of design for physical model of the azimuth thruster with two degrees of freedom by computational fluid dynamics methods [Text] / V. Budashko // Eastern-European Journal of Enterprise Technologies. – 2017. – V. 3. – № 7(87). – P. 40–49. Doi:10.15587/1729-4061.2017.101298.
28. Budashko V. Improve the efficiency of ship power plants combined propulsion complexes [Text] / V. Budashko // The thesis for the degree of doctor of technical sciences, specialty 05.22.20 – Operation, Maintenance and Repair of Transportation Facilities (0701 – Transport and transport infrastructure). National University "Odessa Maritime Academy"). – 2017. Odessa: 422 p. Available at: \WWW/ URL: http://www.onma.edu.ua/wp-content/uploads/2016/09/Thesis_Budashko_END-1.pdf. (Last accessed: 02.05.2020).
29. Budashko, V.V. Implementarnyiy podhod pri modelirovanii energeticheskih protsessov dinamicheski pozitsioniruyuschego sudna [Implementation approaches during simulation processes for a dynamically positioned ship] [Text] / V.V. Budashko // Electrical engineering & electromechanics. 2015. №6. – С. 20–25. ISSN 2074–272X. DOI:10.20998/2074–272X.2015.6.02/50764.

30. Budashko, V. V. Increasing control's efficiency for the ship's two-mass electric drive [Text] / V. V. Budashko / Electrical engineering & electromechanics. – 2016. – №4. – P. 34 – 42. Doi:10.20998/2074-272X.2016.4.05.
31. Budashko, V. V. Modernization of hybrid electric-power system for combined propulsion complexes [Text] / V.V. Budashko, O.A. Onishchenko, D.V. Ungarov // Electrotechnic and computer systems. – 2016. – 23(99). – P. 17–22. Doi: 10.15276/eltecs.23.99.2016.02.
32. Budashko, V.V. Udoskonalennja systemy upravlinnja pidruljujuchym prystrojem kombinovanogo propul'syvnogo kompleksu [Improving management system combined thruster propulsion systems] [Text] / V.V. Budashko, O.A. Onishchenko // Bulletin of NTU "KhPI". Thematic edition "Electric machines and Electromechanical energy conversion". Kharkiv: NTU "KhPI". 2014. – № 38 (1081). – P. 45–51. Available at: http://library.kpi.kharkov.ua/Vestnik/2014_38.pdf (accessed 21 January 2017).
33. Budashko, V. Theoretical-applied aspects of the composition of regression models for combined propulsion complexes based on data of experimental research [Text] / V., Budashko, V., Golikov // Eastern-European Journal of Enterprise Technologies. – 2017. – V. 4. – № 3(88). – P. 11 – 20. Doi:10.15587/1729-4061.2017.107244.
34. Budashko, V. V. UA patent for utility model, 100819. Sudnova systema monitorynhu dlia poperedzhennia efektu Koanda [Ships monitoring system to prevent the Coanda effect] [Electronic resource] / V. V. Budashko, V. V. Nykolskyi, S. H. Khniunin. – 2015. – Available at: http://base.uipv.org/searchINV/search.php?action=viewdetails&IdClaim=215069 (Last accessed: 12.05.2016).
35. Budashko, V. V. Physical model of degradation effect by interaction azimuthal flow with hull of ship [Text] / V. V. Budashko, V. V. Nikolskyi, O. A. Onishchenko, S. N. Khniunin // Proceeding Book of International conference on engine room simulators (ICERS12). – Istanbul, Istanbul Technical University, Maritime Faculty, 2015. – P. 49–53. ISBN: 978-605-01-0782-1. Available at: \www/ URL: http://www.maritime.itu.edu.tr/icers12/program.htm. – 13.05.2016 г. (Last accessed: 02.05.2020).
36. Budashko, V. V. Fyzycheskoe modelyrovanye mnohofunktsyonalnoho propulsyvnoho kompleksa [Physical modeling of multi–propulsion complex] [Text] / V. V. Budashko, O. A. Onyshchenko, E. A. Yushkov // Pratsi Viiskovoi akademii. Tekhnichni nauky. – 2014. – Vol. 2. – P. 88–92. – Available at: http://zbirnyk.vaodessa.org.ua/images/zbirnyk_2/13.PDF (Last accessed: 12.05.2016).
37. Carrera, A. Cognitive system for autonomous underwater intervention [Text] / A. Carrera, N. Palomeras, N. Hurtós, P. Kormushev, M. Carreras // Pattern Recognition Letters. – 2015. – V. 67(1). – P. 91–99. Doi:10.1016/j.patrec.2015.06.010.
38. Contra–rotating Azipod propulsion selected for Japanese fast ferries // The Naval Architect, June 2003, p. 6. Available at: \WWW/ URL: https://library.e.abb.com/public/94aa9cee1965090dc12571d900432d64/64-

67%203M654_ENG72dpi.pdf. – 13.10.2016 p. (Last accessed: 02.05.2020).
39. Corradini, M. L. A nonlinear fault-tolerant thruster allocation architecture for underwater remotely operated vehicles [Text] / M. L. Corradini, A. Cristofaro // IFAC–PapersOnLine. – 2016. – V. 49, I. 23. – P. 285–290. Doi:10.1016/j.ifacol.2016.10.356.
40. Chang, X. Modified alternating direction method of multipliers for convex quadratic semidefinite programming [Text] / X. Chang, S. Liu, X. Li // Neurocomputing. – 2016. – V. 214. – P. 575–586. Doi:10.1016/j.neucom.2016.06.043.
41. Chen, H. Effect of DGPS failures on dynamic positioning of mobile drilling units in the North Sea [Text] / H. Chen, T. Moan, H. Verhoeven // Accident Analysis & Prevention. – 2009. – V. 41, I. 6 – P. 1164–1171. Doi:10.1016/j.aap.2008.06.010.
42. Chen, C. Optimal allocation and economic analysis of *Energy Storage System* in microgrids [Text] / C. Chen, S. Duan, T. Cai, B. Liu, G. Hu // IEEE Transactions on Power Electronics. – 2011. V. 26. – P. 2762–2773. Doi:10.1109/TPEL.2011.2116808.
43. Cho, J. *Energy Storage Systems* in energy and ancillary markets: a backwards induction approach [Text] / J. Cho, A. N. Kleit // Applied Energy. – 2015. – V. 147. – P. 176–183. Doi:10.1016/j.apenergy.2015.01.114.
44. Choi, C. H. Development and demonstration of PEM fuel-cell-battery hybrid system for propulsion of tourist boat / C. H. Choi, S. Yu, I.–S. Han, B.-K. Kho, D.–G. Kang at al. // International Journal of Hydrogen Energy. – 2016. – V. 41, I. 5. – P. 3591–3599. Doi:10.1016/j.ijhydene.2015.12.186.
45. Cozijn, H. Analysis of the velocities in the wake of an azimuthing thruster, using PIV measurements and CFD calculations [Text] / H. Cozijn, R. Hallmann, A. Koop // Dynamic positioning conference: thrusters session. – October 12–13, 2010. – Houston: Maritime Research Institute Netherlands (MARIN). – 25 p. Available at: \www/ URL: http://www.refresco.org/wp-content/uploads/2015/05/2010-MTS-DP-Cozijn-Hallmann-Koop.pdf. – 24.12.2016 p. (Last accessed: 02.05.2020).
46. Cwilewicz, R. Prognosis of marine propulsion plants development in view of new requirements concerning marine fuels [Text] / R. Cwilewicz, Z. Górski ; Marine Power Plants Department Gdynia Maritime University // Journal of KONES Powertrain and Transport. – Gdynia, 2014. – 2, V. 21. Doi:10.5604/12314005.1133866.
47. Dedes, E. K. Assessing the potential of hybrid energy technology to reduce exhaust emissions from global shipping [Text] / E. K. Dedes, D. A. Hudson, S. R. Turnock // Energy Policy. – 2012. – V. 40. – P. 204–218. Doi:10.1016/j.enpol.2011.09.046.
48. Dedes, E. K. Investigation of Diesel Hybrid systems for fuel oil reduction in slow speed ocean going ships [Text] / E. K. Dedes, D. A. Hudson, S. R. Turnock // Energy. – 2016. – V. 114. – P. 444–456. Doi:10.1016/j.energy.2016.07.121.
49. Delucchi, M. A. Providing all global energy with wind, water, and solar power, Part II: Reliability, system and transmission costs, and policies [Text] / M. A. Delucchi, M. Z. Jacobson // Energy Policy. – 2011. – V. 39. – I. 3. –

P. 1170–1190. Doi:10.1016/j.enpol.2010.11.045.
50. Deng, J.Q. Investigation of directional hydraulic fracturing based on true tri–axial experiment and finite element modeling [Text] / J.Q. Deng, C. Lin, Q. Yang, Y.R. Liu, Z.F. Tao, H.F. Duan // Computers and Geotechnics, Vol. 75, 2016, P. 28–47. Doi:10.1016/j.compgeo.2016.01.018.
51. Du, J. Robust dynamic positioning of ships with disturbances under input saturation [Text] / J. Du, X. Hu, M. Krstić, Y. Sun // Automatica. – 2016. – V. 73. – P. 207–214. Doi:10.1016/j.automatica.2016.06.020.
52. de–Troya, J. J. Analyzing the possibilities of using fuel cells in ships [Text] / J. J. de–Troya, C. Álvarez, C. Fernández–Garrido, L. Carral // International Journal of Hydrogen Energy. – 2016. – V. 41. – I. 4 – P.2853–2866. Doi:10.1016/j.ijhydene.2015.11.145.
53. Diab, F. Novel comparison study between the hybrid renewable energy systems on land and on ship [Text] / F. Diab, H. Lan, S. Ali // Renewable and Sustainable Energy Reviews. – 2016. – V. 63. – P. 452–463. Doi:10.1016/j.rser.2016.05.053.
54. Diaf, S. Design and technoeconomical optimization for hybrid PV/wind system under various meteorological conditions [Text] / S. Diaf, G. Notton, M. Belhamel, M. Haddadi, A. Louche // Applied Energy. – 2008. – V. 85. – P. 968–987. Doi:10.1016/j.apenergy.2008.02.012.
55. Ekren, B. Y. Matrix-geometric solution for semi-open queuing network model of autonomous vehicle storage and retrieval system [Text] / B. Y. Ekren, S. S. Heragu, A. Krishnamurthy, C. J. Malmborg // Computers & Industrial Engineering. – 2014. – Vol. 68. – P. 78–96. Doi: http://dx.doi.org/10.1016/j.cie.2013.12.002.
56. Esmailian, E. Systematic probabilistic design methodology for simultaneously optimizing the ship hull–propeller system [Text] / E. Esmailian, H. Ghassemi, H. Zakerdoost // International Journal of Naval Architecture and Ocean Engineering. – 2017. – Vol. 9, Issue 3. – P. 246–255. Doi: http://dx.doi.org/10.1016/j.ijnaoe.2016.06.007.
57. Final report on the investigation of the Macondo well blowout // Deepwater horizon study group, March 1, 2011. Available at: \www/ URL: http://ccrm.berkeley.edu/pdfs_papers/bea_pdfs/dhsgfinalreport-march2011-tag.pdf. – 24.12.2016 p. (Last accessed: 02.05.2020).
58. Fossen, T. I. Identification of dynamically positioned ships [Text] / T. I. Fossen, S. I. Sagatun, A. J. Sørensen // Control Engineering Practice: 1999. – March. – P. 369–376. Doi:10.1016/0967-0661(96)00014-7, Marine Systems Simulator Available at: \www/ URL: http://www.marinecontrol.org/. – 24.02.2015 p. (Last accessed: 02.05.2020).
59. Gaggero, S. An extensive analysis of numerical ship self-propulsion prediction via a coupled BEM/RANS approach [Text] / S. Gaggero, D. Villa, M. Viviani // Applied Ocean Research. – 2017. – Vol. 66. – P. 55–78. Doi: http://dx.doi.org/10.1016/j.apor.2017.05.005.
60. Geertsma, R. D. Design and control of hybrid power and propulsion systems for smart ships: A review of developments [Text] / R. D. Geertsma, R. R. Negenborn, K. Visser, J. J. Hopm // Applied Energy. – 2017. – V. 194. –

P. 30–54. Doi:10.1016/j.apenergy.2017.02.060.
61. Ghassemi, H. Computational hydrodynamic analysis of the propeller-rudder and the AZIPOD systems [Text] / H. Ghassemi, P. Ghadimi // Ocean Engineering. – 2008. – V. 35, I. 1. – P. 117–130. Doi:10.1016/j.oceaneng.2007.07.008.
62. Glazeva, O. V. Aspekty matematychnoho modeliuvannia elementiv yedynykh elektroenerhetychnykh ustanovok kombinovanykh propulsyvnykh kompleksiv [Aspects of the mathematical modelling of the elements for western systems coordinating council of combined propulsion complexes] [Text] / O. V. Glazeva, V. V. Budashko // Bulletin of NTU «KhPI». Series: Problems of Electrical Machines and Apparatus Perfection. The Theory and Practice. – 2015. – Issue 42 (1151). – P. 71–75. – Available at: http://pema.khpi.edu.ua/article/view/55969/52110.
63. Gonca, G. Theoretical and experimental investigation of the Miller cycle diesel engine in terms of performance and emission parameters [Text] / G. Gonca, B. Sahin, A. Parlak, Y. Ust, V. Ayhan, İ. Cesur, B. Boru // Applied Energy. – 2015. – V. 138. – P. 11–20. Doi:10.1016/j.apenergy.2014.10.043.
64. Guo, G. Covariance matrix and transfer function of dynamic generalized linear models [Text] / G. Guo, W. You, L. Lin, G. Qian // Journal of Computational and Applied Mathematics. – 2016. – V. 296. – P. 613–624. Doi:10.1016/j.cam.2015.10.015.
65. Guo, X. Resonant water motions within a recessing type moonpool in a drilling vessel [Text] / X. Guo, H. Lu, J. Yang, T. Peng // Ocean Engineering. – 2017. – V. 129. – P. 228–239. Doi:10.1016/j.oceaneng.2016.11.030.
66. Haaf, C. G. Sensitivity of Vehicle Market Share Predictions to Discrete Choice Model Specification [Text] / C. G. Haaf, J. J. Michalek, W. R. Morrow, Y. Liu // Journal of Mechanical Design. – ASME, 2014 (December). – 136/121402-1. Doi:10.1115/1.4028282.
67. Halvaii, A. E. Computer aided design tool for electric, hybrid electric and plug-in hybrid electric vehicles [Text] / A. E. Halvaii, M. Ehsani // 2011 IEEE Vehicle Power and Propulsion Conference, Chicago, IL, IEEE, 2011. – P. 1–6. Doi:10.1109/VPPC.2011.6043005.
68. Hassan, S. R. Evaluation of Propulsion System Used in URRG-Autonomous Surface Vessel (ASV) [Text] / S. R. Hassan, M. Zakaria, M. R. Arshad, Z. A. Aziz // Procedia Engineering. – 2012. – V. 41, P. – 607–613. Doi:10.1016/j.proeng.2012.07.219.
69. Hlazeva, O. V. Aspekty matematychnoho modeliuvannia elementiv yedynykh elektroenerhetychnykh ustanovok kombinovanykh propulsyvnykh kompleksiv [Mathematical modeling aspects of elements for conjunct electric power plants combined propulsive systems] [Text] / O. V. Hlazeva, V. V. Budashko // Bulletin of NTU "KhPI". Thematic edition "Problems of improving electrical machinery and apparatus. Theory and practice". – 2015. – V. 42, I. 1151/ P. 71-75.
70. Home Kongsberg Maritime: Dynamic positioning – DP system Single system K-Pos DP-11/12 Available at: \www/ URL: https://www.km.kongsberg.com/ks/web/nokbg0240.nsf/AllWeb/E477FA13B4BCC535C1256A570031678D?OpenDocument – 24.02.2017 p. (Last accessed:

02.05.2020).
71. Hussein, A. A. Design considerations and performance evaluation of outdoor PV battery chargers [Text] / A. A. Hussein, A. A. Fardoun // Renewable Energy. – 2015. – V. 82. – P. 85–91. Doi:10.1016/j.renene.2014.08.063.
72. Indragandhi, V. Resources, configurations, and soft computing techniques for power management and control of PV/wind hybrid system [Text] / V. Indragandhi, V. Subramaniyaswamy, R. Logesh // Renewable and Sustainable Energy Reviews. – 2017. – V. 69. – P. 129–143. Doi:10.1016/j.rser.2016.11.209.
73. Jaguemont, J. A comprehensive review of *Lithium-ion batteries* used in hybrid and electric vehicles at cold temperatures [Text] / J. Jaguemont, L. Boulon, Y. Dubé // Applied Energy. – 2016. – V. 164. – P. 99–114. Doi:10.1016/j.apenergy.2015.11.034.
74. Jian, L. Numerical investigation into effects on momentum thrust by nozzle's geometric parameters in water jet propulsion system of autonomous underwater vehicles [Text] / L. Jian, L. Xiwen, Z. Zuti, L. Xiaohui, Z. Yuquan // Ocean Engineering. – 2016. – V. 123. – P. 327–345. Doi:10.1016/j.oceaneng.2016.07.041.
75. Jingjing, X. Queuing Models to Improve Port Terminal Handling Service [Text] / X. Jingjing, L. Dong // Systems Engineering Procedia. – 2012. – Vol. 4. – P. 345–351. Doi: http://dx.doi.org/10.1016/j.sepro.2011.11.085.
76. Johnson, H. Barriers to improving energy efficiency in short sea shipping: an action research case study [Text] / H. Johnson, M. Johansson, K. Andersson // Journal of Cleaner Production. – 2014. – V. 66. – P. 317–327. Doi:10.1016/j.jclepro.2013.10.046.
77. Johnson, H. Increased energy efficiency in short sea shipping through decreased time in port [Text] / H. Johnson, L. Styhre // Transportation Research Part A: Policy and Practice. – 2015. – V. 71. – P. 167–178. Doi:10.1016/j.tra.2014.11.008.
78. Jutao, C. Design and implementation of Marine Electric Propulsion Dynamic Load Simulation System [Text] / Jutao C., Huayao Z., Aibing Y. // 2008 3rd IEEE Conference on Industrial Electronics and Applications. – Singapore, IEEE, 2008. – P. 483–488. Doi:10.1109/ICIEA.2008.4582562.
79. Ketsingsoi, S. An Off-line Battery Charger based on Buck-boost Power Factor Correction Converter for Plug-in Electric Vehicles [Text] / S. Ketsingsoi, Y. Kumsuwan // Energy Procedia. – 2014. – V. 56. – P. 659–666. Doi:10.1016/j.egypro.2014.07.205.
80. Kibi, Y. Fabrication of high-power electric double-layer capacitors [Text] / Y. Kibi, T. Saito, M. Kurata, J. Tabuchi, A. Ochi // Journal of Power Sources. – 1996. – V. 60, I. 2. – P. 219–224. Doi:10.1016/S0378-7753(96)80014-0.
81. Kim, Y.-S. Weather-optimal control of a dynamic positioning vessel using back stepping: simulation and model experiment [Text] / Y.-S. Kim, J. Kim, H.-G. Sung // IFAC–PapersOnLine. – 2016. – V. 49, I. 23. – P. 232–238. Doi:10.1016/j.ifacol.2016.10.348.
82. Kobougias, I. PV Systems Installed in Marine Vessels: Technologies and Specifications: Research Article [Text] / I. Kobougias, E. Tatakis, J. Prousalidis //

Advances in Power Electronics. – 2013. – 8 p. Doi:10.1155/2013/831560.
83. Kobyliński, L. Problems of handling ships equipped with AZIPOD propulsion systems [Text] / L. Kobyliński // Prace naukowe politechniki warszawskiej. – 2013. – V. 95. – P. 232–245. Available at: \www/ URL: https://pbn.nauka.gov.pl/polindex-webapp/browse/article/article-f315dfd7-df06-463e-8de7-b553f8c232db. – 24.12.2016 p. (Last accessed: 02.05.2020).
84. Kritzinger, D. Failure Modes and Effects Analysis [Text] / D. Kritzinger // In Aircraft System Safety, Woodhead Publishing. – 2017. – P. 101–132. Doi:10.1016/B978-0-08-100889-8.00005-2.
85. Kurzweil, P. Post-lithium-ion battery chemistries for hybrid electric vehicles and battery electric vehicles [Text] / P. Kurzweil // Advances in Battery Technologies for Electric Vehicles: A volume in Woodhead Publishing Series in Energy. – 2015. – P. 127–172. Doi:10.1016/B978-1-78242-377-5.00007-8.
86. Lashway, C. R. Hybrid energy storage management in ship power systems with multiple pulsed loads [Text] / C. R. Lashway, A. T. Elsayed, O. A. Mohammed // Electric Power Systems Research. – 2016. – V. 141. – P. 50–62. Doi:10.1016/j.epsr.2016.06.031.
87. Lepisto, V. Dynamic process simulation promotes energy efficient ship design [Text] / V. Lepisto, J. Lappalainen, K. Sillanpaa, P. Ahtila // Ocean Engineering. – 2016. – Vol. 111. – P. 43–45. Doi: http://dx.doi.org/10.1016/j.oceaneng.2015.10.043.
88. Li, C.-Z. Fundamentals of renewable energy processes, 2nd ed. [Text] / C.-Z. Li // Process Safety and Environmental Protection. . – 2006. – V. 84. – I. 6. – P. 476. Doi:10.1205/psep.br.0606.
89. Ling-Chin, J. Investigating the implications of a new-build hybrid power system for Roll-on/Roll-off cargo ships from a sustainability perspective – A life cycle assessment case study [Text] / J. Ling-Chin, A. P. Roskilly // Applied Energy. – 2016. – V. 181. – P. 416–434. Doi:10.1016/j.apenergy.2016.08.065.
90. Livanosa, G. A. Techno-economic investigation of alternative propulsion plants for Ferries and RoRo ships [Text] / G. A. Livanosa, G. Theotokatos, D.-N. Pagonis // Energy Conversion and Management. – V. 79. March, 2014. P. 640–651. Doi:10.1016/j.enconman.2013.12.050.
91. Lujano-Rojas, J. M. Probabilistic modelling and analysis of stand-alone hybrid power systems [Text] / J. M. Lujano-Rojas, R. Dufo-López, J. L. Bernal-Agustín // Energy. – 2013. – V. 63. – P. 19–27. Doi:10.1016/j.energy.2013.10.003.
92. Maciel, P. Modelling Thruster-Hull Interaction with CFD [Text] / P. Maciel, A. Koop, G. Vaz // Proceedings of the ASME 2013 32nd International Conference on Ocean, Offshore and Arctic Engineering. – OMAE2013. – June 9 – 14, 2013. Available at: \www/ URL: http://www.marin.nl/web/Publications/Publication-items/Modelling-ThrusterHull-Interaction-with-CFD.htm. – 24.12.2016 p. (Last accessed: 02.05.2020).
93. Maheri, A. Multi-objective design optimization of standalone hybrid wind-PV-diesel systems under uncertainties [Text] / A. Maheri // Renewable Energy. – 2014. – V. 66. – P. 650–661. Doi:10.1016/j.renene.2014.01.009.

94. Maleki, A. Artificial bee swarm optimization for optimum sizing of a stand-alone PV/WT/FC hybrid system considering LPSP concept [Text] / A. Maleki, A. Askarzadeh // Solar Energy. – 2014. – V. 107. – P. 227–235. Doi:10.1016/j.solener.2014.05.016.
95. Maleki, A. Optimal sizing of a PV/wind/diesel system with battery storage for electrification to an off-grid remote region: a case study of Rafsanjan, Iran [Text] / A. Maleki, A. Askarzadeh // Sustainable Energy Technologies and Assessments. – 2014. – V. 7. – P. 147–153. Doi:10.1016/j.seta.2014.04.005.
96. Mander, S. Slow steaming and a new dawn for wind propulsion: A multi-level analysis of two low carbon shipping transitions [Text] / S. Mander // Marine Policy, In Press, Corrected Proof, Available online. – 2016. Doi:10.1016/j.marpol.2016.03.018.
97. Maragkogianni, A. Evaluating the social cost of cruise ships air emissions in major ports of Greece [Text] / A. Maragkogianni, S. Papaefthimiou // Transportation Research Part D: Transport and Environment. – 2015. – V. 36. – P. 10–17. Doi:10.1016/j.trd.2015.02.014.
98. Matthé, U. Eberle 8-The Voltec System-Energy Storage and Electric Propulsion [Text] / R. Matthé, U. Eberle // Lithium–Ion Batteries: Advances and Applications. – 2014. – P. 51–176. Doi:10.1016/B978-0-444-59513-3.00008-X.
99. Mauro, F. Advantages and disadvantages of thruster allocation procedures in preliminary dynamic positioning predictions [Text] / F. Mauro, R. Nabergoj // Ocean Engineering. – 2016. – V. 123. – P. 96–102. Doi:10.1016/j.oceaneng.2016.06.045.
100. McCamish, B. A backend framework for the efficient management of power system measurements [Text] / B. McCamish, R. Meier, J. Landford, R. B. Bass, D. Chiu, E. Cotilla–Sanchez // Electric Power Systems Research. – 2016. – V. 140. – P. 797–805. Doi:10.1016/j.epsr.2016.05.003.
101. MDL Home Page: Fanbeam® Laser DP reference system [Електронний ресурс]. URL: http://www.mdl-laser.com/en/rugged-laser-equipment-for-extreme-enviro-nments-14735. (дата звернення: 13.10.2016).
102. Militello, L. G. The Role of Cognitive Systems Engineering in the Systems Engineering Design Process [Text] / L. G. Militello, C. O. Dominguez, G. Lintern, G. Klein // Systems Engineering: Regular Paper. – Wiley Periodicals, Inc, 2009. – P. 1–13. Doi:10.1002/sys.20147.
103. Ming, T. Reliability Analysis and Optimization of the Ship Ballast Water System [Text] / T. Ming, Z. Fa-xin, L. Yu-le // The Open Automation and Control Systems Journal. – 2015. – 7. – P. 100–105. Available at: \www/ URL: http://benthamopen.com/contents/pdf/TOAUTOCJ/TOAUTOCJ-7-100.pdf. – 14.05.2016 г. (Last accessed: 02.05.2020).
104. Mishra, C. Rolling element bearing defect diagnosis under variable speed operation through angle synchronous averaging of wavelet de-noised estimate [Text] / C. Mishra, A.K. Samantaray, G. Chakraborty // Mechanical Systems and Signal Processing. – 2016. – V. 72–73. – P. 206–222. Doi:10.1016/j.ymssp.2015.10.019.

105. Montewka, J. Towards probabilistic models for the prediction of a ship performance in dynamic ice [Text] / J. Montewka, F. Goerlandt, P. Kujala, M. Lensu // Cold Regions Science and Technology. – 2015. – Vol. 112. – P. 14–28. Doi: http://dx.doi.org/10.1016/j.coldregions.2014.12.009.
106. Muntean, M.I. Visual A Multidimensional View Proposal of the Data Collected Through a Questionnaire. Associated Data Mart Deployment Framework [Text] / M. I. Muntean, D. Târnăveanu; Technical University Munich // ISPRS International Journal of Geo–Information. – München, 2013. – 2. – P. 813–836. Doi:10.3390/ijgi2030817.
107. Nelson, D. B., Nehrir M. H., Wang C. Unit sizing and cost analysis of stand-alone hybrid wind/PV/fuel cell power generation systems [Text] / D. B. Nelson, M. N. Nehrir, C. Wang // Renewable Energy. – 2006. – V. 31. – P. 1641–1656. Doi:10.1016/j.renene.2005.08.031.
108. Nikolskyi, V. The monitoring system of the Coanda effect for the tension-leg platform's [Text] / V. Nikolskyi, V. Budashko, S. Khniunin // Proceeding Book of International conference on engine room simulators (ICERS12). – Istanbul, Istanbul Technical University, Maritime Faculty, 2015. – P. 45–49. ISBN: 978-605-01-0782-1. Available at: \www/ URL: http://www.maritime.itu.edu.tr/icers12/program.htm. – 13.05.2016 p. (Last accessed: 02.05.2020).
109. Ordoñez, J. Processes and technologies for the recycling and recovery of spent *Lithium-ion batteries* [Text] / J. Ordoñez, E.J. Gago, A. Girard // Renewable and Sustainable Energy Reviews. – 2016. – V. 60. – P. 195–205. Doi:10.1016/j.rser.2015.12.363.
110. Ortolani, F. Investigation of the radial bearing force developed during ship operations. Part 2: Unsteady maneuvers [Text] / F. Ortolani, S. Mauro, G. Dubbioso // Ocean Engineering. – 2015. – V. 106. – P. 424–445. Doi: 10.1016/j.oceaneng.2015.06.058.
111. Ovrum, E. Modelling lithium-ion battery hybrid ship crane operation [Text] / E. Ovrum, T.F. Bergh // Applied Energy. – 2015. – V. 152. – P. 162–172. Doi:10.1016/j.apenergy.2015.01.066.
112. Palmer, A. Modelling Tunnel Thrusters for Autonomous Underwater Vehicles [Text] / A. Palmer, G. E. Hearn, P. Stevenson // IFAC Proceedings Volumes. – 2008. – V. 41, I. 1. – P. 91–96. Doi:10.3182/20080408-3-IE-4914.00017.
113. Pat. No. 100819 UA. Sudova systema monitorynhu dlya poperedzhennya effektu Koanda [Ship monitoring system for the prevention of Coanda effect] [Text] / Budashko V. V., Nikolskyi V. V., Khniunin S. H. – No. u201501854; declareted: 02.03.2015; published: 10.08.2015, Bul. No. 15. – Available at: https://base.uipv.org/searchINV/search.php?action=search.
114. Pat. No. 108074 UA. Systema impulʹsno-fazovoho upravlinnya elektropryvodom sudnovoyi hvynto-kermovoyi ustanovky [The pulse-phase control system of electric ship propeller-steering plant] [Text] / Budashko V. V., Yushkov E. A. – No. u201601510; declareted: 18.02.2016; published: 24.06.2016, Bul. No. 12. – Available at: https://base.uipv.org/searchINV/search.php?action=search.
115. Pat. No. 107006 UA. Sudova systema monitorynhu dlya poperedzhennya effektu

Koanda [Ship system for monitoring for preventing the Coanda effect] [Text] / Khnyunin S. H., Nikolskyi V. V., Budashko V. V. – No. u201512962; declareted: 28.12.2015; published: 10.05.2016, Bul. No. 9. – Available at: https://base.uipv.org/searchINV/search.php?action=search.

116. Pereira, F. C. Text analysis in incident duration prediction [Text] / F. C. Pereira, F. Rodrigues, M. Ben–Akiva // Transportation Research Part: MIT Alliance for Research and Technology (SMART). – Singapore: Elsevier Ltd, 2013. – 37. – P. 177–192. Doi:10.1016/j.trc.2013.10.002.
117. Power, D. J. Model-driven decision support systems: Concepts and research directions [Text] / D. J. Power, R. Sharda // *Decision Support Systems*. – Elsevier B.V., 2007. – 43. – P. 1044–1061. Doi:10.1016/j.dss.2005.05.030.
118. Product catalog modularity redundancy scalability. Power supply modules and systems for industry, power generation & distribution, marine and rail & metro [Text]. Available at: \www/ URL: http://utu.lv/sites/utu.lv/files/attachments/eltek_product_catalog_2012.pdf. – 13.10.2016 p. (Last accessed: 02.05.2020).
119. Ramli, M. Economic analysis of PV/diesel hybrid system with flywheel energy storage [Text] / M. A. M. Ramli, A. Hiendro, S. Twaha // Renewable Energy. – 2015. – V. 78. – P. 398–405. Doi:10.1016/j.renene.2015.01.026.
120. Rezaie, B. Renewable energy options for buildings: case studies [Text] / B. Rezaie, E. Esmailzadeh, I. Dincer // Energy and Buildings. – 2011. – V. 43. – P. 56–65. Doi:10.1016/j.enbuild.2010.08.013.
121. Resolution MEPC.212 (63). 2012 Guidelines on the method of calculation of the attained energy efficiency design index (EEDI) for new ships [Text]. Available at: \www/ URL: http://www.imo.org/en/KnowledgeCentre/IndexofIMOResolutions/Marine-Environment-Protection-Committee-(MEPC)/Documents/MEPC.212(63).pdf. – 13.10.2015 p. (Last accessed: 02.05.2020).
122. Rezzouk, H. Feasibility study and sensitivity analysis of a stand-alone photovoltaic-diesel-battery hybrid energy system in the north of Algeria [Text] / H. Rezzouk, A. Mellit // Renewable and Sustainable Energy Reviews. – 2015. – V. 43. – 1134–1150. Doi:10.1016/j.rser.2014.11.103.
123. Rozali, N. E. M. Process Integration for Hybrid Power System supply planning and demand management [Text] / N. E. M. Rozali, S. R. W. Alwi, Z. A. Manan, J. J. Klemeš // Renewable and Sustainable Energy Reviews. – 2016. – V. 66. – P. 834–842. Doi:10.1016/j.rser.2016.08.045.
124. Rudnichenko, N. D. Nechetko-veroyatnostnaya model otsenok riskov slozhnyih tehnicheskih sistem [Fuzzy-probability model for assessing the risks in complex technical systems] [Text] / N. D. Rudnichenko, V. V. Vychuzhanin // Informatics & Mathematical Methods in Simulation. – 2014. – Vol. 4, Issue 3. – P. 225–232.
125. Saha, N. Speed control with torque ripple reduction of switched reluctance motor by hybrid many optimizing liaison gravitational search technique [Text] / N. Saha, S. Panda // Engineering Science and Technology, an International Journal. – 2016. – Doi:10.1016/j.jestch.2016.11.018.

126. Sørdalen, O. J. Optimal thrust allocation for marine vessels [Text] / O.J. Sørdalen // Control Engineering Practice. – 1997. – V. 5, I. 9. – P. 1223–1231. Doi:10.1016/S0967-0661(97)84361-4.
127. Scherer, T. The Evolution of Machinery Control Systems Support At the Naval Ship Systems Engineering Station [Text] / T. Scherer, J. Cohen; Naval Ship Systems Engineering Station // Naval engineers journal. – American Society of Naval Engineers, 2011. – 2. – P. 85–109. Doi:10.1111/j.1559-3584.2011.00321.x.
128. Sharafi, M. Multi-objective optimal design of hybrid renewable energy systems using PSO–simulation based approach [Text] / M. Sharafi, T. Y. ELMekkawy // Renewable Energy. – 2014. – V. 68. – P. 67–79. Doi:10.1016/j.renene.2014.01.011.
129. Shi, J. P. Past, present, and future of decision support technology [Text] / J. P. Shi, M. Warkentin, J. F. Courtney, D. J. Power, R. Sharda, C. Carlsson // *Decision Support Systems*. – New York: Computer–Supported Decision Making, 2002. – 33(2). – P. 111–126. Doi:10.1016/S01679236(01)00139-7.
130. Sørensen, A. J. High Performance Thrust Allocation Scheme in Positioning of Ships Based on Power and Torque Control [Text] / A. J. Sørensen, A. K. Ådnanes // Marine Technology Society, Dynamic Positioning Conference: Session 9 Control Systems. – Houston, October 21-22, 1997. – P. 1–17. Available at: \www/ URL: https://www.researchgate.net/publication/255649795_High_Performance_Thrust_Allocation_Scheme_in_Positioning_of_Ships_Based_on_Power_and_Torque_Control. – 13.05.2016 г. (Last accessed: 02.05.2020).
131. Taskar, B. The effect of waves on engine-propeller dynamics and propulsion performance of ships [Text] / B. Taskar, K. K. Yum, S. Steen, E. Pedersen // Ocean Engineering. – 2016. – V. 122. – P. 262–277. Doi:10.1016/j.oceaneng.2016.06.034.
132. The essential guide to everything solar 35th Annual Catalog [Text]. Available at: \www/ URL: http://aeesolar.com/wp-content/uploads/2016/04/2016-AEE-Solar-Catalog.pdf. – 13.10.2016 p. (Last accessed: 02.05.2020).
133. The complete propulsion unit [Text]. Available at: \www/ URL: http://www.schottel.de/fileadmin/data/pdf/eng/NAV_EN_0814_web.pdf. – 13.10.2016 p. (Last accessed: 02.05.2020).
134. The SCHOTTEL Rudder propeller. From brilliant invention to global classic [Text]. Available at: \www/ URL: http://www.schottel.de/marine-propulsion/srp-rudderpropeller. – 13.10.2016 p. (Last accessed: 02.05.2020).
135. Thieme, C. A. Safety performance monitoring of autonomous marine systems [Text] / C. A. Thieme, I. B. Utne // Reliability Engineering & System Safety. – 2017. – Vol. 159. – P. 264–275. Doi: http://dx.doi.org/10.1016/j.ress.2016.11.024.
136. .Thiébot, J. Modelling the effect of large arrays of tidal turbines with depth-averaged Actuator Disks [Text] / J. Thiébot, S. Guillou, V. T. Nguyen // Ocean Engineering. – 2016. – V. 126. – P. 265–275. Doi:10.1016/j.oceaneng.2016.09.021.
137. Tsekouras, G. J. Simplified method for the assessment of ship [Text] /

G. J. Tsekouras, J. M. Prousalidis, F. D. Kanellos // IET electrical systems in transportation. – The Institution of Engineering and Technology, 2015. – P. 1–9. Doi:10.1049/iet-est.2013.0011.

138. Vahdani, B. Reliable design of a logistics network under uncertainty: A fuzzy possibilistic-queuing model [Text] / B. Vahdani, R. Tavakkoli-Moghaddam, F. Jolai // Applied Mathematical Modelling. – 2013. – Vol. 37, Issue 5. – P. 3254–3268. Doi: http://dx.doi.org/10.1016/j.apm.2012.07.021.

139. Vahushchenko, L. L. System avtomatycheskoho upravlenyia dvyzhenyem sudna [Motion Control Systems of automatic vehicles] [Text] / L. L. Vahushchenko, N. N. Tsmbal, N. N. – 2002. Odessa, Feniks, 328 p.

140. Vetter, M. Chapter 11 – Rechargeable Batteries with Special Reference to Lithium–Ion Batteries [Text] / M. Vetter, S. Lux // Storing Energy. – 2016. – P. 205–225. Doi:10.1016/B978-0-12-803440-8.00011-7.

141. Vichuzhanin, V. Realization of a fuzzy controller with fuzzy dynamic correction [Text] / V. Vichuzhanin // Open Engineering. – 2012. – Vol. 2, Issue 3. Doi: http://dx.doi.org/10.2478/s13531-012-0003-7.

142. Vrijdag, A. Estimation of uncertainty in ship performance predictions [Text] / A. Vrijdag // Journal of Marine Engineering & Technology. – 2014. – P. 45–55. Doi:10.1080/20464177.2014.11658121.

143. Wang, Q. A critical review of thermal management models and solutions of *Lithium-ion batteries* for the development of pure electric vehicles [Text] / Q. Wang, B. Jiang, B. Li, Y. Yan // Renewable and Sustainable Energy Reviews. – 2016. – V. 64. – P. 106–128. Doi:10.1016/j.rser.2016.05.033.

144. Wei, C. Dynamic Simulation and Control Strategy for Three-Shaft Marine Electric Propulsion Gas Turbine [Text] / C. Wei, S. Zang // ASME Turbo Expo 2010: Power for Land, Sea, and Air, Glasgow, UK, ASME, 2010. – V. 3 : Controls, Diagnostics and Instrumentation ; Cycle Innovations ; Marine. – P. 1099–1104. Doi:10.1115/gt2010-23796.

145. Wilflinger, J. Simulation and control design of hybrid propulsions in boats [Text] / J. Wilflinger, P. Ortner, L. del Re, M. Aschaber // IFAC Proceedings Volumes. – 2010. – V. 43, I. 20. – P. 40–45. Doi:10.3182/20100915-3-DE-3008.00001.

146. Whisper power book marine catalogue 2016 [Text]. Available at: \www/ URL:http://www.whisperpower.com/ru/2/13/phpimg/WhisperPowerBookMarine2016-UK.pdf. – 13.10.2016 p. (Last accessed: 02.05.2020).

147. Yan, R. The combined effects of high penetration of wind and PV on power system frequency response [Text] / R. Yan, T. K. Saha, N. Modi, N.–A. Masood, M. Mosadeghy // Applied Energy. – 2015. – V. 145. – P. 320–330. Doi:10.1016/j.apenergy.2015.02.044.

148. Yang, N. Unbalanced discharging and aging due to temperature differences among the cells in a lithium-ion battery pack with parallel combination [Text] / N. Yang, X. Zhang, B. Shang, G. Li // Journal of Power Sources. – 2016. – V. 306. – P. 733–741. Doi:10.1016/j.jpowsour.2015.12.079.

149. Yipeng, G. Computer based concurrent design and realization of simulated training system for marine electric propulsion system [Text] /

G. Yipeng, Z. Fanming, C. Yutao // Industrial and Information Systems (IIS), 2010 2nd International Conference on, Dalian, IEEE, 2010. – V. 2. – P. 511–513. Doi:10.1109/INDUSIS.2010.5565766.

150. Yoshida, S. Estimation of global tilted irradiance and output energy using meteorological data and performance of photovoltaic modules [Text] / S. Yoshida, S. Ueno, N. Kataoka, H. Takakura, T. Minemoto // Solar Energy. – 2013. – V. 93. – P. 90–99. Doi:10.1016/j.solener.2013.04.001.

151. Yutao, C. Integrated Design Platform for Marine Electric Propulsion System [Text] / C. Yutao, Z. Fanming, W. Jiaming; College of Naval Architecture and Power // 2012 International Conference on Future Electrical Power and Energy System. – Wuhan: Naval University of Engineering, 2012. – 17, Part A. – P. 540–546. Doi:10.1016/j.egypro.2012.02.133.

152. Xiao, H. Quantifying and reducing model-form uncertainties in Reynolds-averaged Navier–Stokes simulations: A data-driven, physics-informed Bayesian approach [Text] / H. Xiao, J.-L. Wu, J.-X. Wang, R. Sun, C.J. Roy // Journal of Computational Physics. – 2016. – V. 324. – P. 115–136. Doi:10.1016/j.jcp.2016.07.038.

153. Xu, S. A thrust sensitivity analysis based on a synthesized positioning capability criterion in DPCap/DynCap analysis for marine vessels [Text] / S. Xu, X. Wang, L. Wang, S. Meng, B. Li // Ocean Engineering. – 2015. – V. 108. – P. 164–172. Doi:10.1016/j.oceaneng.2015.08.001.

154. Zahedi, B. Optimized efficiency of all-electric ships by dc hybrid power systems [Text] / B. Zahedi, L. E. Norum, K. B. Ludvigsen // Journal of Power Sources. – 2014. – V. 255. – P.341–354. Doi:10.1016/j.jpowsour.2014.01.031.

155. Zakeri, B. Electrical *Energy Storage Systems*: a comparative life cycle cost analysis [Text] / B. Zakeri, S. Syri / Renewable and Sustainable Energy Reviews. – 2015. – V. 42. – P. 569–596. Doi:10.1016/j.rser.2014.10.011.

156. Zhang, J. Functional Mechanism: Regression Analysis under Differential Privacy [Text] / J. Zhang, Z. Zhang, X. Xiao, Y. Yang, M. Winslett // The 38th International Conference on Very Large Data Bases: Proceedings. – Istanbul: VLDB Endowment, 2012 (August 27th – 31st). – 11, Vol. 5. – P. 1364–1375. Available at: \www/ URL: http://vldb.org/pvldb/vol5/p1364_junzhang_vldb2012.pdf. – 13.05.2016 г. (Last accessed: 02.05.2020).

157. Zhang, S. Model predictive control for power management in a plug-in hybrid electric vehicle with a hybrid *Energy Storage System* [Text] / S. Zhang, R. Xiong, F. Sun // Applied Energy. – 2017. – V. 185 (2). – P. 1654–1662. Doi:10.1016/j.apenergy.2015.12.035.

158. Zhang, Y. Energy conversion mechanism and regenerative potential of vehicle suspensions [Text] / Y. Zhang, K. Guo, D. Wang, C. Chen, X. Li // Energy. – 2017. – V. 119. – P. 961–970. Doi:10.1016/j.energy.2016.11.045.

159. Zhao, B. Optimal sizing, operating strategy and operational experience of a stand-alone microgrid on Dongfushan Island [Text] / B. Zhao, X. Zhang, P. Li, K. Wang, M. Xue, C. Wang // Applied Energy. – 2014. – V. 113. – P. 1656–1666. Doi:10.1016/j.apenergy.2013.09.015.

160. Zhao, H. Review of *Energy Storage System* for wind power integration support [Text] / H. Zhao, Q. Wu, S. Hu, H. Xu, C. N. Rasmussen // Applied Energy. – 2014. – V. 137. – P. 545–553. Doi:10.1016/j.apenergy.2014.04.103.
161. Zhao, J. Thermal performance of mini-channel liquid cooled cylinder based battery thermal management for cylindrical lithium-ion power battery [Text] / J. Zhao, Z. Rao, Y. Li // Energy Conversion and Management. – 2015. – V. 103. – P. 157–165. Doi:10.1016/j.enconman.2015.06.056.
162. Zhao, P. Capacity allocation of a hybrid *Energy Storage System* for power system peak shaving at high wind power penetration level [Text] / P. Zhao, J. Wang, Y. Dai // Renewable Energy. – 2015. – V. 75. – P. 541–549. Doi:10.1016/j.renene.2014.10.040.
163. Zhou, Y. A novel health indicator for on-line *Lithium-ion batteries* remaining useful life prediction [Text] / Y. Zhou, M. Huang, Y. Chen, Y. Tao // Journal of Power Sources. – 2016. – V. 321. – P. 1–10. Doi:10.1016/j.jpowsour.2016.04.119.

SCIENTIFIC EDITION

MONOGRAPH

PROSPEKTIVE GLOBALE WISSENSCHAFTLICHE TRENDS

MODERNE TECHNOLOGIEN UND FORSCHUNGSKONZEPTE FÜR SCHIFFSKRAFTWERKE KOMBINIERTER ANTRIEBSANLAGEN

PROSPECTIVE GLOBAL SCIENTIFIC TRENDS

MODERN TECHNOLOGIES AND CONCEPTS OF RESEARCHING FOR SHIP POWER PLANTS OF COMBINED PROPULSION COM-PLEXES

MONOGRAPHIC SERIES «EUROPEAN SCIENCE»

BOOK 7. PART 7

Author:
Budashko V.V.

The scientific achievements of the authors of the monograph were also reviewed and recommended for publication at the international scientific symposium
«Prospektive globale wissenschaftliche Trends '2021 / Prospective global scientific trends' 2021»
(November 30, 2021)

The monograph is included in
International scientometric databases

500 copies
December, 2021

Published:
ScientificWorld -NetAkhatAV
Lußstr 13,
Karlsruhe, Germany
in conjunction with Institute «SE&E»
Monograph published in the author's edition

e-mail: orgcom@sworld.education
www.sworld.education

ISBN 978-3-949059-43-8


NEXTAGE